



CERN-PH-EP-2015-018

Submitted to: JHEP

A search for high-mass resonances decaying to $\tau^+\tau^-$ in pp collisions at $\sqrt{s} = 8$ TeV with the ATLAS detector

The ATLAS Collaboration

Abstract

A search for high-mass resonances decaying into $\tau^+\tau^-$ final states using proton–proton collisions at $\sqrt{s} = 8$ TeV produced by the Large Hadron Collider is presented. The data were recorded with the ATLAS detector and correspond to an integrated luminosity of 19.5–20.3 fb^{−1}. No statistically significant excess above the Standard Model expectation is observed; 95% credibility upper limits are set on the cross section times branching fraction of Z' resonances decaying into $\tau^+\tau^-$ pairs as a function of the resonance mass. As a result, Z' bosons of the Sequential Standard Model with masses less than 2.02 TeV are excluded at 95% credibility. The impact of the fermionic couplings on the Z' acceptance is investigated and limits are also placed on a Z' model that exhibits enhanced couplings to third-generation fermions.

A search for high-mass resonances decaying to $\tau^+\tau^-$ in pp collisions at $\sqrt{s} = 8$ TeV with the ATLAS detector

The ATLAS Collaboration

ABSTRACT: A search for high-mass resonances decaying into $\tau^+\tau^-$ final states using proton–proton collisions at $\sqrt{s} = 8$ TeV produced by the Large Hadron Collider is presented. The data were recorded with the ATLAS detector and correspond to an integrated luminosity of 19.5–20.3 fb^{−1}. No statistically significant excess above the Standard Model expectation is observed; 95% credibility upper limits are set on the cross section times branching fraction of Z' resonances decaying into $\tau^+\tau^-$ pairs as a function of the resonance mass. As a result, Z' bosons of the Sequential Standard Model with masses less than 2.02 TeV are excluded at 95% credibility. The impact of the fermionic couplings on the Z' acceptance is investigated and limits are also placed on a Z' model that exhibits enhanced couplings to third-generation fermions.

Contents

1	Introduction	1
2	ATLAS detector	3
3	Event samples	3
4	Physics objects	5
5	Event selection	7
6	Background estimation	8
6.1	Multijet background in the $\tau_{\text{had}}\tau_{\text{had}}$ channel	8
6.2	Jet background in the $\tau_{\text{lep}}\tau_{\text{had}}$ channel	9
6.3	Jet background other than multijet in the $\tau_{\text{had}}\tau_{\text{had}}$ channel	11
7	Systematic uncertainties	12
8	Z' signal models	14
8.1	Z' signal acceptance	15
8.2	Non-universal $G(221)$ model	16
9	Results and discussion	17
10	Conclusion	21

1 Introduction

Searches for new heavy resonances decaying to tau lepton pairs are both theoretically and experimentally well motivated [1–6]. Heavy Z' bosons often arise in grand unified theories and while they are typically considered to obey lepton universality, this is not necessarily a requirement. In particular, some models offering an explanation for the high mass of the top quark predict that such bosons preferentially couple to third-generation fermions [7, 8]. Models containing non-universal Z' bosons can explain the anomalous dimuon production observed at the D0 experiment [9, 10] and the excess in semileptonic B -meson decays into tau leptons observed at the Belle and BaBar experiments [11–13]. Searches in the ditau channel are also sensitive to goldstino-like scalars in supersymmetric models [14, 15], hidden sector Z' models [16] and to the anomalous tau lepton dipole moments and higher-order tau–gluon couplings [17].

In this article, a search for high-mass resonances decaying into $\tau^+\tau^-$ final states using proton-proton (pp) collisions at a center-of-mass energy of $\sqrt{s} = 8$ TeV produced by the

Large Hadron Collider (LHC) [18] is presented. The data were recorded with the ATLAS detector [19] and correspond to an integrated luminosity of 19.5–20.3 fb⁻¹. Tau leptons can decay into a charged lepton and two neutrinos ($\tau_{\text{lep}} = \tau_e$ or τ_μ), or hadronically (τ_{had}), predominantly into one or three charged pions, a neutrino and often additional neutral pions. The $\tau_{\text{had}}\tau_{\text{had}}$, $\tau_\mu\tau_{\text{had}}$ and $\tau_e\tau_{\text{had}}$ channels are analysed, accounting for 42%, 23% and 23% of the total $\tau^+\tau^-$ branching fraction, respectively. A counting experiment is performed in each channel from events that pass a high-transverse-mass requirement. Due to the different dominant background contributions and signal sensitivities, each channel is analysed separately and a statistical combination is used to maximise the sensitivity.

The Sequential Standard Model (SSM), which contains a Z'_{SSM} boson with couplings identical to the Standard Model Z boson, is chosen as the benchmark model to optimise the analysis and to quantify the experimental sensitivity. Limits on the Z'_{SSM} cross section times the branching fraction in tau pairs, $\sigma(pp \rightarrow Z'_{\text{SSM}} + X) \cdot \mathcal{B}(Z'_{\text{SSM}} \rightarrow \tau^+\tau^-) \equiv \sigma\mathcal{B}_{\text{SSM}}$, are provided as a function of the resonance mass, $m_{Z'}$. The impact on the signal acceptance times efficiency from changing the Z'_{SSM} couplings is assessed, which allows the limits on Z'_{SSM} to be reinterpreted for a broad range of models. Limits are also placed on the non-universal $G(221)$ model [8, 20, 21], which contains a Z'_{NU} boson that can exhibit enhanced couplings to tau leptons.

Direct searches for high-mass ditau resonances have been performed by the ATLAS and CMS collaborations using 5 fb⁻¹ of integrated luminosity at $\sqrt{s} = 7$ TeV [22, 23]. The searches exclude Z'_{SSM} with masses below 1.4 TeV at 95% CL.¹ For comparison, the most stringent limits on Z'_{SSM} in the dielectron and dimuon decay channels combined are 2.90 TeV at 95% CL from both ATLAS [24] and CMS [25]. While the limits on $\sigma(pp \rightarrow Z'_{\text{SSM}} + X) \cdot \mathcal{B}(Z' \rightarrow e^+e^-/\mu^+\mu^-)$ are in general stronger than those on $\sigma\mathcal{B}_{\text{SSM}}$, they may be evaded by models with weak couplings to electrons and muons. Indirect limits on Z' bosons with non-universal flavour couplings have been set using measurements from LEP and LEP II [26] and translate to a lower bound on the Z' mass of 1.09 TeV at 95% CL. Indirect limits have also been placed on the non-universal $G(221)$ model [8, 27–29]. The strongest exclude Z'_{NU} with a mass lower than 1.8 TeV at 95% CL.

This article is structured as follows. Section 2 provides an overview of the ATLAS detector. The event samples used in the analysis, recorded by the ATLAS detector or simulated using the ATLAS simulation framework, are described in section 3. The reconstruction of physics objects within the event samples is described in section 4. A description of the selection criteria used to define Z' signal regions is given in section 5. Section 6 describes the estimation of background contributions, followed by a description of systematic uncertainties in section 7. In section 8, the impact of altering the Z' couplings on the signal acceptance is described and the non-universal $G(221)$ model is introduced. A presentation of the results is given in section 9, followed by concluding remarks in section 10.

¹CL is used interchangeably throughout this article to refer to both confidence level (frequentist) and credibility limit (Bayesian).

2 ATLAS detector

The ATLAS detector at the LHC covers nearly the entire solid angle around the collision point. It consists of an inner tracking detector surrounded by a thin superconducting solenoid, electromagnetic (EM) and hadronic calorimeters, and a muon spectrometer incorporating large superconducting toroid magnets.

The inner-detector system is immersed in a 2 T axial magnetic field and provides charged-particle tracking in the range $|\eta| < 2.5$.² A high-granularity silicon pixel detector covers the vertex region and typically provides three measurements per track. It is followed by a silicon microstrip tracker, which usually provides four pairs of measurements per track. These silicon detectors are complemented by a transition radiation tracker (TRT), which enables radially extended track reconstruction up to $|\eta| = 2.0$. The TRT also provides electron/pion discrimination based on the fraction of hits (typically 30 in total) above a higher energy-deposit threshold corresponding to transition radiation.

The calorimeter system covers the pseudorapidity range $|\eta| < 4.9$. Within the region $|\eta| < 3.2$, EM calorimetry is provided by high-granularity barrel and endcap liquid-argon (LAr) EM calorimeters with lead absorbers, with an additional thin LAr presampler covering $|\eta| < 1.8$ to correct for upstream energy loss. Hadronic calorimetry is provided by a steel/scintillator-tile calorimeter, segmented into three barrel structures within $|\eta| < 1.7$, and two copper/LAr hadronic endcap calorimeters. Coverage in the forward region is achieved by copper/LAr and tungsten/LAr calorimeter modules optimised for EM and hadronic measurements, respectively.

The muon spectrometer comprises separate trigger and high-precision tracking chambers measuring the deflection of muons in a magnetic field generated by superconducting air-core toroids. The precision chamber system covers the region $|\eta| < 2.7$ with three layers of monitored drift tubes, complemented by cathode strip chambers in the forward region, where the background is highest. The muon trigger system covers the range $|\eta| < 2.4$ with resistive plate chambers in the barrel, and thin gap chambers in the endcap regions.

A three-level trigger system is used to select interesting events [30]. The Level-1 trigger is implemented in hardware and uses a subset of detector information to reduce the event rate to a design value of at most 75 kHz. This is followed by two software-based trigger levels which together reduce the event rate to a maximum of 1 kHz.

3 Event samples

The data used in this search were recorded with the ATLAS detector in pp collisions at a centre-of-mass energy of $\sqrt{s} = 8$ TeV during the 2012 run of the LHC. Only data taken with pp collisions in stable beam conditions and with all ATLAS subsystems operational are used, resulting in an integrated luminosity of 20.3 fb^{-1} . For the analysis of the $\tau_{\text{had}}\tau_{\text{had}}$

²ATLAS uses a right-handed coordinate system with its origin at the nominal interaction point (IP) in the centre of the detector and the z -axis along the beam pipe. The x -axis points from the IP to the centre of the LHC ring, and the y -axis points upward. Cylindrical coordinates (r, ϕ) are used in the transverse plane, ϕ being the azimuthal angle around the beam pipe. The pseudorapidity is defined in terms of the polar angle θ as $\eta = -\ln \tan(\theta/2)$. The geometrical distance between objects is defined as $\Delta R = \sqrt{(\Delta\phi)^2 + (\Delta\eta)^2}$.

channel, a small fraction of data from the initial running period are discarded as the trigger conditions are not accounted for by the simulation, resulting in an integrated luminosity of 19.5 fb^{-1} . The $\tau_{\text{had}}\tau_{\text{had}}$ channel uses events passing a single-tau trigger with a transverse momentum (p_{T}) threshold of 125 GeV, designed to select hadronic tau decays. The $\tau_{\mu}\tau_{\text{had}}$ channel uses events passing a single-muon trigger, either with a p_{T} threshold of 24 GeV including an isolation requirement or with a threshold of 36 GeV without an isolation requirement. The $\tau_e\tau_{\text{had}}$ channel uses events passing a single-electron trigger, either with a p_{T} threshold of 24 GeV including an isolation requirement, or with a threshold of 60 GeV without an isolation requirement. Events that pass the trigger are selected if they contain a vertex with at least four associated tracks, each with $p_{\text{T}} > 0.5 \text{ GeV}$. Events may have several vertices satisfying this requirement due to multiple pp interactions occurring in the same or neighbouring bunch crossings, referred to as pile-up. The event vertex is chosen as the one with the largest sum of the squared track transverse momenta.

Monte Carlo (MC) simulation is used to estimate signal efficiencies and some background contributions. Simulated samples of events from the following background processes are used: $Z/\gamma^* \rightarrow \tau\tau$ and $Z/\gamma^*(\rightarrow \ell\ell)+\text{jets}$ ($\ell = e, \mu$) enriched in high-mass events, and $W+\text{jets}$, $t\bar{t}$, single-top-quark (Wt , s -channel and t -channel) and diboson (WW , WZ , and ZZ) production. Each sample is produced with one of the following event generators: PYTHIA 8.165 [31], SHERPA 1.4.1 [32], MC@NLO 4.01 [33–35], ACERMC 3.8 [36], HERWIG 6.520 [37] or POWHEG-BOX 1.0 [38–41]. The most consistent set of available samples was chosen. The $Z/\gamma^* \rightarrow \tau\tau$ process is generated at leading order so that the sample can also be reweighted to describe the Z' signal. The combination of $t\bar{t}$ and single-top-quark production are referred to as *top*. In some cases the generators are interfaced to the following external software for parton showering, hadronisation and multiple parton interactions: PYTHIA 8, PYTHIA 6.421 [42] or HERWIG (which is itself interfaced to JIMMY 4.31 [43] for multiple parton interactions). The tau lepton decay is performed by either PYTHIA 8, SHERPA or TAUOLA [44]. For PYTHIA 8, the *sophisticated tau decay* option is used, which provides fully modelled hadronic currents with spin correlations for tau-lepton decays [45]. In all samples other than those generated with SHERPA, final-state photon radiation is performed by PHOTOS [46]. The CTEQ6L1 [47] and CT10 [48] parton distribution functions (PDFs) and the AU2, AUET2, AUET2B [49] and CT10 [32] MC tunes are used. A summary is given in table 1.

The contributions from simulated processes are normalised using theoretical cross sections. The Z/γ^* cross section is calculated up to next-to-next-to-leading order (NNLO) in QCD including next-to-leading order (NLO) electroweak corrections using FEWZ 3.1 [50] configured with the MSTW2008NNLO PDF set [51]. This cross section is used to derive mass-dependent K -factors that are used to weight the simulated Z/γ^* samples. Cross sections for the other background processes are calculated without the use of differential K -factors to at least NLO in QCD, as specified in table 1.

The contributions of the various Z' signal models are estimated by reweighting the $Z/\gamma^* \rightarrow \tau\tau$ sample using TAUSPINNER [60–62], which correctly accounts for spin effects in the tau decays. The algorithm relies on a leading order approximation in which spin amplitudes are used to calculate the spin density matrices for hard $2 \rightarrow 2$ Born level

Process	Generator	PS+MPI	Tau decay	PDF set	MC tune	Cross section
$Z/\gamma^* \rightarrow \tau\tau$	PYTHIA 8	PYTHIA 8	PYTHIA 8	CTEQ6L1	AU2	NNLO [50]
W +jets	SHERPA	SHERPA	SHERPA	CT10	CT10	NNLO [52, 53]
$t\bar{t}$	MC@NLO	HERWIG	TAUOLA	CT10	AUET2	\sim NNLO [54–56]
Single top						
(Wt)	MC@NLO	HERWIG	TAUOLA	CT10	AUET2	\sim NNLO [57]
(s -channel)	MC@NLO	HERWIG	TAUOLA	CT10	AUET2	NNLL [58]
(t -channel)	ACERMC	PYTHIA 6	TAUOLA	CTEQ6L1	AUET2B	\sim NNLO [57]
Diboson	HERWIG	HERWIG	TAUOLA	CTEQ6L1	AUET2	NLO [59]
$Z/\gamma^* \rightarrow \ell\ell$	POWHEG-BOX	PYTHIA 8	PYTHIA 8	CT10	AU2	NNLO [50]

Table 1. Details regarding the MC simulated samples. The following information is provided for each sample: the generator of the hard interaction, the parton shower and hadronisation (PS), multiple parton interactions (MPI) and the tau decay; the PDF set; the MC tune and the order in QCD of the cross section calculation. All cross sections are calculated at either NLO, NNLO, approximate NNLO (\sim NNLO) or next-to-next-to-leading logarithm (NNLL).

processes. The impact of interference between Z' and Z/γ^* is typically small (as discussed in section 8.1), so it is not included. For each signal model, several mass hypotheses are considered, ranging from 500 to 2500 GeV in steps of 125 GeV.

All generated events are propagated through a detailed GEANT4 simulation [63] of the ATLAS detector and subdetector-specific digitisation algorithms [64] and are reconstructed with the same algorithms as the data. Pile-up is simulated by overlaying minimum-bias interactions generated with PYTHIA 8 (with an MC tune specific to the LHC [65]) on the generated signal and background events. The resulting events are reweighted so that the distribution of the number of minimum-bias interactions per bunch crossing agrees with data. Due to the high momenta of the tau decay products, however, pile-up has little impact on the analysis. The effective luminosity of most simulated samples is at least as large as the integrated luminosity of the data; the statistical uncertainty from the limited sample size is accounted for in the statistical analysis.

4 Physics objects

In this section the reconstruction of electrons, muons, hadronic tau decays and the missing transverse momentum is described. Preliminary selections are applied to all electrons, muons and tau candidates. Further selection is applied to some of the objects as part of the *event selection* described in section 5. Corrections are applied to the kinematics and efficiencies of reconstructed electrons, muons and hadronic tau decays in simulated samples so that they match the performance measured from the data.

The reconstruction, energy calibration and identification of hadronic tau decays in ATLAS is described in detail in ref. [66]. Candidates for hadronic tau decays are built from jets reconstructed using the anti- k_t algorithm [67, 68] with a radius parameter value of 0.4. The jets are calibrated to the hadronic energy scale with correction factors based on simulation and validated using test-beam and collision data [69]. Only the *visible* tau-decay products (all products excluding neutrinos), $\tau_{\text{had-vis}}$, are considered when calculating

kinematic properties. The calculation of the four-momentum uses clusters with $\Delta R < 0.2$ from the initial jet-axis and includes a final tau-specific calibration derived from simulated samples, which accounts for out-of-cone energy, energy lost in dead material, underlying-event and pile-up contributions and the typical composition of hadrons in hadronic tau decays. The size of the tau-specific calibration is typically a few percent. The calibrated energy scale in data and simulation have been compared and agree within the $\sim 1.5\%$ uncertainty of the measurement. Candidates are required to have either one or three associated tracks (prongs) reconstructed in the inner detector. The tau charge is reconstructed from the sum of the charges of the associated tracks and is required to be ± 1 . The charge misidentification probability is found to be negligible. Hadronic tau decays are identified with a multivariate algorithm that employs boosted decision trees (BDTs) to discriminate against quark- and gluon-initiated jets using shower shape and tracking information. Working points with a tau identification (ID) efficiency for 1-prong/3-prong candidates of about 55%/40% (*medium*) for the $\tau_\mu\tau_{\text{had}}$ and $\tau_e\tau_{\text{had}}$ channels and 65%/45% (*loose*) for the $\tau_{\text{had}}\tau_{\text{had}}$ channel are chosen, leading to rates of false identification for quark- and gluon-initiated jets of below a percent. The tau ID efficiency is independent of p_T and pile-up. Corrections of a few percent are applied to the efficiency in simulation. Candidates arising from the misidentification of electrons are rejected using a separate BDT. In the $\tau_\mu\tau_{\text{had}}$ channel, a dedicated selection is applied to suppress candidates arising from the misidentification of muons. Tau candidates are required to have $p_T > 30$ GeV and to be in the fiducial volume of the inner detector, $|\eta| < 2.47$. The transition region between the barrel and endcap EM calorimeters, with $1.37 < |\eta| < 1.52$, is excluded. In the $\tau_{\text{ep}}\tau_{\text{had}}$ channels, candidates that have the highest- p_T track in the range $|\eta| < 0.05$ are rejected. This region corresponds to a gap in the TRT, which reduces the power of electron/pion discrimination.

Muon candidates are reconstructed by combining an inner-detector track with a track from the muon spectrometer. The candidates are required to have $p_T > 10$ GeV and $|\eta| < 2.5$. Muon quality criteria are applied to achieve a precise measurement of the muon momentum and reduce the misidentification rate [70]. These quality requirements correspond to a muon reconstruction and identification efficiency greater than 95%.

Electrons are reconstructed by matching clustered energy deposits in the EM calorimeter to tracks reconstructed in the inner detector [71]. The tracks are then refitted using the Gaussian Sum Filter algorithm [72], which accounts for energy loss through bremsstrahlung. The electron candidates are required to have $p_T > 15$ GeV and to be within the fiducial volume of the inner detector, $|\eta| < 2.47$ (the EM calorimeter transition region is excluded). The candidates are required to satisfy quality criteria based on the expected calorimeter shower shape and amount of radiation in the TRT. These quality requirements correspond to an electron identification efficiency of approximately 95% [73].

Electrons and muons are considered isolated if they are away from large deposits of energy in the calorimeter and tracks with large p_T consistent with originating from the same vertex. Lepton isolation is defined using the sum of the transverse energy, E_T , deposited in calorimeter cells with $\Delta R < 0.2$ from the lepton, $E_T^{0.2}$, and the scalar sum of the p_T of tracks with $p_T > 0.5$ GeV consistent with the same vertex as the lepton and with $\Delta R < 0.3$, $p_T^{0.3}$. Muons are considered isolated if they have $p_T^{0.3}/p_T < 5\%$. Isolated electrons must

have $p_T^{0.3}/p_T < 5\%$ and $E_T^{0.2} < 5 \text{ GeV} + 0.7\% \times p_T$ and must pass a tighter identification requirement corresponding to an efficiency of approximately 70%.

Geometric overlap of objects with $\Delta R < 0.2$ is resolved by selecting only one of the overlapping objects in the following order of priority: muons, electrons, tau candidates. The order is determined by the ability to identify the objects from their detector signatures. The missing transverse momentum, with magnitude E_T^{miss} , is calculated from the vector sum of the transverse momenta of all high- p_T objects reconstructed in the event, as well as a term for the remaining activity in the calorimeter [74]. Clusters associated with electrons, hadronic tau decays and jets are calibrated separately. The remaining clusters are weighted using tracking information to reduce the effect of pile-up on the E_T^{miss} resolution. A single weight is calculated for each event using all tracks that are not matched to high- p_T objects. The tracks are categorised based on whether or not they are matched to the primary vertex. The weight is then defined as the ratio of the sum of the p_T of tracks originating from the primary vertex to the sum of the p_T of all tracks.

5 Event selection

Selected events in the $\tau_{\text{had}}\tau_{\text{had}}$ channel must contain no electrons with $p_T > 15 \text{ GeV}$ or muons with $p_T > 10 \text{ GeV}$ and at least two tau candidates: one with $p_T > 150 \text{ GeV}$ that is matched to the object that passed the trigger and the other with $p_T > 50 \text{ GeV}$. This constitutes the *preselection*. If multiple tau candidates are selected, the two highest- p_T candidates are chosen. This decision is made before applying the BDT tau ID, to avoid kinematic biases in control regions defined by reversing the ID requirement. The tau candidates are then required to have charges of opposite sign (OS). Finally, the angle between the tau candidates in the transverse plane, $\Delta\phi(\tau_1, \tau_2)$, must be greater than 2.7 radians, as tau leptons from the decay of heavy neutral resonances are typically produced back-to-back in the transverse plane.

Selected events in the $\tau_{\text{lep}}\tau_{\text{had}}$ channels must contain exactly one isolated muon with $p_T > 30 \text{ GeV}$ or one isolated electron with $p_T > 30 \text{ GeV}$; no additional electrons with $p_T > 15 \text{ GeV}$ or muons with $p_T > 10 \text{ GeV}$; and at least one tau candidate with $p_T > 30 \text{ GeV}$. This constitutes the *preselection*. If multiple tau candidates are selected, the highest- p_T candidate is chosen. As in the $\tau_{\text{had}}\tau_{\text{had}}$ channel, this choice is made before applying the BDT tau ID. The angle between the lepton and tau candidate in the transverse plane, $\Delta\phi(\ell, \tau)$, must be greater than 2.7 radians, and they must have opposite charge. The *transverse mass* is defined as:

$$m_T(p^A, p^B) = \sqrt{2p_T^A p_T^B (1 - \cos \Delta\phi(p^A, p^B))},$$

where p^A and p^B are two reconstructed physics objects with transverse momenta p_T^A and p_T^B , respectively, which subtend an angle of $\Delta\phi(p^A, p^B)$ in the transverse plane. The W +jets background is suppressed by requiring the transverse mass of the lepton- E_T^{miss} system, $m_T(\ell, E_T^{\text{miss}})$, to be less than 50 GeV.

The search in all channels is performed by counting events in signal regions with *total transverse mass* above thresholds optimised separately for each signal mass hypothesis in

each channel to give the best expected exclusion limits. The same thresholds are found to be optimal for all channels. The total transverse mass, m_T^{tot} , is defined as

$$m_T^{\text{tot}}(\tau_1, \tau_2, E_T^{\text{miss}}) = \sqrt{m_T^2(\tau_1, \tau_2) + m_T^2(\tau_1, E_T^{\text{miss}}) + m_T^2(\tau_2, E_T^{\text{miss}})},$$

where τ_1 and τ_2 denote the reconstructed visible decay products of the two tau leptons (e , μ or $\tau_{\text{had-vis}}$).

6 Background estimation

The dominant background process in the $\tau_{\text{had}}\tau_{\text{had}}$ channel at high mass is $Z/\gamma^* \rightarrow \tau\tau$, which is estimated using simulation. The modelling of the $pp \rightarrow Z/\gamma^*$ process has been shown to be very reliable by using decays to electrons and muons [24, 75]. Additional uncertainties related to the modelling of high- p_T tau decays are also considered, as described in section 7. Multijet production makes a large contribution at low mass in the $\tau_{\text{had}}\tau_{\text{had}}$ channel and is estimated by weighting events in data where the subleading tau candidate fails tau ID, with *fake-factors* that parameterise the rate for jets to pass tau ID (section 6.1). Due to the relatively large size of the sample that fails tau ID, this procedure provides high statistical precision, which is particularly crucial in the high-mass tail. The fake-factors are measured from data in a separate control region. Diboson, W +jets, $t\bar{t}$, $Z/\gamma^*(\rightarrow \ell\ell)$ +jets, and single-top-quark production make minor contributions and are estimated using simulation. To improve the modelling of these background processes, events in the simulation that contain jets misidentified as hadronic tau decays are weighted by *fake-rates* measured in a W +jets control region in data (section 6.3).

The dominant background contributions in the $\tau_{\text{lep}}\tau_{\text{had}}$ channels come from $Z/\gamma^* \rightarrow \tau\tau$, which is estimated using simulation, and from processes in which a jet is misidentified as a hadronic tau decay. The latter is mainly composed of W +jets events and is estimated using fake-factors to weight events in data where the tau candidate fails ID, similarly to the procedure in the $\tau_{\text{had}}\tau_{\text{had}}$ channel (section 6.2). Diboson, $t\bar{t}$, $Z/\gamma^*(\rightarrow \ell\ell)$ +jets and single-top-quark production in which the tau candidate does not originate from a jet make minor contributions and are estimated using simulation. In the following subsections, the data-driven background estimates are described in more detail.

6.1 Multijet background in the $\tau_{\text{had}}\tau_{\text{had}}$ channel

To estimate the multijet background in the $\tau_{\text{had}}\tau_{\text{had}}$ channel, two control regions are used. Events in the first control region are required to pass the same selection as in the analysis, except for the subleading tau candidate, which is required to fail the BDT tau ID. The multijet contribution in the signal region is estimated by weighting these events with a tau ID fake-factor. The fake-factor, $f_{\text{tau-ID}}$, is defined as the ratio of the number of tau candidates that pass the BDT tau ID, $N^{\text{pass tau-ID}}$, to the number that fail, $N^{\text{fail tau-ID}}$. The fake-factors are calculated from a second control region that is highly pure in multijet events, the *multijet control region* (described below), and they depend on the p_T and track

multiplicity, N_{track} , of the subleading tau candidate:

$$f_{\text{tau-ID}}(p_T, N_{\text{track}}) \equiv \frac{N^{\text{pass tau-ID}}(p_T, N_{\text{track}})}{N^{\text{fail tau-ID}}(p_T, N_{\text{track}})} \Big|_{\text{multijet}}.$$

The fake-factors have no significant dependence on η . The number of multijet events in a bin of p_T , N_{track} and any additional variable that is uncorrelated to the BDT tau ID, x , is given by:

$$N_{\text{multijet}}(p_T, N_{\text{track}}, x) = f_{\text{tau-ID}}(p_T, N_{\text{track}}) \times N_{\text{data}}^{\text{fail tau-ID}}(p_T, N_{\text{track}}, x).$$

The multijet control region is designed to be as similar to the signal region as possible, while avoiding contamination from hadronic tau decays. This is achieved by loosening the tau ID requirements. Specifically, the selection for this control region is the same as for the signal region except with the following alterations. The BDT tau ID is not applied to either tau candidate. Instead of using the single-tau trigger, events are selected using single-jet triggers with thresholds ranging from 45 to 360 GeV, with all but the highest threshold trigger being prescaled. The p_T of the subleading tau candidate must be at least 40% of the p_T of the leading tau candidate (p_T -balance > 0.4) to avoid bias at low p_T due to the disproportionate fraction of events coming from the unprescaled 360 GeV jet trigger. The opposite-sign requirement on the charges of the two tau candidates is removed to increase the sample size.

Figures 1(left) and 1(right) show the fake-factors for 1-prong and 3-prong candidates, respectively. Use of these fake-factors relies on the assumption that they are insensitive to the alteration of the selection between the signal region and multijet control region. Systematic uncertainties on the fake-factors are derived by altering the selection on the p_T -balance, the charge product, and the identification of the leading- p_T tau candidate. These variations modify the fractional contribution of quark- and gluon-initiated jets in the sample, leading to large variations in the fake-factors at low p_T where the composition is mixed and little variation to the fake-factors at high p_T where the sample is quark dominated.

6.2 Jet background in the $\tau_{\text{lep}}\tau_{\text{had}}$ channel

The background contributions originating from quark- and gluon-initiated jets that are misidentified as hadronic tau decays in the $\tau_{\text{lep}}\tau_{\text{had}}$ channels are modelled using a fake-factor method, similar to that used in the $\tau_{\text{had}}\tau_{\text{had}}$ channel. In contrast to the $\tau_{\text{had}}\tau_{\text{had}}$ channel, the background is dominated by W +jets production, with a minor contribution from multijet production. To reduce the sensitivity to the differing fake-factors in W +jets and multijet events (due to a different quark/gluon fraction), events failing a *very loose* level of BDT tau identification (corresponding to efficiencies of 98% and 90% for 1-prong and 3-prong hadronic tau decays, respectively) are rejected. This significantly suppresses the gluon contribution, which typically consists of wider jets with higher hadron multiplicity which are more readily rejected by the tau ID. In the $\tau_{\text{lep}}\tau_{\text{had}}$ channels, there is also a non-negligible contribution to the first control region (fail-ID control region) from background

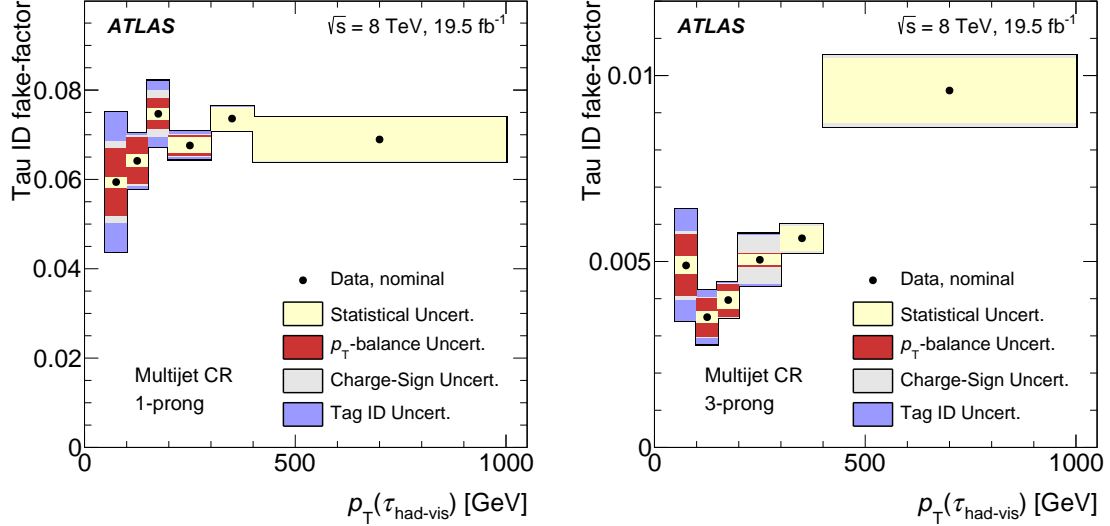


Figure 1. Tau ID fake-factors for (left) 1-prong and (right) 3-prong tau candidates, measured in the multijet control region of the $\tau_{\text{had}}\tau_{\text{had}}$ channel. The statistical and systematic uncertainties are shown, successively added in quadrature.

processes containing hadronic tau decays, which is subtracted using simulation. The fake-factors are measured in a high-purity W +jets control region and they depend on p_T , η and N_{track} of the tau candidate. The W +jets control region uses the same selection as the signal region but with the medium BDT tau ID replaced by very loose BDT tau ID and the m_T requirement replaced by $70 \text{ GeV} \leq m_T \leq 200 \text{ GeV}$. A second control region enriched in multijet events is defined, which has a higher fraction of gluon-initiated jets and represent an extreme variation in the jet composition. This control region uses the same selection as the W +jets control region but the lepton is required to fail isolation, the m_T requirement is replaced by $m_T < 30 \text{ GeV}$ and $E_T^{\text{miss}} < 30 \text{ GeV}$ is required. A 30% systematic uncertainty is derived from the difference in the fake-factors in the multijet and W +jets control regions. Figures 2(left) and 2(right) show the fake-factors measured in each of the two control regions in the $\tau_\mu\tau_{\text{had}}$ channel, integrated across all $|\eta|$ regions, for 1-prong and 3-prong candidates, respectively. The fake-factors in the $\tau_e\tau_{\text{had}}$ channel are similar.

Finally, in the $\tau_{\text{lep}}\tau_{\text{had}}$ channel, two additional steps are taken to ensure E_T^{miss} is modelled well by the fake-factor estimate. Firstly, the standard E_T^{miss} reconstruction treats the selected tau candidate in the fail-ID control region as a jet rather than a hadronic tau decay. Therefore, the E_T^{miss} is recalculated in the fail-ID control region using the tau hypothesis for the selected tau candidate. Following this, a slight bias in the shape of the E_T^{miss} distribution is corrected for by reweighting in bins of the E_T^{miss} projected along the direction of the tau candidate. An additional 20% uncertainty is applied to the estimate of the jet background event yield obtained after the full event selection, derived from the difference in the estimate between applying and not applying the E_T^{miss} reweighting.

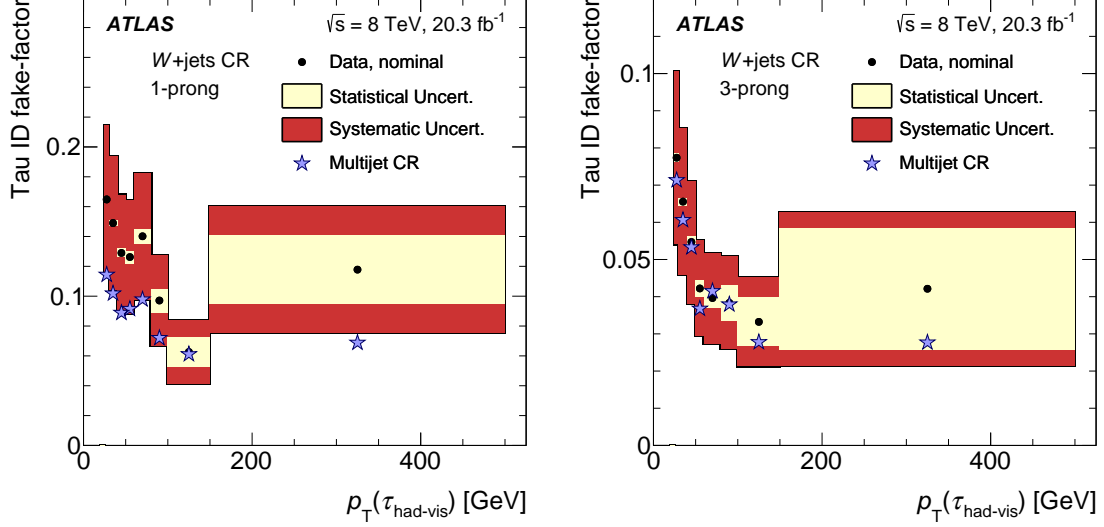


Figure 2. Tau ID fake-factors for (left) 1-prong and (right) 3-prong tau candidates, measured in the W +jets control region of the $\tau_\mu\tau_{\text{had}}$ channel, integrated across all $|\eta|$ regions. The statistical and systematic uncertainties are shown, successively added in quadrature. The fake-factors measured in the alternative multijet control region are overlaid.

6.3 Jet background other than multijet in the $\tau_{\text{had}}\tau_{\text{had}}$ channel

In the $\tau_{\text{had}}\tau_{\text{had}}$ channel, backgrounds originating from quark- and gluon-initiated jets that are misidentified as hadronic tau decays in processes other than multijet production are estimated using simulation (predominantly W +jets). Rather than applying the tau ID to the simulated jets, they are weighted by fake-rates. This not only ensures the correct fake-rate, but enhances the statistical precision of the estimate, as events failing the tau ID are not discarded. The fake-rate for the sub-leading tau candidate, $R_{\text{tau-ID}}^{\text{sub-lead}}$, is defined as the ratio of the number of tau candidates that pass tau ID, $N^{\text{pass tau-ID}}$, to the total number of tau candidates, N^{total} . The fake-rate for the leading tau candidate, $R_{\text{tau-ID}}^{\text{lead}}$, is defined as the ratio of the number of tau candidates that pass tau ID and the single-tau trigger requirement, $N^{\text{pass tau-ID + trigger}}$, to N^{total} . The fake-rates are calculated from a second control region that is high in W +jets purity (described below), and they depend on p_T and N_{track} of the tau candidate:

$$R_{\text{tau-ID}}^{\text{lead}}(p_T, N_{\text{track}}) \equiv \left. \frac{N^{\text{pass tau-ID + trigger}}(p_T, N_{\text{track}})}{N^{\text{total}}(p_T, N_{\text{track}})} \right|_{W+\text{jets}},$$

$$R_{\text{tau-ID}}^{\text{sub-lead}}(p_T, N_{\text{track}}) \equiv \left. \frac{N^{\text{pass tau-ID}}(p_T, N_{\text{track}})}{N^{\text{total}}(p_T, N_{\text{track}})} \right|_{W+\text{jets}}.$$

All simulated events are assigned a weight:

$$w_{\text{MC}} = \prod_{i \in \{\text{lead, sub-lead}\}} (1 - \delta^i [1 - R_{\text{tau-ID}}^i(p_T^i, N_{\text{track}}^i)])$$

where δ^i is 1 if the tau candidate originates from a jet and 0 otherwise. The tau ID and trigger selection criteria for simulated events are modified as follows: the BDT tau ID

criteria for the sub-leading tau candidate is removed if the candidate originates from a jet, the BDT tau ID criteria for the leading tau candidate and the trigger requirement are removed if the leading tau candidate originates from a jet.

Events in the W +jets control region are selected by a single-muon trigger with a p_T threshold of 36 GeV. The events are required to contain one isolated muon that: has $p_T > 40$ GeV, has $E_T^{0.2}/p_T < 6\%$ and is matched to the object that passed the trigger. There must be no additional muons or electrons and at least one tau candidate with opposite charge to the muon. The remaining contamination from multijet events is suppressed by requiring $\cos \Delta\phi(\mu, E_T^{\text{miss}}) + \cos \Delta\phi(\tau_{\text{had-vis}}, E_T^{\text{miss}}) < -0.15$, which disfavors back-to-back topologies where the E_T^{miss} vector points either in the direction of the muon or the tau candidate. The leading- p_T tau candidate is used to measure the fake-rate. Figures 3(left) and 3(right) show $R_{\text{tau-ID}}^{\text{sub-lead}}$ for 1-prong and 3-prong tau candidates, respectively. The fake-rates $R_{\text{tau-ID}}^{\text{lead}}$ (including the trigger requirement in the numerator) have a similar behaviour but are a factor of two to four lower. The requirement of opposite charge between the muon and the tau candidate enhances the contribution of the leading-order $qg \rightarrow W\bar{q}'$ process in which the tau candidate originates from a quark-initiated jet. To evaluate the systematic uncertainty from applying these fake-rates to simulated samples with different jet origin, the fake-rates are also calculated for events where the tau candidate has the same charge sign as the muon. These events have a higher fraction of gluon-initiated jets and represent an extreme variation in the jet composition, resulting in lower fake-rates as shown in Fig. 3(left) and Fig. 3(right). A 60% uncertainty is assigned to cover the range of the measured fake-rates for events with opposite- or same-sign tau candidates. The uncertainty is omitted for W +jets events as they are expected to have the same jet composition as events in the control region. The statistical uncertainty from the limited size of the W +jets control region is also considered.

7 Systematic uncertainties

Systematic effects on the contributions of signal and background processes estimated from simulation are discussed in this section. These include theoretical uncertainties on the cross sections of simulated processes and experimental uncertainties on the trigger, reconstruction and identification efficiencies; on the energy and momentum scales and resolutions; and on the measurement of the integrated luminosity. Uncertainties on the background contributions estimated from data are discussed in their respective sections.

The overall uncertainty on the Z' signal and the $Z/\gamma^* \rightarrow ee/\mu\mu/\tau\tau$ background due to choice of the PDFs, α_S , and the renormalisation and factorisation scales is estimated to be 14% for a ditau mass of 1750 GeV, dominated by the PDF uncertainty [24]. The uncertainty is evaluated using 90% CL MSTW2008NNLO PDF error sets and also takes into account potential differences between the following PDFs at the same α_S : MSTW2008NNLO, CT10NNLO, NNPDF2.3 [76], ABM11 [77] and HERAPDF1.5 [78]. Additionally, for $Z/\gamma^* \rightarrow \tau\tau$, a mass-dependent systematic uncertainty of up to 4% is attributed to electroweak corrections [24]. This uncertainty is not considered for the signal as it is strongly model dependent. An uncertainty of 5% is estimated for diboson production, derived from

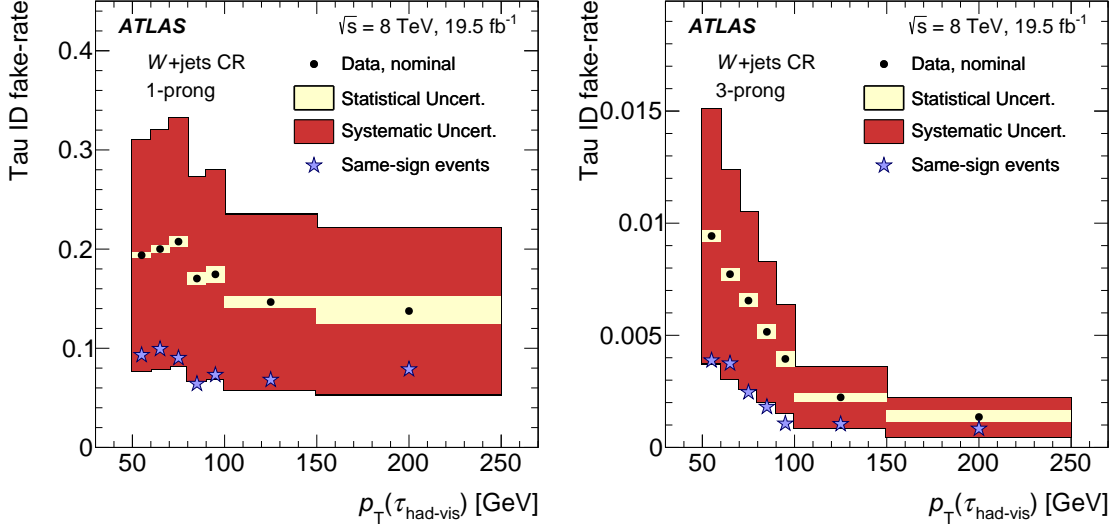


Figure 3. Tau identification fake-rate measured in $W(\rightarrow \mu\nu)+\text{jets}$ data events for the BDT loose identification working point for (left) 1-prong and (right) 3-prong tau candidates. The fake-rate is parameterised in the charge product of the muon and fake tau candidate. Opposite-sign events are depicted by black circles and same-sign events by blue stars. The systematic uncertainty covers differences due to jet composition and is added to the statistical uncertainty in quadrature.

scale, PDF and α_s variations. A 6% uncertainty on the $W+\text{jets}$ normalisation is derived from comparisons to data in the $W+\text{jets}$ control region used to measure jet-to-tau fake-rates in the $\tau_{\text{had}}\tau_{\text{had}}$ channel. For $t\bar{t}$ and single-top-quark production, the uncertainties from variations in the renormalisation and factorisation scales are in the range of 3–6% [57, 79, 80], while those related to the proton PDFs amount to 8% [48, 51, 81–83].

The uncertainty on the integrated luminosity is 2.8%. It is derived from a preliminary calibration of the luminosity scale derived from beam-separation scans performed in November 2012, following the same methodology as that detailed in ref. [84]. Comparisons of the efficiency of the hadronic tau trigger measured in data and in simulation are used to derive an uncertainty of 10% on the trigger efficiency. Differences between data and simulation in the reconstruction and identification efficiency and the energy scale of hadronic tau decays are taken into account. The associated uncertainties for muons and electrons are negligible for this analysis.

The systematic uncertainty on the identification efficiency of hadronic tau decays is estimated at low p_T from data samples enriched in $Z \rightarrow \tau\tau$ events, yielding an uncertainty of 2–7% depending on the number of tracks and $|\eta|$ of the tau candidate. At high p_T , there are no abundant sources of real hadronic tau decays from which an efficiency measurement could be made. Rather, the tau identification is studied in high- p_T dijet events as a function of the jet p_T , which indicates that there is no degradation in the modelling of the detector response as a function of the p_T of tau candidates. Based on the limited precision of these studies, an additional uncertainty of $14\% \cdot p_T/\text{TeV}$ for 1-prong tau candidates and $8\% \cdot p_T/\text{TeV}$ for 3-prong tau candidates is added in quadrature to the low- p_T uncertainty

for candidates with $p_T > 100$ GeV. The reconstruction efficiency for 3-prong tau candidates decreases at high p_T due to track merging. An uncertainty of $50\% \cdot p_T/\text{TeV}$ above $p_T = 150$ GeV is assigned for 3-prong candidates, derived from data/MC comparisons of tracking performance within jets. The energy scale uncertainty for hadronic tau decays and jets is evaluated based on the single-hadron response in the calorimeters [66, 69]. In addition, the tau energy scale is validated in data samples enriched in $Z \rightarrow \tau\tau$ events. The systematic uncertainty related to the tau energy scale is a function of η , p_T and the number of prongs, and is generally near 3%. Energy scale and resolution uncertainties for all objects are propagated to the E_T^{miss} calculation. The uncertainty on the E_T^{miss} due to clusters that do not belong to any reconstructed object has a minor effect.

Table 2 summarises the systematic uncertainties across all channels for the 1750 GeV Z'_{SSM} mass point. In the $\tau_{\text{had}}\tau_{\text{had}}$ channel the dominant uncertainties on both the signal and background come from the tau efficiency and energy scale, while in the $\tau_{\text{lep}}\tau_{\text{had}}$ channels the statistical uncertainty on the background coming from the fake-factor estimate also makes a major contribution. The uncertainties are the same for background and similar for the signal for all higher signal mass points, since the same m_T^{tot} thresholds are used. The uncertainties for the lower mass points are typically very similar, except for the tau ID efficiency, the 3-prong tau reconstruction efficiency, the Z/γ^* cross section and the statistical uncertainties, which are all a few percent lower, and the uncertainty on the tau energy scale for the signal, which can be up to 11% at low mass since the m_T^{tot} requirement is much tighter relative to the Z' mass. The small data-driven uncertainty contribution to the signal in the $\tau_{\text{had}}\tau_{\text{had}}$ channel comes from jets that are misidentified as hadronic tau decays.

Uncertainty [%]	Signal			Background		
	$\tau_{\text{had}}\tau_{\text{had}}$	$\tau_{\mu}\tau_{\text{had}}$	$\tau_e\tau_{\text{had}}$	$\tau_{\text{had}}\tau_{\text{had}}$	$\tau_{\mu}\tau_{\text{had}}$	$\tau_e\tau_{\text{had}}$
Statistical uncertainty	2.4	4	4	6	21	21
Efficiency	16	8	8	12	5	4
Energy scale and resolution	2.9	5	5	10	11	9
Theory cross section	–	–	–	6	6	6
Luminosity	2.8	2.8	2.8	2.5	2.2	1.9
Data-driven methods	0.2	–	–	2.7	8	12
Total	17	11	10	18	27	28

Table 2. Uncertainties on the estimated Z'_{SSM} contribution ($m_{Z'_{\text{SSM}}} = 1750$ GeV) and the corresponding total background contribution in percent for each channel. A dash denotes that the uncertainty is not applicable. The statistical uncertainty corresponds to the uncertainty due to the limited size of the samples produced via simulation or selected in control regions. The total consists of all uncertainties added in quadrature.

8 Z' signal models

In this section, the impact on the signal acceptance times efficiency from altering the Z' couplings and from including interference between Z' and Z/γ^* is discussed. The accep-

tance times efficiency for a given Z' model is defined as:

$$\mathcal{A}\varepsilon = \frac{N_S}{\mathcal{L}_{\text{int}} \cdot \sigma\mathcal{B}}$$

where N_S is the expected number of Z' events passing the full analysis selection, $\sigma\mathcal{B}$ is the Z' production cross section times $\tau^+\tau^-$ branching fraction and \mathcal{L}_{int} is the integrated luminosity. The impact on $\mathcal{A}\varepsilon$ is presented as a fraction of the SSM value, $\mathcal{A}\varepsilon_{\text{SSM}}$. The corresponding impact on the acceptance alone, \mathcal{A} , is also evaluated by replacing N_S with the expected number of Z' events after applying the kinematic selection directly to the generated particles before simulation. A Z' model that couples preferentially to third-generation fermions is also discussed.

8.1 Z' signal acceptance

Changing the fermionic couplings of the Z' from their SSM values can alter the signal acceptance of the analysis. Such changes are primarily due to alterations in either the tau polarisation or the total Z' decay width. Alteration of the tau polarisation changes the tau decay kinematics. Most importantly it affects the visible momentum fraction, which enters the analysis through the p_T thresholds of the reconstructed visible tau decay products and via the threshold on m_T^{tot} . The most extreme impact on the acceptance is seen for models that couple only to left-handed or right-handed tau leptons: Z'_L and Z'_R , respectively. Alteration of the quark couplings can impact the acceptance if it alters the tau polarisation. However, the maximum impact is much smaller than when altering the couplings to tau leptons. As the kinematic limit (due to the collision energy) for high-mass Z' production is approached, the signal exhibits an increased fraction of low-mass off-shell production. The fraction of off-shell events increases rapidly as a function of the decay width. Figure 4 shows $\mathcal{A}\varepsilon$ for the Z'_L and Z'_R models, and two models with artificially altered decay widths: Z'_{narrow} ($\Gamma/m_{Z'} = 1\%$) and Z'_{wide} ($\Gamma/m_{Z'} = 20\%$), each divided by $\mathcal{A}\varepsilon$ for Z'_{SSM} ($\Gamma/m_{Z'} \approx 3\%$). Interference between Z' and Z/γ^* is not included. The statistical uncertainty is typically below 5% but can be up to 14% at low mass. A smoothing is applied to reduce fluctuations. For Z'_L and Z'_R , the largest impact is observed at low mass, where the p_T and m_T^{tot} thresholds are much more stringent on the signal. In this case, alteration of the tau couplings can lead to changes of up to +50% and -25%. The impact on the $\tau_{\text{had}}\tau_{\text{had}}$ and $\tau_{\text{lep}}\tau_{\text{had}}$ channels are different due to the different effect of polarisation on leptonic and hadronic tau decays. For Z'_{narrow} and Z'_{wide} , the impact is most prominent at high mass where changes of up to +20% and -45% are observed. At low mass, $\mathcal{A}\varepsilon$ only changes for widths above 10%. The impact is the same for all channels. For all Z' models, the change in \mathcal{A} is very similar to that in $\mathcal{A}\varepsilon$, indicating that the efficiency is insensitive to changes in the Z' couplings.

The impact of interference between Z' and Z/γ^* is typically small. For the SSM, it leads to a reduction in the expected Z' contribution of up to 10% for $m_{Z'} \leq 2$ TeV, and up to 35% for the highest mass hypotheses. For Z'_L , Z'_R and Z'_{narrow} the impact is negligible. For Z'_{wide} the impact can be substantial and is highly dependent on the choice of the fermionic couplings. An exhaustive treatment is outside the scope of this

article. Reinterpretations of the SSM results for models with large widths should specifically calculate the impact from interference.

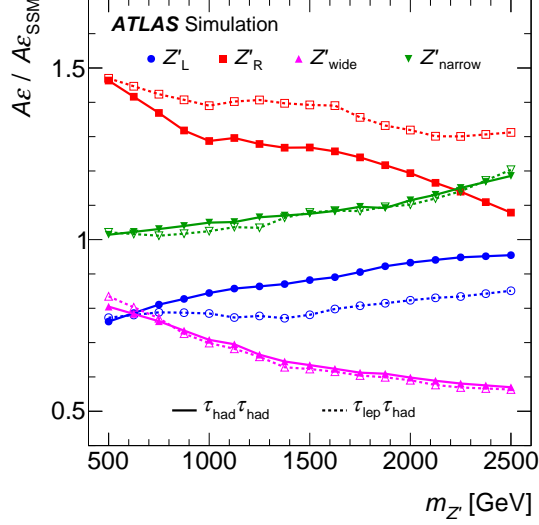


Figure 4. Signal acceptance times efficiency for Z'_L , Z'_R , Z'_{narrow} and Z'_{wide} divided by the acceptance times efficiency for Z'_{SSM} as a function of $m_{Z'}$, separately for the $\tau_{\text{had}}\tau_{\text{had}}$ (solid lines with filled markers) and $\tau_{\text{lep}}\tau_{\text{had}}$ (dashed lines with empty markers) channels. The statistical uncertainty is typically below 5% but can increase to 14% at low mass.

8.2 Non-universal $G(221)$ model

The non-universal $G(221)$ model [8, 20, 21] (also known by other names such as *Topflavor*) is an extension of the SM, containing additional heavy gauge bosons, Z'_{NU} and W'^{\pm}_{NU} , that may couple preferentially to third-generation fermions. The model is motivated by the idea that the large mass of the top-quark may suggest that the third fermion generation has a dynamical behaviour different from the first two generations. Accordingly, the SM weak $SU(2)$ gauge group is split into two parts: one coupling to *light* fermions (the first two generations), $SU(2)_{\text{l}}$ and one coupling to *heavy* fermions (the third generation), $SU(2)_{\text{h}}$. The extended gauge group breaks to the SM $SU(2)_{\text{l+h}}$ at a high energy scale, u , and then eventually to $U(1)_{\text{EM}}$ at the usual electroweak scale, $v = 246$ GeV:

$$SU(2)_{\text{l}} \times SU(2)_{\text{h}} \times U(1)_Y \xrightarrow{u} SU(2)_{\text{l+h}} \times U(1)_Y \xrightarrow{v} U(1)_{\text{EM}}.$$

The mixing between $SU(2)_{\text{l}}$ and $SU(2)_{\text{h}}$ is described by the parameter $\sin^2 \phi$. The Z'_{NU} and W'^{\pm}_{NU} bosons are degenerate in mass; the mass is defined at tree level by $\sin^2 \phi$ and u . Large mixing between τ and μ leptons has been considered as an additional feature of the model, but is ignored here as it would lead to stronger limits via the dielectron and dimuon searches. The Z'_{NU} couples almost exclusively to left-handed fermions, and while the coupling strength differs for light and heavy fermions, it is largely insensitive to the electric charge or weak isospin, leading to almost universal couplings for all light and heavy fermions.

Figure 5(left) shows the Z'_{NU} cross section times $\tau^+\tau^-$ branching fraction, $\sigma\mathcal{B}_{\text{NU}}$, divided by $\sigma\mathcal{B}_{\text{SSM}}$. For much of the parameter space $\sigma\mathcal{B}_{\text{NU}}$ is larger than $\sigma\mathcal{B}_{\text{SSM}}$, peaking at moderate values of $\sin^2\phi$. For extreme values of $\sin^2\phi$ either the cross section is suppressed by weakened couplings to light quarks ($\sin^2\phi \sim 0$) or the branching fraction is suppressed by weakened couplings to tau leptons ($\sin^2\phi \sim 1$). Figures 5(middle) and 5(right) show the Z'_{NU} acceptance times efficiency, $\mathcal{A}\varepsilon_{\text{NU}}$, divided by $\mathcal{A}\varepsilon_{\text{SSM}}$, for the $\tau_{\text{had}}\tau_{\text{had}}$ and $\tau_{\text{lep}}\tau_{\text{had}}$ channels, respectively. In general $\mathcal{A}\varepsilon_{\text{NU}}$ is lower than $\mathcal{A}\varepsilon_{\text{SSM}}$. At low mass this is mainly due to the left-handed couplings, which result in softer visible tau decays. Near $\sin^2\phi \sim 0$ and $\sin^2\phi \sim 1$, the acceptance loss comes mainly from the significantly increased decay width, which causes a large fraction of the signal to be produced off shell.

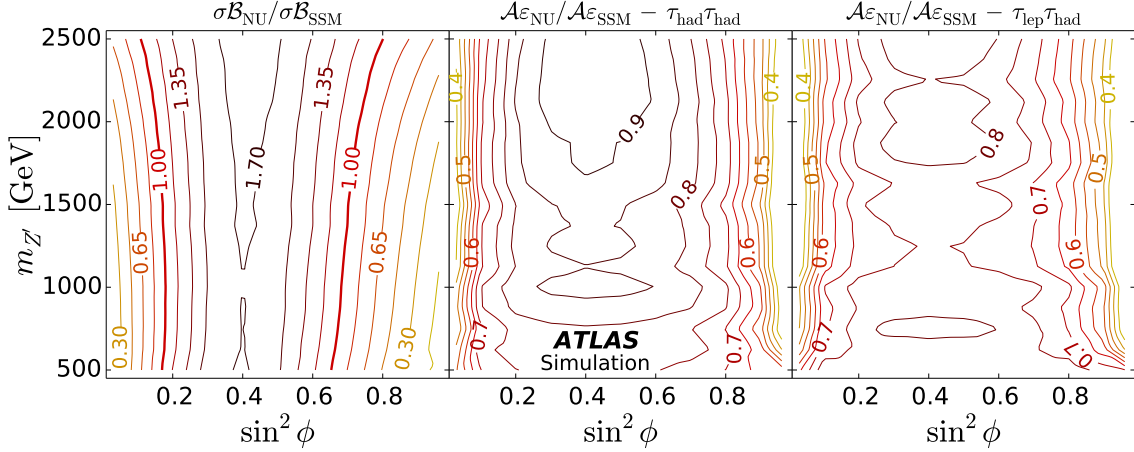


Figure 5. Signal production cross section times $\tau^+\tau^-$ branching fraction for Z'_{NU} , $\sigma\mathcal{B}_{\text{NU}}$, divided by $\sigma\mathcal{B}_{\text{SSM}}$ (left) and acceptance times efficiency for Z'_{NU} , $\mathcal{A}\varepsilon_{\text{NU}}$, divided by $\mathcal{A}\varepsilon_{\text{SSM}}$ for the (middle) $\tau_{\text{had}}\tau_{\text{had}}$ and (right) $\tau_{\text{lep}}\tau_{\text{had}}$ channels, as a function of $\sin^2\phi$ and $m_{Z'}$.

9 Results and discussion

A summary of the expected number of events remaining after successively applying each selection requirement, up to the $m_{\text{T}}^{\text{tot}}$ threshold, for the signal and dominant background processes is given in table 3. Figures 6(left) and 6(right) show the $m_{\text{T}}^{\text{tot}}$ distribution after event selection in the $\tau_{\text{had}}\tau_{\text{had}}$ and $\tau_{\text{lep}}\tau_{\text{had}}$ channels, respectively. The numbers of observed and expected events (including their total uncertainties) after applying the $m_{\text{T}}^{\text{tot}}$ thresholds in all channels are summarised in table 4. In all cases, the number of observed events is consistent with the expected Standard Model background. Therefore, upper limits are set on the production of a high-mass resonance decaying to $\tau^+\tau^-$ pairs. The acceptance and acceptance times efficiency for Z'_{SSM} is shown in figure 7.

The statistical combination of the channels employs a likelihood function constructed as the product of Poisson-distributed random numbers describing the total number of events observed in each channel. The probability in each channel is evaluated for the observed number of data events given the signal-plus-background expectation. Systematic

	$Z/\gamma^* \rightarrow \tau\tau$	$\tau_{\text{had}}\tau_{\text{had}}$ channel			Z'_{SSM}
		Multijet	$W/Z/\gamma^* + \text{jets}$	Top + diboson	
Preselection	276(18)	611(5)	64(1)	24(2)	10.1(2)
OS	270(18)	316(4)	53(1)	21(2)	9.5(2)
$\Delta\phi(\tau_1, \tau_2) > 2.7$	117(2)	209(3)	35(1)	11(2)	9.2(2)

	$Z/\gamma^* \rightarrow \tau\tau$	$\tau_{\text{lep}}\tau_{\text{had}}$ channel			Z'_{SSM}
		Jet $\rightarrow \tau$ fake	$Z/\gamma^* \rightarrow \ell\ell$	Top + diboson	
Preselection	46 800(300)	154 670(130)	17 340(250)	12 330(70)	14.3(2)
OS	46 300(300)	111 270(120)	16 180(240)	11 830(70)	13.9(2)
$\Delta\phi(\ell, \tau) > 2.7$	32 200(300)	47 650(80)	12 490(210)	3530(40)	13.5(2)
$m_T < 50$ GeV	29 490(230)	22 660(60)	11 240(210)	808(16)	8.5(2)

Table 3. Number of expected signal ($m_{Z'_{\text{SSM}}} = 1750$ GeV) and background events in the $\tau_{\text{had}}\tau_{\text{had}}$ and $\tau_{\text{lep}}\tau_{\text{had}}$ channels after successively applying each selection criterion. The statistical uncertainty in the least significant digit(s) is shown in parentheses.

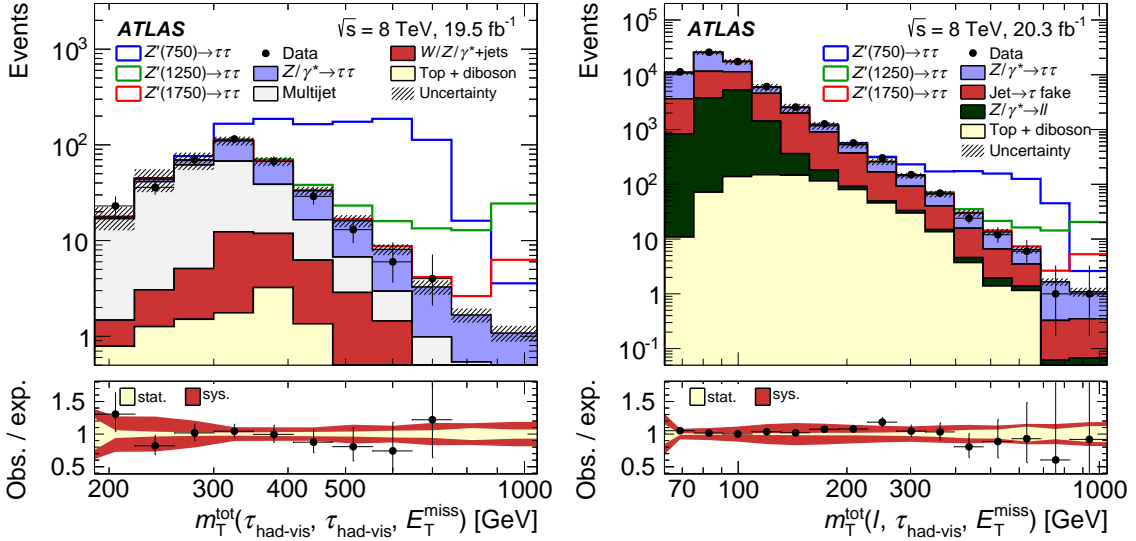


Figure 6. The m_T^{tot} distribution after event selection in the (left) $\tau_{\text{had}}\tau_{\text{had}}$ and (right) $\tau_{\text{lep}}\tau_{\text{had}}$ channels. The estimated contributions from SM processes are stacked and appear in the same order as in the legend. The expected contributions from three Z'_{SSM} signals with masses of 750, 1250 and 1750 GeV are shown, stacked on the total SM expectation. The events observed in data are overlaid. The hatched area indicates the uncertainty on the total estimated background. The bins have a constant width of (left) 0.153 and (right) 0.184 in $\log(m_T^{\text{tot}})$. The last bin includes overflow events. The inset shows the ratio of the observed events over the total expected SM contribution. The statistical uncertainty from the observed events and the expected SM contribution are shown on the points and by the yellow band, respectively. The red band depicts the total systematic and statistical uncertainties on the SM contribution added in quadrature.

uncertainties on the expected number of events are incorporated into the likelihood via nuisance parameters constrained by Gaussian distributions. Correlations between signal and background and across channels are taken into account. A signal-strength parameter

$m_{Z'}$ [GeV]	m_T^{tot}	$\tau_{\text{had}}\tau_{\text{had}}$			$\tau_{\text{lep}}\tau_{\text{had}}$		
		N_S	N_B	N	N_S	N_B	N
500	400	1030(170)	70(8)	56	570(90)	49(6)	42
625	450	650(100)	40(5)	30	420(50)	29(4)	23
750	500	410(60)	24.0(30)	18	270(29)	18.2(23)	15
875	550	206(30)	14.6(20)	11	152(14)	11.2(16)	10
1000	600	119(17)	9.4(13)	4	82(8)	6.7(11)	6
1125	700	60(9)	4.0(6)	0	45(5)	2.5(4)	2
1250	750	35(6)	2.8(5)	0	27.0(29)	1.78(32)	1
1375	800	20.8(34)	1.93(32)	0	15.7(16)	1.24(23)	1
1500	850	13.4(22)	1.32(24)	0	9.6(10)	0.96(20)	1
1625	850	8.4(14)	1.32(24)	0	6.5(7)	0.96(20)	1
1750	850	5.4(9)	1.32(24)	0	4.0(4)	0.96(20)	1
1875	850	3.6(6)	1.32(24)	0	2.70(27)	0.96(20)	1
2000	850	2.4(4)	1.32(24)	0	1.85(18)	0.96(20)	1
2125	850	1.54(28)	1.32(24)	0	1.19(12)	0.96(20)	1
2250	850	1.02(19)	1.32(24)	0	0.81(8)	0.96(20)	1
2375	850	0.66(12)	1.32(24)	0	0.52(5)	0.96(20)	1
2500	850	0.43(8)	1.32(24)	0	0.330(34)	0.96(20)	1

Table 4. Number of expected Z'_{SSM} signal (N_S), background (N_B) and observed (N) events in the $\tau_{\text{had}}\tau_{\text{had}}$ and $\tau_{\text{lep}}\tau_{\text{had}}$ channels. The signal mass ($m_{Z'}$) and corresponding m_T^{tot} thresholds are given in units of GeV. The total uncertainty (statistical and systematic added in quadrature) in the least significant digit(s) is shown in parentheses.

multiplies the expected signal in each channel, for which a positive uniform prior probability distribution is assumed. Theoretical uncertainties on the signal cross section are not included in the calculation of the experimental limit as they are model dependent.

Bayesian 95% credibility upper limits are set on $\sigma\mathcal{B}_{\text{SSM}}$ as a function of $m_{Z'}$, using the Bayesian Analysis Toolkit [85]. Figures 8(left) and 8(right) show the limits for the individual channels and for the combination, respectively. The resulting 95% CL lower limit on the mass of a Z'_{SSM} decaying to $\tau^+\tau^-$ pairs is 2.02 TeV, with an expected limit of 1.95 TeV. The observed and expected limits in the individual channels are, respectively: 1.89 and 1.80 TeV ($\tau_{\text{had}}\tau_{\text{had}}$); 1.59 and 1.59 TeV ($\tau_{\mu}\tau_{\text{had}}$); and 1.55 and 1.65 TeV ($\tau_e\tau_{\text{had}}$). Alteration of the Z' couplings can impact the signal acceptance as described in section 8.1. These changes translate linearly to the limits on $\sigma\mathcal{B}_{\text{SSM}}$. Limits on the Z'_L and Z'_R models are shown in figure 8 (right). The impact of the choice of the prior on the signal-strength parameter is evaluated by also considering the *reference prior* [86]. Use of the reference prior improves the limit on $\sigma\mathcal{B}_{\text{SSM}}$ by a maximum of 10%, corresponding to an increase of 20 GeV in the observed mass limit.

Limits on the non-universal $G(221)$ model are also calculated. The signal contributions in the $\tau_{\text{had}}\tau_{\text{had}}$ and $\tau_{\text{lep}}\tau_{\text{had}}$ channels are rescaled by $\sigma\mathcal{B}_{\text{NU}}/\sigma\mathcal{B}_{\text{SSM}} \cdot \mathcal{A}_{\text{NU}}/\mathcal{A}_{\text{SSM}}$ (as derived

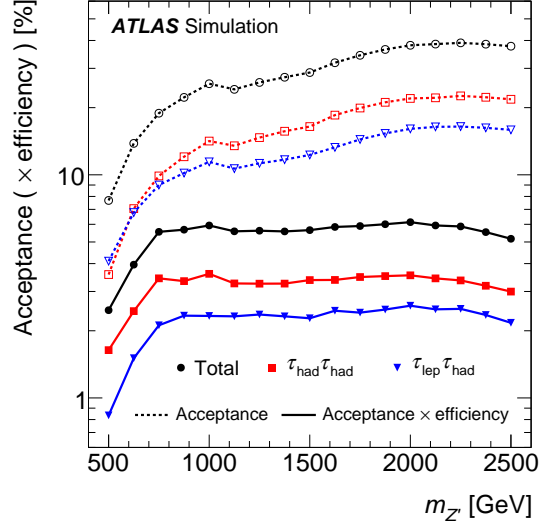


Figure 7. Acceptance (dashed lines with empty markers) and acceptance times efficiency (solid lines with filled markers) for Z'_{SSM} as a function of the Z'_{SSM} mass. Contributions from the individual channels and the full analysis are given.

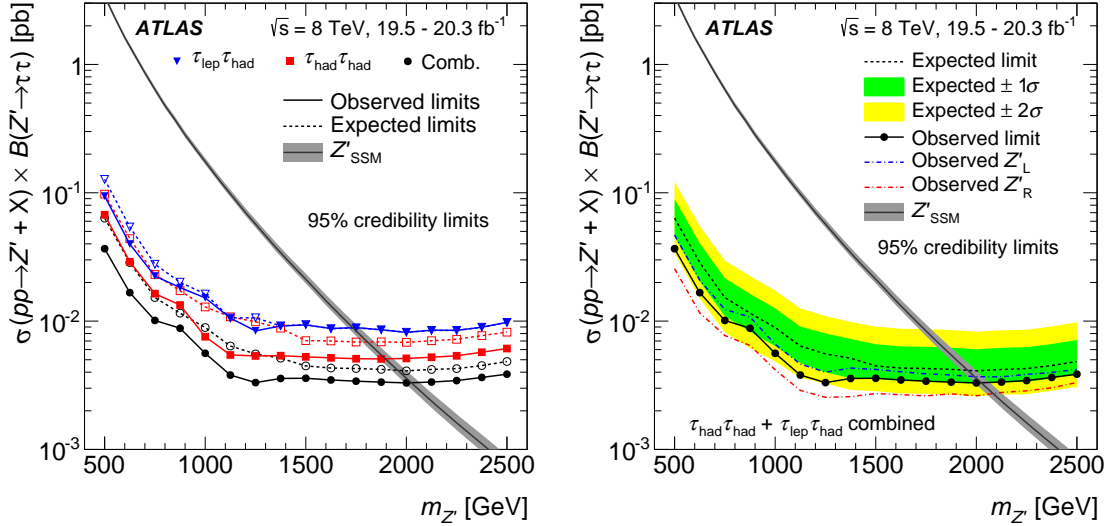


Figure 8. Bayesian 95% credibility upper limits on the cross section times ditau branching fraction for a Z' in the Sequential Standard Model. The figure shows (left) an overlay of the observed (solid lines with filled markers) and expected (dashed lines with empty markers) limits in each channel and for the combination, and (right) the combined limit with 1σ and 2σ uncertainty bands and an overlay of the impact of the Z'_L/Z'_R models. The width of the Z'_{SSM} theory band represents the theoretical uncertainty from the PDF error set, the choice of PDF as well as the strong coupling constant.

in section 8.2). In addition, the systematic uncertainties are re-evaluated for each point in parameter space. Figure 9 shows the region in the Z'_{NU} parameter space excluded at 95% credibility: Z'_{NU} bosons with masses below 1.3–2.1 TeV are excluded in the range

$0.03 < \sin^2 \phi < 0.5$ assuming no μ - τ mixing. Indirect limits are also overlaid.

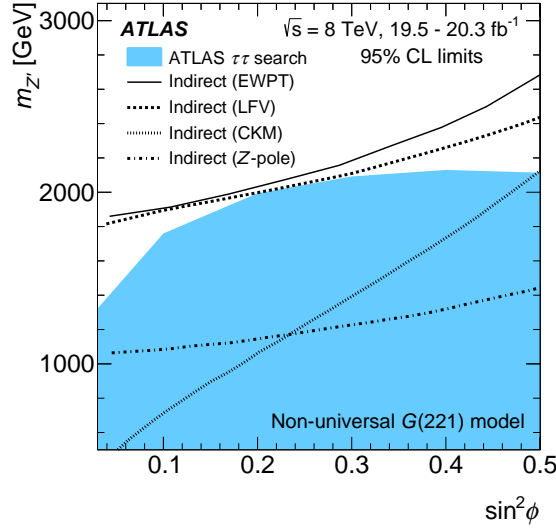


Figure 9. Observed 95% CL exclusion in the non-universal $G(221)$ parameter space from the combination of the $\tau_{\text{had}}\tau_{\text{had}}$ and $\tau_{\text{lep}}\tau_{\text{had}}$ channels (blue). Indirect limits at 95% CL from fits to electroweak precision measurements (EWPT) [27], lepton flavour violation (LFV) [28], CKM unitarity [29] and the original Z -pole data [8] are overlaid.

10 Conclusion

A search for high-mass ditau resonances was performed using $19.5\text{--}20.3\text{ fb}^{-1}$ of data collected with the ATLAS detector in pp collisions at $\sqrt{s} = 8\text{ TeV}$ at the LHC. The $\tau_{\text{had}}\tau_{\text{had}}$, $\tau_{\mu}\tau_{\text{had}}$ and $\tau_e\tau_{\text{had}}$ channels are analysed. The observed number of events in regions with high total transverse mass are consistent with the SM expectations. Limits are set on the cross section times branching fraction for such resonances. The resulting lower limit on the mass of a Z' decaying to $\tau^+\tau^-$ in the Sequential Standard Model is 2.02 TeV at 95% credibility, in agreement with the expected limit of 1.95 TeV in the absence of a signal. The impact on the Z' acceptance from altering the Z' couplings and the total decay width is found to be significant, and can be up to 50%. The impact from interference between Z' and Z/γ^* is only important when the total decay width of the Z' is large. Limits on the non-universal $G(221)$ model are also established, where Z' bosons with masses below $1.3\text{--}2.1\text{ TeV}$ are excluded in the range $0.03 < \sin^2 \phi < 0.5$ assuming no μ - τ mixing.

Acknowledgements

We thank CERN for the very successful operation of the LHC, as well as the support staff from our institutions without whom ATLAS could not be operated efficiently.

We acknowledge the support of ANPCyT, Argentina; YerPhI, Armenia; ARC, Australia; BMWFW and FWF, Austria; ANAS, Azerbaijan; SSTC, Belarus; CNPq and FAPESP, Brazil; NSERC, NRC and CFI, Canada; CERN; CONICYT, Chile; CAS, MOST

and NSFC, China; COLCIENCIAS, Colombia; MSMT CR, MPO CR and VSC CR, Czech Republic; DNRF, DNSRC and Lundbeck Foundation, Denmark; EPLANET, ERC and NSRF, European Union; IN2P3-CNRS, CEA-DSM/IRFU, France; GNSF, Georgia; BMBF, DFG, HGF, MPG and AvH Foundation, Germany; GSRT and NSRF, Greece; RGC, Hong Kong SAR, China; ISF, MINERVA, GIF, I-CORE and Benoziyo Center, Israel; INFN, Italy; MEXT and JSPS, Japan; CNRST, Morocco; FOM and NWO, Netherlands; BRF and RCN, Norway; MNiSW and NCN, Poland; GRICES and FCT, Portugal; MNE/IFA, Romania; MES of Russia and NRC KI, Russian Federation; JINR; MSTĐ, Serbia; MSSR, Slovakia; ARRS and MIZŠ, Slovenia; DST/NRF, South Africa; MINECO, Spain; SRC and Wallenberg Foundation, Sweden; SER, SNSF and Cantons of Bern and Geneva, Switzerland; NSC, Taiwan; TAEK, Turkey; STFC, the Royal Society and Leverhulme Trust, United Kingdom; DOE and NSF, United States of America.

The crucial computing support from all WLCG partners is acknowledged gratefully, in particular from CERN and the ATLAS Tier-1 facilities at TRIUMF (Canada), NDGF (Denmark, Norway, Sweden), CC-IN2P3 (France), KIT/GridKA (Germany), INFN-CNAF (Italy), NL-T1 (Netherlands), PIC (Spain), ASGC (Taiwan), RAL (UK) and BNL (USA) and in the Tier-2 facilities worldwide.

References

- [1] J. L. Hewett and T. G. Rizzo, *Low-energy phenomenology of superstring-inspired E_6 models*, *Phys. Rept.* **183** (1989) 193–381.
- [2] M. Cvetič and S. Godfrey, *Discovery and identification of extra gauge bosons*, [hep-ph/9504216](#).
- [3] A. Leike, *The Phenomenology of extra neutral gauge bosons*, *Phys. Rept.* **317** (1999) 143–250, [[hep-ph/9805494](#)].
- [4] T. G. Rizzo, *Z' phenomenology and the LHC*, [hep-ph/0610104](#). In Proceedings of Theoretical Advanced Study Institute in Elementary Particle Physics: Exploring New Frontiers Using Colliders and Neutrinos (TASI 2006), World Scientific Publishing, 2008, 537–575.
- [5] R. Diener, S. Godfrey, and T. A. Martin, *Unravelling an Extra Neutral Gauge Boson at the LHC using Third Generation Fermions*, *Phys. Rev. D* **83** (2011) 115008, [[arXiv:1006.2845](#)].
- [6] P. Langacker, *The Physics of Heavy Z' Gauge Bosons*, *Rev. Mod. Phys.* **81** (2009) 1199–1228, [[arXiv:0801.1345](#)].
- [7] K. R. Lynch, E. H. Simmons, M. Narain, and S. Mrenna, *Finding Z' bosons coupled preferentially to the third family at CERN-LEP and the Tevatron*, *Phys. Rev. D* **63** (2001) 035006, [[hep-ph/0007286](#)].
- [8] E. Malkawi, T. M. P. Tait, and C.-P. Yuan, *A model of strong flavor dynamics for the top quark*, *Phys. Lett. B* **385** (1996) 304–310, [[hep-ph/9603349](#)].
- [9] H. D. Kim, S.-G. Kim, and S. Shin, *$D0$ dimuon charge asymmetry from B_s system with Z' couplings and the recent LHCb result*, *Phys. Rev. D* **88** (2013) 015005, [[arXiv:1205.6481](#)].
- [10] D0 Collaboration, V. M. Abazov, et al., *Measurement of the anomalous like-sign dimuon charge asymmetry with 9 fb^{-1} of $p\bar{p}$ collisions*, *Phys. Rev. D* **84** (2011) 052007, [[arXiv:1106.6308](#)].

- [11] X.-G. He and G. Valencia, *B decays with τ leptons in nonuniversal left-right models*, *Phys. Rev. D* **87** (2013) 014014, [[arXiv:1211.0348](#)].
- [12] Belle Collaboration, A. Bozek, et al., *Observation of $B^+ \rightarrow \bar{D}^{*0} \tau^+ \nu_\tau$ and Evidence for $B^+ \rightarrow \bar{D}^0 \tau^+ \nu_\tau$ at Belle*, *Phys. Rev. D* **82** (2010) 072005, [[arXiv:1005.2302](#)].
- [13] BaBar Collaboration, J. Lees, et al., *Evidence for an excess of $\bar{B} \rightarrow D^{(*)} \tau^- \bar{\nu}_\tau$ decays*, *Phys. Rev. Lett.* **109** (2012) 101802, [[arXiv:1205.5442](#)].
- [14] E. Dudas, C. Petersson, and R. Torre, *Collider signatures of low scale supersymmetry breaking: A Snowmass 2013 White Paper*, [arXiv:1309.1179](#).
- [15] C. Petersson, A. Romagnoni, and R. Torre, *Liberating Higgs couplings in supersymmetry*, *Phys. Rev. D* **87** (2013) 013008, [[arXiv:1211.2114](#)].
- [16] V. Barger, D. Marfatia, and A. Peterson, *LHC and dark matter signals of Z' bosons*, *Phys. Rev. D* **87** (2013) 015026, [[arXiv:1206.6649](#)].
- [17] A. Hayreter and G. Valencia, *Constraining τ -lepton dipole moments and gluon couplings at the LHC*, *Phys. Rev. D* **88** (2013) 013015, [[arXiv:1305.6833](#)].
- [18] L. Evans and P. Bryant, *LHC Machine*, *JINST* **3** (2008) S08001.
- [19] ATLAS Collaboration, *The ATLAS Experiment at the CERN Large Hadron Collider*, *JINST* **3** (2008) S08003.
- [20] D. J. Muller and S. Nandi, *Topflavor: a separate $SU(2)$ for the third family*, *Phys. Lett. B* **383** (1996) 345–350, [[hep-ph/9602390](#)].
- [21] K. Hsieh, K. Schmitz, J.-H. Yu, and C.-P. Yuan, *Global analysis of general $SU(2) \times SU(2) \times U(1)$ models with precision data*, *Phys. Rev. D* **82** (2010) 035011, [[arXiv:1003.3482](#)].
- [22] ATLAS Collaboration, *A search for high-mass resonances decaying to $\tau^+ \tau^-$ in pp collisions at $\sqrt{s} = 7$ TeV with the ATLAS detector*, *Phys. Lett. B* **719** (2013) 242–260, [[arXiv:1210.6604](#)].
- [23] CMS Collaboration, *Search for high-mass resonances decaying into τ -lepton pairs in pp collisions at $\sqrt{s} = 7$ TeV*, *Phys. Lett. B* **716** (2012) 82, [[arXiv:1206.1725](#)].
- [24] ATLAS Collaboration, *Search for high-mass dilepton resonances in pp collisions at $\sqrt{s} = 8$ TeV with the ATLAS detector*, *Phys. Rev. D* **90** (2014) 052005, [[arXiv:1405.4123](#)].
- [25] CMS Collaboration, *Search for physics beyond the standard model in dilepton mass spectra in proton-proton collisions at $\sqrt{s} = 8$ TeV*, [arXiv:1412.6302](#).
- [26] R. S. Chivukula and E. H. Simmons, *Electroweak limits on nonuniversal Z' bosons*, *Phys. Rev. D* **66** (2002) 015006, [[hep-ph/0205064](#)].
- [27] Q.-H. Cao, Z. Li, J.-H. Yu, and C.-P. Yuan, *Discovery and identification of W' and Z' in $SU(2)_1 \otimes SU(2)_2 \otimes U(1)_X$ models at the LHC*, *Phys. Rev. D* **86** (2012) 095010, [[arXiv:1205.3769](#)].
- [28] K. Y. Lee, *Lepton flavor violation in a nonuniversal gauge interaction model*, *Phys. Rev. D* **82** (2010) 097701, [[arXiv:1009.0104](#)].
- [29] K. Y. Lee, *Unitarity violation of the CKM matrix in a nonuniversal gauge interaction model*, *Phys. Rev. D* **71** (2005) 115008, [[hep-ph/0410381](#)].

- [30] ATLAS Collaboration, *Performance of the ATLAS Trigger System in 2010*, *Eur. Phys. J. C* **72** (2012) 1849, [[arXiv:1110.1530](#)].
- [31] T. Sjöstrand, S. Mrenna, and P. Skands, *A brief introduction to PYTHIA 8.1*, *Comput. Phys. Commun.* **178** (2008) 852–867, [[arXiv:0710.3820](#)].
- [32] T. Gleisberg et al., *Event generation with SHERPA 1.1*, *JHEP* **02** (2009) 7, [[arXiv:0811.4622](#)].
- [33] S. Frixione and B. R. Webber, *Matching NLO QCD computations and parton shower simulations*, *JHEP* **06** (2002) 29, [[hep-ph/0204244](#)].
- [34] S. Frixione, E. Laenen, P. Motylinski, and B. R. Webber, *Single-top production in MC@NLO*, *JHEP* **03** (2006) 92, [[hep-ph/0512250](#)].
- [35] S. Frixione, E. Laenen, P. Motylinski, C. White, and B. R. Webber, *Single-top hadroproduction in association with a W boson*, *JHEP* **07** (2008) 29, [[arXiv:0805.3067](#)].
- [36] B. P. Kersevan and E. Richter-Was, *The Monte Carlo Event Generator AcerMC 2.0 with Interfaces to PYTHIA 6.2 and HERWIG 6.5*, [hep-ph/0405247](#).
- [37] G. Corcella et al., *HERWIG 6: an event generator for hadron emission reactions with interfering gluons (including supersymmetric processes)*, *JHEP* **01** (2001) 10, [[hep-ph/0011363](#)].
- [38] P. Nason, *A New method for combining NLO QCD with shower Monte Carlo algorithms*, *JHEP* **11** (2004) 040, [[hep-ph/0409146](#)].
- [39] S. Frixione, P. Nason, and C. Oleari, *Matching NLO QCD computations with Parton Shower simulations: the POWHEG method*, *JHEP* **11** (2007) 070, [[arXiv:0709.2092](#)].
- [40] S. Alioli, P. Nason, C. Oleari, and E. Re, *A general framework for implementing NLO calculations in shower Monte Carlo programs: the POWHEG BOX*, *JHEP* **06** (2010) 043, [[arXiv:1002.2581](#)].
- [41] S. Alioli, P. Nason, C. Oleari, and E. Re, *NLO vector-boson production matched with shower in POWHEG*, *JHEP* **07** (2008) 060, [[arXiv:0805.4802](#)].
- [42] T. Sjöstrand, S. Mrenna, and P. Skands, *PYTHIA 6.4 physics and manual*, *JHEP* **05** (2006) 26, [[hep-ph/0603175](#)].
- [43] J. M. Butterworth, J. R. Forshaw, and M. H. Seymour, *Multiparton interactions in photoproduction at HERA*, *Z Phys. C* **72** (1996) 637–646, [[hep-ph/9601371](#)].
- [44] N. Davidson, G. Nanava, T. Przedziński, E. Richter-Was, and Z. Was, *Universal interface of TAUOLA: Technical and physics documentation*, *Comput. Phys. Commun.* **183** (2012) 821–843, [[arXiv:1002.0543](#)].
- [45] P. Ilten, *Tau Decays in Pythia 8*, *Nucl. Phys. B* **253** (2014) 255, [[arXiv:1211.6730](#)].
- [46] P. Golonka and Z. Was, *PHOTOS Monte Carlo: a precision tool for QED corrections in Z and W decays*, *Eur. Phys. J. C* **45** (2006) 97–107, [[hep-ph/0506026](#)].
- [47] P. M. Nadolsky et al., *Implications of CTEQ global analysis for collider observables*, *Phys. Rev. D* **78** (2008) 013004, [[arXiv:0802.0007](#)].
- [48] H.-L. Lai et al., *New parton distributions for collider physics*, *Phys. Rev. D* **82** (2010) 074024, [[arXiv:1007.2241](#)].

- [49] ATLAS Collaboration, *New ATLAS event generator tunes to 2010 data*, ATL-PHYS-PUB-2011-008. <http://cdsweb.cern.ch/record/1345343>.
- [50] Y. Li and F. Petriello, *Combining QCD and electroweak corrections to dilepton production in the framework of the FEWZ simulation code*, *Phys. Rev. D* **86** (2012) 094034, [[arXiv:1208.5967](#)].
- [51] A. D. Martin, W. J. Stirling, R. S. Thorne, and G. Watt, *Parton distributions for the LHC*, *Eur. Phys. J. C* **63** (2009) 189–285, [[arXiv:0901.0002](#)].
- [52] K. Melnikov and F. Petriello, *Electroweak gauge boson production at hadron colliders through $O(\alpha_s^2)$* , *Phys. Rev. D* **74** (2006) 114017, [[hep-ph/0609070](#)].
- [53] R. Gavin, Y. Li, F. Petriello, and S. Quackenbush, *FEWZ 2.0: A code for hadronic Z production at next-to-next-to-leading order*, *Comput. Phys. Commun.* **182** (2011) 2388–2403, [[arXiv:1011.3540](#)].
- [54] S. Moch and P. Uwer, *Theoretical status and prospects for top-quark pair production at hadron colliders*, *Phys. Rev. D* **78** (2008) 034003, [[arXiv:0804.1476](#)].
- [55] U. Langenfeld, S. Moch, and P. Uwer, *New results for $t\bar{t}$ production at hadron colliders*, [arXiv:0907.2527](#).
- [56] M. Aliev et al., *HATHOR - HAdronic Top and Heavy quarks crOss section calculatoR*, *Comput. Phys. Commun.* **182** (2011) 1034–1046, [[arXiv:1007.1327](#)].
- [57] N. Kidonakis, *Next-to-next-to-leading-order collinear and soft gluon corrections for t-channel single top quark production*, *Phys. Rev. D* **83** (2011) 091503, [[arXiv:1103.2792](#)].
- [58] N. Kidonakis, *Next-to-next-to-leading logarithm resummation for s-channel single top quark production*, *Phys. Rev. D* **81** (2010) 054028, [[arXiv:1001.5034](#)].
- [59] J. M. Campbell and R. K. Ellis, *Update on vector boson pair production at hadron colliders*, *Phys. Rev. D* **60** (1999) 113006, [[hep-ph/9905386](#)].
- [60] Z. Czyzula, T. Przedzinski, and Z. Was, *TauSpinner program for studies on spin effect in tau production at the LHC*, *Eur. Phys. J. C* **72** (2012) 1988, [[arXiv:1201.0117](#)].
- [61] A. Kaczmarska, J. Piatlicki, T. Przedzinski, E. Richter-Was, and Z. Was, *Application of TauSpinner for studies on tau-lepton polarization and spin correlations in Z, W and H decays at LHC*, [arXiv:1402.2068](#).
- [62] S. Banerjee, J. Kalinowski, W. Kotlarski, T. Przedzinski, and Z. Was, *Ascertaining the spin for new resonances decaying into $\tau^+\tau^-$ at hadron colliders*, *Eur. Phys. J. C* **73** (2013) 2313, [[arXiv:1212.2873](#)].
- [63] GEANT4 Collaboration, S. Agostinelli, et al., *Geant4 – a simulation toolkit*, *Nucl. Instr. and Meth. A* **506** (2003) 250 – 303.
- [64] ATLAS Collaboration, *The ATLAS Simulation Infrastructure*, *Eur. Phys. J. C* **70** (2010) 823–874, [[arXiv:1005.4568](#)].
- [65] ATLAS Collaboration, *ATLAS tunes of PYTHIA 6 and Pythia 8 for MC11*, ATL-PHYS-PUB-2011-009. <http://cdsweb.cern.ch/record/1363300>.
- [66] ATLAS Collaboration, *Identification and energy calibration of hadronically decaying tau leptons with the ATLAS experiment in pp collisions at $\sqrt{s} = 8$ TeV, submitted to Eur. Phys. J. C* (2014) [[arXiv:1412.7086](#)].

- [67] M. Cacciari, G. P. Salam, and G. Soyez, *The anti- k_t jet clustering algorithm*, *JHEP* **04** (2008) 063, [[arXiv:0802.1189](#)].
- [68] M. Cacciari and G. P. Salam, *Dispelling the N^3 myth for the k_t jet-finder*, *Phys. Lett. B* **641** (2006) 57–61, [[hep-ph/0512210](#)].
- [69] ATLAS Collaboration, *Jet energy measurement with the ATLAS detector in proton-proton collisions at $\sqrt{s} = 7$ TeV*, *Eur. Phys. J. C* **73** (2013) 2304, [[arXiv:1112.6426](#)].
- [70] ATLAS Collaboration, *Measurement of the muon reconstruction performance of the ATLAS detector using 2011 and 2012 LHC proton-proton collision data*, *Eur. Phys. J. C* **74** (2014) 3130, [[arXiv:1407.3935](#)].
- [71] ATLAS Collaboration, *Electron and photon energy calibration with the ATLAS detector using LHC Run 1 data*, *Eur. Phys. J. C* **74** (2014) 3071, [[arXiv:1407.5063](#)].
- [72] ATLAS Collaboration, *Improved electron reconstruction in ATLAS using the Gaussian Sum Filter-based model for bremsstrahlung*, ATLAS-CONF-2012-047. <https://cds.cern.ch/record/1449796>.
- [73] ATLAS Collaboration, *Electron efficiency measurements with the ATLAS detector using the 2012 LHC proton-proton collision data*, ATLAS-CONF-2014-032. <https://cds.cern.ch/record/1706245>.
- [74] ATLAS Collaboration, *Performance of missing transverse momentum reconstruction in proton-proton collisions at $\sqrt{s} = 7$ TeV with ATLAS*, *Eur. Phys. J. C* **72** (2012) 1844, [[arXiv:1108.5602](#)].
- [75] ATLAS Collaboration, *Measurement of the high-mass Drell–Yan differential cross-section in pp collisions at $\sqrt{s} = 7$ TeV with the ATLAS detector*, *Phys. Lett. B* **725** (2013) 223–242, [[arXiv:1305.4192](#)].
- [76] R. D. Ball et al., *Parton distributions with LHC data*, *Nucl. Phys. B* **867** (2013) 244–289, [[arXiv:1207.1303](#)].
- [77] S. Alekhin, J. Blumlein, and S. Moch, *Parton Distribution Functions and Benchmark Cross Sections at NNLO*, *Phys. Rev. D* **86** (2012) 054009, [[arXiv:1202.2281](#)].
- [78] H1 and ZEUS Collaborations, F. Aaron, et al., *Combined Measurement and QCD Analysis of the Inclusive $e^\pm p$ Scattering Cross Sections at HERA*, *JHEP* **01** (2010) 109, [[arXiv:0911.0884](#)].
- [79] S. Moch and P. Uwer, *Theoretical status and prospects for top-quark pair production at hadron colliders*, *Phys. Rev. D* **78** (2008) 034003, [[arXiv:0804.1476](#)].
- [80] M. Beneke, M. Czakon, P. Falgari, A. Mitov, and C. Schwinn, *Threshold expansion of the $gg(q\bar{q}) \rightarrow Q\bar{Q} + X$ cross section at $O(\alpha_s^4)$* , *Phys. Lett. B* **690** (2010) 483–490, [[arXiv:0911.5166](#)].
- [81] M. Botje et al., *The PDF4LHC Working Group Interim Recommendations*, [arXiv:1101.0538](#).
- [82] S. Alekhin et al., *The PDF4LHC Working Group Interim Report*, [arXiv:1101.0536](#).
- [83] NNPDF Collaboration, R. D. Ball, et al., *Impact of heavy quark masses on parton distributions and LHC phenomenology*, *Nucl. Phys. B* **849** (2011) 296–363, [[arXiv:1101.1300](#)].

- [84] ATLAS Collaboration, *Improved luminosity determination in pp collisions at $\sqrt{s} = 7$ TeV using the ATLAS detector at the LHC*, *Eur. Phys. J. C* **73** (2013) 2518, [[arXiv:1302.4393](#)].
- [85] A. Caldwell, D. Kollár, and K. Kröninger, *BAT - The Bayesian analysis toolkit*, *Comput. Phys. Commun.* **180** (2009) 2197–2209, [[arXiv:0808.2552](#)].
- [86] D. Casadei, *Reference analysis of the signal + background model in counting experiments*, *JINST* **7** (2012) 1012, [[arXiv:1108.4270](#)].

The ATLAS Collaboration

G. Aad⁸⁵, B. Abbott¹¹³, J. Abdallah¹⁵², S. Abdel Khalek¹¹⁷, O. Abdinov¹¹, R. Aben¹⁰⁷, B. Abi¹¹⁴, M. Abolins⁹⁰, O.S. AbouZeid¹⁵⁹, H. Abramowicz¹⁵⁴, H. Abreu¹⁵³, R. Abreu³⁰, Y. Abulaiti^{147a,147b}, B.S. Acharya^{165a,165b,a}, L. Adamczyk^{38a}, D.L. Adams²⁵, J. Adelman¹⁰⁸, S. Adomeit¹⁰⁰, T. Adye¹³¹, T. Agatonovic-Jovin¹³, J.A. Aguilar-Saavedra^{126a,126f}, M. Agustoni¹⁷, S.P. Ahlen²², F. Ahmadov^{65,b}, G. Aielli^{134a,134b}, H. Akerstedt^{147a,147b}, T.P.A. Åkesson⁸¹, G. Akimoto¹⁵⁶, A.V. Akimov⁹⁶, G.L. Alberghi^{20a,20b}, J. Albert¹⁷⁰, S. Albrand⁵⁵, M.J. Alconada Verzini⁷¹, M. Aleksa³⁰, I.N. Aleksandrov⁶⁵, C. Alexa^{26a}, G. Alexander¹⁵⁴, G. Alexandre⁴⁹, T. Alexopoulos¹⁰, M. Alhroob¹¹³, G. Alimonti^{91a}, L. Alio⁸⁵, J. Alison³¹, B.M.M. Allbrooke¹⁸, L.J. Allison⁷², P.P. Allport⁷⁴, A. Aloisio^{104a,104b}, A. Alonso³⁶, F. Alonso⁷¹, C. Alpigiani⁷⁶, A. Altheimer³⁵, B. Alvarez Gonzalez⁹⁰, M.G. Alviggi^{104a,104b}, K. Amako⁶⁶, Y. Amaral Coutinho^{24a}, C. Amelung²³, D. Amidei⁸⁹, S.P. Amor Dos Santos^{126a,126c}, A. Amorim^{126a,126b}, S. Amoroso⁴⁸, N. Amram¹⁵⁴, G. Amundsen²³, C. Anastopoulos¹⁴⁰, L.S. Ancu⁴⁹, N. Andari³⁰, T. Andeen³⁵, C.F. Anders^{58b}, G. Anders³⁰, K.J. Anderson³¹, A. Andreazza^{91a,91b}, V. Andrei^{58a}, X.S. Anduaga⁷¹, S. Angelidakis⁹, I. Angelozzi¹⁰⁷, P. Anger⁴⁴, A. Angerami³⁵, F. Anghinolfi³⁰, A.V. Anisenkov^{109,c}, N. Anjos¹², A. Annovi^{124a,124b}, M. Antonelli⁴⁷, A. Antonov⁹⁸, J. Antos^{145b}, F. Anulli^{133a}, M. Aoki⁶⁶, L. Aperio Bella¹⁸, G. Arabidze⁹⁰, Y. Arai⁶⁶, J.P. Araque^{126a}, A.T.H. Arce⁴⁵, F.A. Arduh⁷¹, J-F. Arguin⁹⁵, S. Argyropoulos⁴², M. Arik^{19a}, A.J. Armbruster³⁰, O. Arnæz³⁰, V. Arnal⁸², H. Arnold⁴⁸, M. Arratia²⁸, O. Arslan²¹, A. Artamonov⁹⁷, G. Artoni²³, S. Asai¹⁵⁶, N. Asbah⁴², A. Ashkenazi¹⁵⁴, B. Åsman^{147a,147b}, L. Asquith¹⁵⁰, K. Assamagan²⁵, R. Astalos^{145a}, M. Atkinson¹⁶⁶, N.B. Atlay¹⁴², B. Auerbach⁶, K. Augsten¹²⁸, M. Auresseau^{146b}, G. Avolio³⁰, B. Axen¹⁵, M.K. Ayoub¹¹⁷, G. Azuelos^{95,d}, M.A. Baak³⁰, A.E. Baas^{58a}, C. Bacci^{135a,135b}, H. Bachacou¹³⁷, K. Bachas¹⁵⁵, M. Backes³⁰, M. Backhaus³⁰, P. Bagiacchi^{133a,133b}, P. Bagnaia^{133a,133b}, Y. Bai^{33a}, T. Bain³⁵, J.T. Baines¹³¹, O.K. Baker¹⁷⁷, P. Balek¹²⁹, T. Balestri¹⁴⁹, F. Balli⁸⁴, E. Banas³⁹, Sw. Banerjee¹⁷⁴, A.A.E. Bannoura¹⁷⁶, H.S. Bansil¹⁸, L. Barak³⁰, S.P. Baranov⁹⁶, E.L. Barberio⁸⁸, D. Barberis^{50a,50b}, M. Barbero⁸⁵, T. Barillari¹⁰¹, M. Barisonzi^{165a,165b}, T. Barklow¹⁴⁴, N. Barlow²⁸, S.L. Barnes⁸⁴, B.M. Barnett¹³¹, R.M. Barnett¹⁵, Z. Barnovska⁵, A. Baroncelli^{135a}, G. Barone⁴⁹, A.J. Barr¹²⁰, F. Barreiro⁸², J. Barreiro Guimarães da Costa⁵⁷, R. Bartoldus¹⁴⁴, A.E. Barton⁷², P. Bartos^{145a}, A. Bassalat¹¹⁷, A. Basye¹⁶⁶, R.L. Bates⁵³, S.J. Batista¹⁵⁹, J.R. Batley²⁸, M. Battaglia¹³⁸, M. Bause^{133a,133b}, F. Bauer¹³⁷, H.S. Bawa^{144,e}, J.B. Beacham¹¹¹, M.D. Beattie⁷², T. Beau⁸⁰, P.H. Beauchemin¹⁶², R. Beccherle^{124a,124b}, P. Bechtel²¹, H.P. Beck^{17,f}, K. Becker¹²⁰, S. Becker¹⁰⁰, M. Beckingham¹⁷¹, C. Becot¹¹⁷, A.J. Beddall^{19c}, A. Beddall^{19c}, V.A. Bednyakov⁶⁵, C.P. Bee¹⁴⁹, L.J. Beemster¹⁰⁷, T.A. Beermann¹⁷⁶, M. Begel²⁵, K. Behr¹²⁰, C. Belanger-Champagne⁸⁷, P.J. Bell⁴⁹, W.H. Bell⁴⁹, G. Bella¹⁵⁴, L. Bellagamba^{20a}, A. Bellerive²⁹, M. Bellomo⁸⁶, K. Belotskiy⁹⁸, O. Beltramello³⁰, O. Benary¹⁵⁴, D. Bencheikroun^{136a}, M. Bender¹⁰⁰, K. Bendtz^{147a,147b}, N. Benekos¹⁰, Y. Benhammou¹⁵⁴, E. Benhar Nocchioli⁴⁹, J.A. Benitez Garcia^{160b}, D.P. Benjamin⁴⁵, J.R. Bensinger²³, S. Bentvelsen¹⁰⁷, L. Beresford¹²⁰, M. Beretta⁴⁷,

D. Berge¹⁰⁷, E. Bergeaas Kuutmann¹⁶⁷, N. Berger⁵, F. Berghaus¹⁷⁰, J. Beringer¹⁵,
C. Bernard²², N.R. Bernard⁸⁶, C. Bernius¹¹⁰, F.U. Bernlochner²¹, T. Berry⁷⁷,
P. Berta¹²⁹, C. Bertella⁸³, G. Bertoli^{147a,147b}, F. Bertolucci^{124a,124b}, C. Bertsche¹¹³,
D. Bertsche¹¹³, M.I. Besana^{91a}, G.J. Besjes¹⁰⁶, O. Bessidskaia Bylund^{147a,147b},
M. Bessner⁴², N. Besson¹³⁷, C. Betancourt⁴⁸, S. Bethke¹⁰¹, A.J. Bevan⁷⁶, W. Bhimji⁴⁶,
R.M. Bianchi¹²⁵, L. Bianchini²³, M. Bianco³⁰, O. Biebel¹⁰⁰, S.P. Bieniek⁷⁸,
M. Biglietti^{135a}, J. Bilbao De Mendizabal⁴⁹, H. Bilokon⁴⁷, M. Bindi⁵⁴, S. Binet¹¹⁷,
A. Bingul^{19c}, C. Bini^{133a,133b}, C.W. Black¹⁵¹, J.E. Black¹⁴⁴, K.M. Black²²,
D. Blackburn¹³⁹, R.E. Blair⁶, J.-B. Blanchard¹³⁷, J.E. Blanco⁷⁷, T. Blazek^{145a}, I. Bloch⁴²,
C. Blocker²³, W. Blum^{83,*}, U. Blumenschein⁵⁴, G.J. Bobbink¹⁰⁷, V.S. Bobrovnikov^{109,c},
S.S. Bocchetta⁸¹, A. Bocci⁴⁵, C. Bock¹⁰⁰, M. Boehler⁴⁸, J.A. Bogaerts³⁰,
A.G. Bogdanchikov¹⁰⁹, C. Bohm^{147a}, V. Boisvert⁷⁷, T. Bold^{38a}, V. Boldea^{26a},
A.S. Boldyrev⁹⁹, M. Bomben⁸⁰, M. Bona⁷⁶, M. Boonekamp¹³⁷, A. Borisov¹³⁰,
G. Borissov⁷², S. Borroni⁴², J. Bortfeldt¹⁰⁰, V. Bortolotto^{60a,60b,60c}, K. Bos¹⁰⁷,
D. Boscherini^{20a}, M. Bosman¹², J. Boudreau¹²⁵, J. Bouffard², E.V. Bouhova-Thacker⁷²,
D. Boumediene³⁴, C. Bourdarios¹¹⁷, N. Bousson¹¹⁴, S. Boutouil^{136d}, A. Boveia³⁰,
J. Boyd³⁰, I.R. Boyko⁶⁵, I. Bozic¹³, J. Bracinik¹⁸, A. Brandt⁸, G. Brandt¹⁵, O. Brandt^{58a},
U. Bratzler¹⁵⁷, B. Brau⁸⁶, J.E. Brau¹¹⁶, H.M. Braun^{176,*}, S.F. Brazzale^{165a,165c},
K. Brendlinger¹²², A.J. Brennan⁸⁸, L. Brenner¹⁰⁷, R. Brenner¹⁶⁷, S. Bressler¹⁷³,
K. Bristow^{146c}, T.M. Bristow⁴⁶, D. Britton⁵³, D. Britzger⁴², F.M. Brochu²⁸, I. Brock²¹,
R. Brock⁹⁰, J. Bronner¹⁰¹, G. Brooijmans³⁵, T. Brooks⁷⁷, W.K. Brooks^{32b},
J. Brosamer¹⁵, E. Brost¹¹⁶, J. Brown⁵⁵, P.A. Bruckman de Renstrom³⁹, D. Bruncko^{145b},
R. Bruneliere⁴⁸, A. Bruni^{20a}, G. Bruni^{20a}, M. Bruschi^{20a}, L. Bryngemark⁸¹, T. Buanes¹⁴,
Q. Buat¹⁴³, F. Bucci⁴⁹, P. Buchholz¹⁴², A.G. Buckley⁵³, S.I. Buda^{26a}, I.A. Budagov⁶⁵,
F. Buehrer⁴⁸, L. Bugge¹¹⁹, M.K. Bugge¹¹⁹, O. Bulekov⁹⁸, H. Burckhart³⁰, S. Burdin⁷⁴,
B. Burghgrave¹⁰⁸, S. Burke¹³¹, I. Burmeister⁴³, E. Busato³⁴, D. Büscher⁴⁸, V. Büscher⁸³,
P. Bussey⁵³, C.P. Buszello¹⁶⁷, J.M. Butler²², A.I. Butt³, C.M. Buttar⁵³,
J.M. Butterworth⁷⁸, P. Butti¹⁰⁷, W. Buttinger²⁵, A. Buzatu⁵³, S. Cabrera Urbán¹⁶⁸,
D. Caforio¹²⁸, O. Cakir^{4a}, P. Calafiura¹⁵, A. Calandri¹³⁷, G. Calderini⁸⁰, P. Calfayan¹⁰⁰,
L.P. Caloba^{24a}, D. Calvet³⁴, S. Calvet³⁴, R. Camacho Toro⁴⁹, S. Camarda⁴²,
D. Cameron¹¹⁹, L.M. Caminada¹⁵, R. Caminal Armadans¹², S. Campana³⁰,
M. Campanelli⁷⁸, A. Campoverde¹⁴⁹, V. Canale^{104a,104b}, A. Canepa^{160a}, M. Cano Bret⁷⁶,
J. Cantero⁸², R. Cantrill^{126a}, T. Cao⁴⁰, M.D.M. Capeans Garrido³⁰, I. Caprini^{26a},
M. Caprini^{26a}, M. Capua^{37a,37b}, R. Caputo⁸³, R. Cardarelli^{134a}, T. Carli³⁰,
G. Carlino^{104a}, L. Carminati^{91a,91b}, S. Caron¹⁰⁶, E. Carquin^{32a}, G.D. Carrillo-Montoya⁸,
J.R. Carter²⁸, J. Carvalho^{126a,126c}, D. Casadei⁷⁸, M.P. Casado¹², M. Casolino¹²,
E. Castaneda-Miranda^{146b}, A. Castelli¹⁰⁷, V. Castillo Gimenez¹⁶⁸, N.F. Castro^{126a,g},
P. Catastini⁵⁷, A. Catinaccio³⁰, J.R. Catmore¹¹⁹, A. Cattai³⁰, G. Cattani^{134a,134b},
J. Caudron⁸³, V. Cavaliere¹⁶⁶, D. Cavalli^{91a}, M. Cavalli-Sforza¹², V. Cavasinni^{124a,124b},
F. Ceradini^{135a,135b}, B.C. Cerio⁴⁵, K. Cerny¹²⁹, A.S. Cerqueira^{24b}, A. Cerri¹⁵⁰,
L. Cerrito⁷⁶, F. Cerutti¹⁵, M. Cerv³⁰, A. Cervelli¹⁷, S.A. Cetin^{19b}, A. Chafaq^{136a},
D. Chakraborty¹⁰⁸, I. Chalupkova¹²⁹, P. Chang¹⁶⁶, B. Chapleau⁸⁷, J.D. Chapman²⁸,
D. Charfeddine¹¹⁷, D.G. Charlton¹⁸, C.C. Chau¹⁵⁹, C.A. Chavez Barajas¹⁵⁰,

S. Cheatham¹⁵³, A. Chegwidien⁹⁰, S. Chekanov⁶, S.V. Chekulaev^{160a}, G.A. Chelkov^{65,h},
 M.A. Chelstowska⁸⁹, C. Chen⁶⁴, H. Chen²⁵, K. Chen¹⁴⁹, L. Chen^{33d,i}, S. Chen^{33c},
 X. Chen^{33f}, Y. Chen⁶⁷, H.C. Cheng⁸⁹, Y. Cheng³¹, A. Cheplakov⁶⁵, E. Cheremushkina¹³⁰,
 R. Cherkaoui El Moursli^{136e}, V. Chernyatin^{25,*}, E. Cheu⁷, L. Chevalier¹³⁷, V. Chiarella⁴⁷,
 J.T. Childers⁶, A. Chilingarov⁷², G. Chiodini^{73a}, A.S. Chisholm¹⁸, R.T. Chislett⁷⁸,
 A. Chitan^{26a}, M.V. Chizhov⁶⁵, K. Choi⁶¹, S. Chouridou⁹, B.K.B. Chow¹⁰⁰,
 V. Christodoulou⁷⁸, D. Chromek-Burckhart³⁰, M.L. Chu¹⁵², J. Chudoba¹²⁷,
 J.J. Chwastowski³⁹, L. Chytka¹¹⁵, G. Ciapetti^{133a,133b}, A.K. Ciftci^{4a}, D. Cinca⁵³,
 V. Cindro⁷⁵, A. Ciocio¹⁵, Z.H. Citron¹⁷³, M. Ciubancan^{26a}, A. Clark⁴⁹, P.J. Clark⁴⁶,
 R.N. Clarke¹⁵, W. Cleland¹²⁵, C. Clement^{147a,147b}, Y. Coadou⁸⁵, M. Cobal^{165a,165c},
 A. Coccaro¹³⁹, J. Cochran⁶⁴, L. Coffey²³, J.G. Cogan¹⁴⁴, B. Cole³⁵, S. Cole¹⁰⁸,
 A.P. Colijn¹⁰⁷, J. Collot⁵⁵, T. Colombo^{58c}, G. Compostella¹⁰¹, P. Conde Muino^{126a,126b},
 E. Coniavitis⁴⁸, S.H. Connell^{146b}, I.A. Connelly⁷⁷, S.M. Consonni^{91a,91b}, V. Consorti⁴⁸,
 S. Constantinescu^{26a}, C. Conta^{121a,121b}, G. Conti³⁰, F. Conventi^{104a,j}, M. Cooke¹⁵,
 B.D. Cooper⁷⁸, A.M. Cooper-Sarkar¹²⁰, K. Copic¹⁵, T. Cornelissen¹⁷⁶, M. Corradi^{20a},
 F. Corriveau^{87,k}, A. Corso-Radu¹⁶⁴, A. Cortes-Gonzalez¹², G. Cortiana¹⁰¹, M.J. Costa¹⁶⁸,
 D. Costanzo¹⁴⁰, D. Côté⁸, G. Cottin²⁸, G. Cowan⁷⁷, B.E. Cox⁸⁴, K. Cranmer¹¹⁰,
 G. Cree²⁹, S. Crépé-Renaudin⁵⁵, F. Crescioli⁸⁰, W.A. Cribbs^{147a,147b},
 M. Crispin Ortuzar¹²⁰, M. Cristinziani²¹, V. Croft¹⁰⁶, G. Crosetti^{37a,37b},
 T. Cuhadar Donszelmann¹⁴⁰, J. Cummings¹⁷⁷, M. Curatolo⁴⁷, C. Cuthbert¹⁵¹,
 H. Czirr¹⁴², P. Czodrowski³, S. D'Auria⁵³, M. D'Onofrio⁷⁴,
 M.J. Da Cunha Sargedas De Sousa^{126a,126b}, C. Da Via⁸⁴, W. Dabrowski^{38a},
 A. Dafinca¹²⁰, T. Dai⁸⁹, O. Dale¹⁴, F. Dallaire⁹⁵, C. Dallapiccola⁸⁶, M. Dam³⁶,
 J.R. Dandoy³¹, A.C. Daniells¹⁸, M. Danninger¹⁶⁹, M. Dano Hoffmann¹³⁷, V. Dao⁴⁸,
 G. Darbo^{50a}, S. Darmora⁸, J. Dassoulas³, A. Dattagupta⁶¹, W. Davey²¹, C. David¹⁷⁰,
 T. Davidek¹²⁹, E. Davies^{120,l}, M. Davies¹⁵⁴, P. Davison⁷⁸, Y. Davygora^{58a}, E. Dawe¹⁴³,
 I. Dawson¹⁴⁰, R.K. Daya-Ishmukhametova⁸⁶, K. De⁸, R. de Asmundis^{104a},
 S. De Castro^{20a,20b}, S. De Cecco⁸⁰, N. De Groot¹⁰⁶, P. de Jong¹⁰⁷, H. De la Torre⁸²,
 F. De Lorenzi⁶⁴, L. De Nooij¹⁰⁷, D. De Pedis^{133a}, A. De Salvo^{133a}, U. De Sanctis¹⁵⁰,
 A. De Santo¹⁵⁰, J.B. De Vivie De Regie¹¹⁷, W.J. Dearnaley⁷², R. Debbé²⁵,
 C. Debenedetti¹³⁸, D.V. Dedovich⁶⁵, I. Deigaard¹⁰⁷, J. Del Peso⁸², T. Del Prete^{124a,124b},
 D. Delgove¹¹⁷, F. Deliot¹³⁷, C.M. Delitzsch⁴⁹, M. Deliyergiyev⁷⁵, A. Dell'Acqua³⁰,
 L. Dell'Asta²², M. Dell'Orso^{124a,124b}, M. Della Pietra^{104a,j}, D. della Volpe⁴⁹,
 M. Delmastro⁵, P.A. Delsart⁵⁵, C. Deluca¹⁰⁷, D.A. DeMarco¹⁵⁹, S. Demers¹⁷⁷,
 M. Demichev⁶⁵, A. Demilly⁸⁰, S.P. Denisov¹³⁰, D. Derendarz³⁹, J.E. Derkaoui^{136d},
 F. Derue⁸⁰, P. Dervan⁷⁴, K. Desch²¹, C. Deterre⁴², P.O. Deviveiros³⁰, A. Dewhurst¹³¹,
 S. Dhaliwal¹⁰⁷, A. Di Ciaccio^{134a,134b}, L. Di Ciaccio⁵, A. Di Domenico^{133a,133b},
 C. Di Donato^{104a,104b}, A. Di Girolamo³⁰, B. Di Girolamo³⁰, A. Di Mattia¹⁵³,
 B. Di Micco^{135a,135b}, R. Di Nardo⁴⁷, A. Di Simone⁴⁸, R. Di Sipio¹⁵⁹, D. Di Valentino²⁹,
 C. Diaconu⁸⁵, M. Diamond¹⁵⁹, F.A. Dias⁴⁶, M.A. Diaz^{32a}, E.B. Diehl⁸⁹, J. Dietrich¹⁶,
 S. Diglio⁸⁵, A. Dimitrievska¹³, J. Dingfelder²¹, F. Dittus³⁰, F. Djama⁸⁵, T. Djobava^{51b},
 J.I. Djuvsland^{58a}, M.A.B. do Vale^{24c}, D. Dobos³⁰, M. Dobre^{26a}, C. Doglioni⁴⁹,
 T. Dohmae¹⁵⁶, J. Dolejsi¹²⁹, Z. Dolezal¹²⁹, B.A. Dolgoshein^{98,*}, M. Donadelli^{24d},

S. Donati^{124a,124b}, P. Dondero^{121a,121b}, J. Donini³⁴, J. Dopke¹³¹, A. Doria^{104a},
 M.T. Dova⁷¹, A.T. Doyle⁵³, E. Drechsler⁵⁴, M. Dris¹⁰, E. Dubreuil³⁴, E. Duchovni¹⁷³,
 G. Duckeck¹⁰⁰, O.A. Ducu^{26a,85}, D. Duda¹⁷⁶, A. Dudarev³⁰, L. Duflot¹¹⁷, L. Duguid⁷⁷,
 M. Dührssen³⁰, M. Dunford^{58a}, H. Duran Yildiz^{4a}, M. Düren⁵², A. Durglishvili^{51b},
 D. Duschinger⁴⁴, M. Dwuznik^{38a}, M. Dyndal^{38a}, K.M. Ecker¹⁰¹, W. Edson²,
 N.C. Edwards⁴⁶, W. Ehrenfeld²¹, T. Eifert³⁰, G. Eigen¹⁴, K. Einsweiler¹⁵, T. Ekelof¹⁶⁷,
 M. El Kacimi^{136c}, M. Ellert¹⁶⁷, S. Elles⁵, F. Ellinghaus⁸³, A.A. Elliot¹⁷⁰, N. Ellis³⁰,
 J. Elmsheuser¹⁰⁰, M. Elsing³⁰, D. Emeliyanov¹³¹, Y. Enari¹⁵⁶, O.C. Endner⁸³,
 M. Endo¹¹⁸, R. Engelmann¹⁴⁹, J. Erdmann⁴³, A. Ereditato¹⁷, D. Eriksson^{147a},
 G. Ernis¹⁷⁶, J. Ernst², M. Ernst²⁵, S. Errede¹⁶⁶, E. Ertel⁸³, M. Escalier¹¹⁷, H. Esch⁴³,
 C. Escobar¹²⁵, B. Esposito⁴⁷, A.I. Etienvre¹³⁷, E. Etzion¹⁵⁴, H. Evans⁶¹, A. Ezhilov¹²³,
 L. Fabbri^{20a,20b}, G. Facini³¹, R.M. Fakhruddinov¹³⁰, S. Falciano^{133a}, R.J. Falla⁷⁸,
 J. Faltova¹²⁹, Y. Fang^{33a}, M. Fanti^{91a,91b}, A. Farbin⁸, A. Farilla^{135a}, T. Farooque¹²,
 S. Farrell¹⁵, S.M. Farrington¹⁷¹, P. Farthouat³⁰, F. Fassi^{136e}, P. Fassnacht³⁰,
 D. Fassouliotis⁹, A. Favareto^{50a,50b}, L. Fayard¹¹⁷, P. Federic^{145a}, O.L. Fedin^{123,m},
 W. Fedorko¹⁶⁹, S. Feigl³⁰, L. Feligioni⁸⁵, C. Feng^{33d}, E.J. Feng⁶, H. Feng⁸⁹,
 A.B. Fenyuk¹³⁰, P. Fernandez Martinez¹⁶⁸, S. Fernandez Perez³⁰, S. Ferrag⁵³,
 J. Ferrando⁵³, A. Ferrari¹⁶⁷, P. Ferrari¹⁰⁷, R. Ferrari^{121a}, D.E. Ferreira de Lima⁵³,
 A. Ferrer¹⁶⁸, D. Ferrere⁴⁹, C. Ferretti⁸⁹, A. Ferretto Parodi^{50a,50b}, M. Fiassarini³¹,
 F. Fiedler⁸³, A. Filipčič⁷⁵, M. Filipuzzi⁴², F. Filthaut¹⁰⁶, M. Fincke-Keeler¹⁷⁰,
 K.D. Finelli¹⁵¹, M.C.N. Fiolhais^{126a,126c}, L. Fiorini¹⁶⁸, A. Firan⁴⁰, A. Fischer²,
 C. Fischer¹², J. Fischer¹⁷⁶, W.C. Fisher⁹⁰, E.A. Fitzgerald²³, M. Flechl⁴⁸, I. Fleck¹⁴²,
 P. Fleischmann⁸⁹, S. Fleischmann¹⁷⁶, G.T. Fletcher¹⁴⁰, G. Fletcher⁷⁶, T. Flick¹⁷⁶,
 A. Floderus⁸¹, L.R. Flores Castillo^{60a}, M.J. Flowerdew¹⁰¹, A. Formica¹³⁷, A. Forti⁸⁴,
 D. Fournier¹¹⁷, H. Fox⁷², S. Fracchia¹², P. Francavilla⁸⁰, M. Franchini^{20a,20b}, D. Francis³⁰,
 L. Franconi¹¹⁹, M. Franklin⁵⁷, M. Fraternali^{121a,121b}, D. Freeborn⁷⁸, S.T. French²⁸,
 F. Friedrich⁴⁴, D. Froidevaux³⁰, J.A. Frost¹²⁰, C. Fukunaga¹⁵⁷, E. Fullana Torregrosa⁸³,
 B.G. Fulsom¹⁴⁴, J. Fuster¹⁶⁸, C. Gabaldon⁵⁵, O. Gabizon¹⁷⁶, A. Gabrielli^{20a,20b},
 A. Gabrielli^{133a,133b}, S. Gadatsch¹⁰⁷, S. Gadomski⁴⁹, G. Gagliardi^{50a,50b}, P. Gagnon⁶¹,
 C. Galea¹⁰⁶, B. Galhardo^{126a,126c}, E.J. Gallas¹²⁰, B.J. Gallop¹³¹, P. Gallus¹²⁸,
 G. Galster³⁶, K.K. Gan¹¹¹, J. Gao^{33b,85}, Y. Gao⁴⁶, Y.S. Gao^{144,e}, F.M. Garay Walls⁴⁶,
 F. Garbersson¹⁷⁷, C. García¹⁶⁸, J.E. García Navarro¹⁶⁸, M. Garcia-Sciveres¹⁵,
 R.W. Gardner³¹, N. Garelli¹⁴⁴, V. Garonne³⁰, C. Gatti⁴⁷, G. Gaudio^{121a}, B. Gaur¹⁴²,
 L. Gauthier⁹⁵, P. Gauzzi^{133a,133b}, I.L. Gavrilenko⁹⁶, C. Gay¹⁶⁹, G. Gaycken²¹,
 E.N. Gazis¹⁰, P. Ge^{33d}, Z. Gece¹⁶⁹, C.N.P. Gee¹³¹, D.A.A. Geerts¹⁰⁷,
 Ch. Geich-Gimbel²¹, C. Gemme^{50a}, M.H. Genest⁵⁵, S. Gentile^{133a,133b}, M. George⁵⁴,
 S. George⁷⁷, D. Gerbaudo¹⁶⁴, A. Gershon¹⁵⁴, H. Ghazlane^{136b}, N. Ghodbane³⁴,
 B. Giacobbe^{20a}, S. Giagu^{133a,133b}, V. Giangiobbe¹², P. Giannetti^{124a,124b}, F. Gianotti³⁰,
 B. Gibbard²⁵, S.M. Gibson⁷⁷, M. Gilchriese¹⁵, T.P.S. Gillam²⁸, D. Gillberg³⁰, G. Gilles³⁴,
 D.M. Gingrich^{3,d}, N. Giokaris⁹, M.P. Giordani^{165a,165c}, F.M. Giorgi^{20a}, F.M. Giorgi¹⁶,
 P.F. Giraud¹³⁷, P. Giromini⁴⁷, D. Giugni^{91a}, C. Giuliani⁴⁸, M. Giuliani^{58b},
 B.K. Gjelsten¹¹⁹, S. Gkaitatzis¹⁵⁵, I. Gkialas¹⁵⁵, E.L. Gkoukousis¹¹⁷, L.K. Gladilin⁹⁹,
 C. Glasman⁸², J. Glatzer³⁰, P.C.F. Glaysheer⁴⁶, A. Glazov⁴², M. Goblirsch-Kolb¹⁰¹,

J.R. Goddard⁷⁶, J. Godlewski³⁹, S. Goldfarb⁸⁹, T. Golling⁴⁹, D. Golubkov¹³⁰,
 A. Gomes^{126a,126b,126d}, R. Gonalo^{126a}, J. Goncalves Pinto Firmino Da Costa¹³⁷,
 L. Gonella²¹, S. Gonzlez de la Hoz¹⁶⁸, G. Gonzalez Parra¹², S. Gonzalez-Sevilla⁴⁹,
 L. Goossens³⁰, P.A. Gorbounov⁹⁷, H.A. Gordon²⁵, I. Gorelov¹⁰⁵, B. Gorini³⁰,
 E. Gorini^{73a,73b}, A. Gorišek⁷⁵, E. Gornicki³⁹, A.T. Goshaw⁴⁵, C. Gssling⁴³,
 M.I. Gostkin⁶⁵, M. Goughri^{136a}, D. Goujdami^{136c}, A.G. Goussiou¹³⁹, H.M.X. Grabas¹³⁸,
 L. Graber⁵⁴, I. Grabowska-Bold^{38a}, P. Grafstrm^{20a,20b}, K.-J. Grahm⁴², J. Gramling⁴⁹,
 E. Gramstad¹¹⁹, S. Grancagnolo¹⁶, V. Grassi¹⁴⁹, V. Gratchev¹²³, H.M. Gray³⁰,
 E. Graziani^{135a}, Z.D. Greenwood^{79,n}, K. Gregersen⁷⁸, I.M. Gregor⁴², P. Grenier¹⁴⁴,
 J. Griffiths⁸, A.A. Grillo¹³⁸, K. Grimm⁷², S. Grinstein^{12,o}, Ph. Gris³⁴,
 Y.V. Grishkevich⁹⁹, J.-F. Grivaz¹¹⁷, J.P. Grohs⁴⁴, A. Grohsjean⁴², E. Gross¹⁷³,
 J. Grosse-Knetter⁵⁴, G.C. Grossi^{134a,134b}, Z.J. Groust¹⁵⁰, L. Guan^{33b}, J. Guenther¹²⁸,
 F. Guescini⁴⁹, D. Guest¹⁷⁷, O. Gueta¹⁵⁴, E. Guido^{50a,50b}, T. Guillemin¹¹⁷, S. Guindon²,
 U. Gul⁵³, C. Gumpert⁴⁴, J. Guo^{33e}, S. Gupta¹²⁰, P. Gutierrez¹¹³, N.G. Gutierrez Ortiz⁵³,
 C. Gutsche⁴⁴, N. Guttman¹⁵⁴, C. Guyot¹³⁷, C. Gwenlan¹²⁰, C.B. Gwilliam⁷⁴,
 A. Haas¹¹⁰, C. Haber¹⁵, H.K. Hadavand⁸, N. Haddad^{136e}, P. Haefner²¹, S. Hagebck²¹,
 Z. Hajduk³⁹, H. Hakobyan¹⁷⁸, M. Haleem⁴², J. Haley¹¹⁴, D. Hall¹²⁰, G. Halladjian⁹⁰,
 G.D. Hallewell⁸⁵, K. Hamacher¹⁷⁶, P. Hamal¹¹⁵, K. Hamano¹⁷⁰, M. Hamer⁵⁴,
 A. Hamilton^{146a}, S. Hamilton¹⁶², G.N. Hamity^{146c}, P.G. Hamnett⁴², L. Han^{33b},
 K. Hanagaki¹¹⁸, K. Hanawa¹⁵⁶, M. Hance¹⁵, P. Hanke^{58a}, R. Hanna¹³⁷, J.B. Hansen³⁶,
 J.D. Hansen³⁶, P.H. Hansen³⁶, K. Hara¹⁶¹, A.S. Hard¹⁷⁴, T. Harenberg¹⁷⁶, F. Hariri¹¹⁷,
 S. Harkusha⁹², R.D. Harrington⁴⁶, P.F. Harrison¹⁷¹, F. Hartjes¹⁰⁷, M. Hasegawa⁶⁷,
 S. Hasegawa¹⁰³, Y. Hasegawa¹⁴¹, A. Hasib¹¹³, S. Hassani¹³⁷, S. Haug¹⁷, R. Hauser⁹⁰,
 L. Hauswald⁴⁴, M. Havranek¹²⁷, C.M. Hawkes¹⁸, R.J. Hawkings³⁰, A.D. Hawkins⁸¹,
 T. Hayashi¹⁶¹, D. Hayden⁹⁰, C.P. Hays¹²⁰, J.M. Hays⁷⁶, H.S. Hayward⁷⁴,
 S.J. Haywood¹³¹, S.J. Head¹⁸, T. Heck⁸³, V. Hedberg⁸¹, L. Heelan⁸, S. Heim¹²²,
 T. Heim¹⁷⁶, B. Heinemann¹⁵, L. Heinrich¹¹⁰, J. Hejbal¹²⁷, L. Helary²², M. Heller³⁰,
 S. Hellman^{147a,147b}, D. Hellmich²¹, C. Helsen³⁰, J. Henderson¹²⁰, R.C.W. Henderson⁷²,
 Y. Heng¹⁷⁴, C. Hengler⁴², A. Henrichs¹⁷⁷, A.M. Henriques Correia³⁰,
 S. Henrot-Versille¹¹⁷, G.H. Herbert¹⁶, Y. Hernndez Jimnez¹⁶⁸, R. Herrberg-Schubert¹⁶,
 G. Herten⁴⁸, R. Hertenberger¹⁰⁰, L. Hervas³⁰, G.G. Hesketh⁷⁸, N.P. Hessey¹⁰⁷,
 J.W. Hetherly⁴⁰, R. Hickling⁷⁶, E. Hign-Rodríguez¹⁶⁸, E. Hill¹⁷⁰, J.C. Hill²⁸,
 K.H. Hiller⁴², S.J. Hillier¹⁸, I. Hinchliffe¹⁵, E. Hines¹²², R.R. Hinman¹⁵, M. Hirose¹⁵⁸,
 D. Hirschbuehl¹⁷⁶, J. Hobbs¹⁴⁹, N. Hod¹⁰⁷, M.C. Hodgkinson¹⁴⁰, P. Hodgson¹⁴⁰,
 A. Hoecker³⁰, M.R. Hoefkamp¹⁰⁵, F. Hoenig¹⁰⁰, M. Hohlfeld⁸³, D. Hohn²¹,
 T.R. Holmes¹⁵, T.M. Hong¹²², L. Hooft van Huysduynen¹¹⁰, W.H. Hopkins¹¹⁶,
 Y. Hori¹⁰³, A.J. Horton¹⁴³, J.-Y. Hostachy⁵⁵, S. Hou¹⁵², A. Hoummada^{136a}, J. Howard¹²⁰,
 J. Howarth⁴², M. Hrabovsky¹¹⁵, I. Hristova¹⁶, J. Hrivnac¹¹⁷, T. Hryn'ova⁵,
 A. Hrynevich⁹³, C. Hsu^{146c}, P.J. Hsu^{152,p}, S.-C. Hsu¹³⁹, D. Hu³⁵, Q. Hu^{33b}, X. Hu⁸⁹,
 Y. Huang⁴², Z. Hubacek³⁰, F. Hubaut⁸⁵, F. Huegging²¹, T.B. Huffman¹²⁰,
 E.W. Hughes³⁵, G. Hughes⁷², M. Huhtinen³⁰, T.A. Hlsing⁸³, N. Huseynov^{65,b},
 J. Huston⁹⁰, J. Huth⁵⁷, G. Iacobucci⁴⁹, G. Iakovidis²⁵, I. Ibragimov¹⁴²,
 L. Iconomidou-Fayard¹¹⁷, E. Ideal¹⁷⁷, Z. Idrissi^{136e}, P. Iengo^{104a}, O. Igonkina¹⁰⁷,

T. Iizawa¹⁷², Y. Ikegami⁶⁶, K. Ikematsu¹⁴², M. Ikeno⁶⁶, Y. Ilchenko^{31,q}, D. Iliadis¹⁵⁵,
 N. Ilic¹⁵⁹, Y. Inamaru⁶⁷, T. Ince¹⁰¹, P. Ioannou⁹, M. Iodice^{135a}, K. Iordanidou⁹,
 V. Ippolito⁵⁷, A. Irles Quiles¹⁶⁸, C. Isaksson¹⁶⁷, M. Ishino⁶⁸, M. Ishitsuka¹⁵⁸,
 R. Ishmukhametov¹¹¹, C. Issever¹²⁰, S. Istin^{19a}, J.M. Iturbe Ponce⁸⁴, R. Iuppa^{134a,134b},
 J. Ivarsson⁸¹, W. Iwanski³⁹, H. Iwasaki⁶⁶, J.M. Izen⁴¹, V. Izzo^{104a}, S. Jabbar³,
 B. Jackson¹²², M. Jackson⁷⁴, P. Jackson¹, M.R. Jaekel³⁰, V. Jain², K. Jakobs⁴⁸,
 S. Jakobsen³⁰, T. Jakoubek¹²⁷, J. Jakubek¹²⁸, D.O. Jamin¹⁵², D.K. Jana⁷⁹, E. Jansen⁷⁸,
 R.W. Jansky⁶², J. Janssen²¹, M. Janus¹⁷¹, G. Jarlskog⁸¹, N. Javadov^{65,b}, T. Javůrek⁴⁸,
 L. Jeanty¹⁵, J. Jejelava^{51a,r}, G.-Y. Jeng¹⁵¹, D. Jennens⁸⁸, P. Jenni^{48,s}, J. Jentzsch⁴³,
 C. Jeske¹⁷¹, S. Jézéquel⁵, H. Ji¹⁷⁴, J. Jia¹⁴⁹, Y. Jiang^{33b}, J. Jimenez Pena¹⁶⁸, S. Jin^{33a},
 A. Jinaru^{26a}, O. Jinnouchi¹⁵⁸, M.D. Joergensen³⁶, P. Johansson¹⁴⁰, K.A. Johns⁷,
 K. Jon-And^{147a,147b}, G. Jones¹⁷¹, R.W.L. Jones⁷², T.J. Jones⁷⁴, J. Jongmanns^{58a},
 P.M. Jorge^{126a,126b}, K.D. Joshi⁸⁴, J. Jovicevic¹⁴⁸, X. Ju¹⁷⁴, C.A. Jung⁴³, P. Jussel⁶²,
 A. Juste Rozas^{12,o}, M. Kaci¹⁶⁸, A. Kaczmarzka³⁹, M. Kado¹¹⁷, H. Kagan¹¹¹,
 M. Kagan¹⁴⁴, S.J. Kahn⁸⁵, E. Kajomovitz⁴⁵, C.W. Kalderon¹²⁰, S. Kama⁴⁰,
 A. Kamenshchikov¹³⁰, N. Kanaya¹⁵⁶, M. Kaneda³⁰, S. Kaneti²⁸, V.A. Kantserov⁹⁸,
 J. Kanzaki⁶⁶, B. Kaplan¹¹⁰, A. Kapliy³¹, D. Kar⁵³, K. Karakostas¹⁰, A. Karamaoun³,
 N. Karastathis^{10,107}, M.J. Kareem⁵⁴, M. Karneviskiy⁸³, S.N. Karpov⁶⁵, Z.M. Karpova⁶⁵,
 K. Karthik¹¹⁰, V. Kartvelishvili⁷², A.N. Karyukhin¹³⁰, L. Kashif¹⁷⁴, R.D. Kass¹¹¹,
 A. Kastanas¹⁴, Y. Kataoka¹⁵⁶, A. Katre⁴⁹, J. Katzy⁴², K. Kawagoe⁷⁰, T. Kawamoto¹⁵⁶,
 G. Kawamura⁵⁴, S. Kazama¹⁵⁶, V.F. Kazanin^{109,c}, M.Y. Kazarinov⁶⁵, R. Keeler¹⁷⁰,
 R. Kehoe⁴⁰, M. Keil⁵⁴, J.S. Keller⁴², J.J. Kempster⁷⁷, H. Keoshkerian⁸⁴, O. Kepka¹²⁷,
 B.P. Kerševan⁷⁵, S. Kersten¹⁷⁶, R.A. Keyes⁸⁷, F. Khalil-zada¹¹, H. Khandanyan^{147a,147b},
 A. Khanov¹¹⁴, A. Kharlamov¹⁰⁹, A. Khodinov⁹⁸, T.J. Khoo²⁸, G. Khorauli²¹,
 V. Khovanskiy⁹⁷, E. Khramov⁶⁵, J. Khubua^{51b,t}, H.Y. Kim⁸, H. Kim^{147a,147b},
 S.H. Kim¹⁶¹, Y. Kim³¹, N. Kimura¹⁵⁵, O.M. Kind¹⁶, B.T. King⁷⁴, M. King¹⁶⁸,
 R.S.B. King¹²⁰, S.B. King¹⁶⁹, J. Kirk¹³¹, A.E. Kiryunin¹⁰¹, T. Kishimoto⁶⁷,
 D. Kisielewska^{38a}, F. Kiss⁴⁸, K. Kiuchi¹⁶¹, E. Kladiva^{145b}, M.H. Klein³⁵, M. Klein⁷⁴,
 U. Klein⁷⁴, K. Kleinknecht⁸³, P. Klimek^{147a,147b}, A. Klimentov²⁵, R. Klingenberg⁴³,
 J.A. Klinger⁸⁴, T. Klioutchnikova³⁰, P.F. Klok¹⁰⁶, E.-E. Kluge^{58a}, P. Kluit¹⁰⁷,
 S. Kluth¹⁰¹, E. Kneringer⁶², E.B.F.G. Knoops⁸⁵, A. Knue⁵³, D. Kobayashi¹⁵⁸,
 T. Kobayashi¹⁵⁶, M. Kobel⁴⁴, M. Kocian¹⁴⁴, P. Kodys¹²⁹, T. Koffas²⁹, E. Koffeman¹⁰⁷,
 L.A. Kogan¹²⁰, S. Kohlmann¹⁷⁶, Z. Kohout¹²⁸, T. Kohriki⁶⁶, T. Koi¹⁴⁴, H. Kolanoski¹⁶,
 I. Koletsou⁵, A.A. Komar^{96,*}, Y. Komori¹⁵⁶, T. Kondo⁶⁶, N. Kondrashova⁴²,
 K. Köneke⁴⁸, A.C. König¹⁰⁶, S. König⁸³, T. Kono^{66,u}, R. Konoplich^{110,v},
 N. Konstantinidis⁷⁸, R. Kopeliansky¹⁵³, S. Koperny^{38a}, L. Köpke⁸³, A.K. Kopp⁴⁸,
 K. Korcyl³⁹, K. Kordas¹⁵⁵, A. Korn⁷⁸, A.A. Korol^{109,c}, I. Korolkov¹², E.V. Korolkova¹⁴⁰,
 O. Kortner¹⁰¹, S. Kortner¹⁰¹, T. Kosek¹²⁹, V.V. Kostyukhin²¹, V.M. Kotov⁶⁵,
 A. Kotwal⁴⁵, A. Kourkouveli-Charalampidi¹⁵⁵, C. Kourkouvelis⁹, V. Kouskoura²⁵,
 A. Koutsman^{160a}, R. Kowalewski¹⁷⁰, T.Z. Kowalski^{38a}, W. Kozanecki¹³⁷, A.S. Kozhin¹³⁰,
 V.A. Kramarenko⁹⁹, G. Kramberger⁷⁵, D. Krasnopevtsev⁹⁸, M.W. Krasny⁸⁰,
 A. Krasznahorkay³⁰, J.K. Kraus²¹, A. Kravchenko²⁵, S. Kreiss¹¹⁰, M. Kretz^{58c},
 J. Kretzschmar⁷⁴, K. Kreutzfeldt⁵², P. Krieger¹⁵⁹, K. Krizka³¹, K. Kroeninger⁴³,

H. Kroha¹⁰¹, J. Kroll¹²², J. Kroseberg²¹, J. Krstic¹³, U. Kruchonak⁶⁵, H. Krüger²¹,
 N. Krumnack⁶⁴, Z.V. Krumshteyn⁶⁵, A. Kruse¹⁷⁴, M.C. Kruse⁴⁵, M. Kruskal²²,
 T. Kubota⁸⁸, H. Kucuk⁷⁸, S. Kuday^{4c}, S. Kuehn⁴⁸, A. Kugel^{58c}, F. Kuger¹⁷⁵, A. Kuhl¹³⁸,
 T. Kuhl⁴², V. Kukhtin⁶⁵, Y. Kulchitsky⁹², S. Kuleshov^{32b}, M. Kuna^{133a,133b}, T. Kunigo⁶⁸,
 A. Kupco¹²⁷, H. Kurashige⁶⁷, Y.A. Kurochkin⁹², R. Kurumida⁶⁷, V. Kus¹²⁷,
 E.S. Kuwertz¹⁴⁸, M. Kuze¹⁵⁸, J. Kvita¹¹⁵, T. Kwan¹⁷⁰, D. Kyriazopoulos¹⁴⁰,
 A. La Rosa⁴⁹, J.L. La Rosa Navarro^{24d}, L. La Rotonda^{37a,37b}, C. Lacasta¹⁶⁸,
 F. Lacava^{133a,133b}, J. Lacey²⁹, H. Lacker¹⁶, D. Lacour⁸⁰, V.R. Lacuesta¹⁶⁸, E. Ladygin⁶⁵,
 R. Lafaye⁵, B. Laforge⁸⁰, T. Lagouri¹⁷⁷, S. Lai⁴⁸, L. Lambourne⁷⁸, S. Lammers⁶¹,
 C.L. Lampen⁷, W. Lampl⁷, E. Lançon¹³⁷, U. Landgraf⁴⁸, M.P.J. Landon⁷⁶, V.S. Lang^{58a},
 A.J. Lankford¹⁶⁴, F. Lanni²⁵, K. Lantzsche³⁰, S. Laplace⁸⁰, C. Lapoire³⁰, J.F. Laporte¹³⁷,
 T. Lari^{91a}, F. Lasagni Manghi^{20a,20b}, M. Lassnig³⁰, P. Laurelli⁴⁷, W. Lavrijsen¹⁵,
 A.T. Law¹³⁸, P. Laycock⁷⁴, O. Le Dortz⁸⁰, E. Le Guirriec⁸⁵, E. Le Menedeu¹²,
 T. LeCompte⁶, F. Ledroit-Guillon⁵⁵, C.A. Lee^{146b}, S.C. Lee¹⁵², L. Lee¹, G. Lefebvre⁸⁰,
 M. Lefebvre¹⁷⁰, F. Legger¹⁰⁰, C. Leggett¹⁵, A. Lehan⁷⁴, G. Lehmann Miotto³⁰, X. Lei⁷,
 W.A. Leight²⁹, A. Leisos¹⁵⁵, A.G. Leister¹⁷⁷, M.A.L. Leite^{24d}, R. Leitner¹²⁹,
 D. Lellouch¹⁷³, B. Lemmer⁵⁴, K.J.C. Leney⁷⁸, T. Lenz²¹, G. Lenzen¹⁷⁶, B. Lenzi³⁰,
 R. Leone⁷, S. Leone^{124a,124b}, C. Leonidopoulos⁴⁶, S. Leontsinis¹⁰, C. Leroy⁹⁵,
 C.G. Lester²⁸, M. Levchenko¹²³, J. Levêque⁵, D. Levin⁸⁹, L.J. Levinson¹⁷³, M. Levy¹⁸,
 A. Lewis¹²⁰, A.M. Leyko²¹, M. Leyton⁴¹, B. Li^{33b,w}, B. Li⁸⁵, H. Li¹⁴⁹, H.L. Li³¹, L. Li⁴⁵,
 L. Li^{33e}, S. Li⁴⁵, Y. Li^{33c,x}, Z. Liang¹³⁸, H. Liao³⁴, B. Liberti^{134a}, A. Liblong¹⁵⁹,
 P. Lichard³⁰, K. Lie¹⁶⁶, J. Liebal²¹, W. Liebig¹⁴, C. Limbach²¹, A. Limosani¹⁵¹,
 S.C. Lin^{152,y}, T.H. Lin⁸³, F. Linde¹⁰⁷, B.E. Lindquist¹⁴⁹, J.T. Linnemann⁹⁰, E. Lipeles¹²²,
 A. Lipniacka¹⁴, M. Lisovyi⁴², T.M. Liss¹⁶⁶, D. Lissauer²⁵, A. Lister¹⁶⁹, A.M. Litke¹³⁸,
 B. Liu¹⁵², D. Liu¹⁵², J. Liu⁸⁵, J.B. Liu^{33b}, K. Liu^{33b,z}, L. Liu⁸⁹, M. Liu⁴⁵, M. Liu^{33b},
 Y. Liu^{33b}, M. Livan^{121a,121b}, A. Lleres⁵⁵, J. Llorente Merino⁸², S.L. Lloyd⁷⁶,
 F. Lo Sterzo¹⁵², E. Lobodzinska⁴², P. Loch⁷, W.S. Lockman¹³⁸, F.K. Loebinger⁸⁴,
 A.E. Loevschall-Jensen³⁶, A. Loginov¹⁷⁷, T. Lohse¹⁶, K. Lohwasser⁴², M. Lokajicek¹²⁷,
 B.A. Long²², J.D. Long⁸⁹, R.E. Long⁷², K.A. Looper¹¹¹, L. Lopes^{126a}, D. Lopez Mateos⁵⁷,
 B. Lopez Paredes¹⁴⁰, I. Lopez Paz¹², J. Lorenz¹⁰⁰, N. Lorenzo Martinez⁶¹, M. Losada¹⁶³,
 P. Loscutoff¹⁵, P.J. Lösel¹⁰⁰, X. Lou^{33a}, A. Lounis¹¹⁷, J. Love⁶, P.A. Love⁷², N. Lu⁸⁹,
 H.J. Lubatti¹³⁹, C. Luci^{133a,133b}, A. Lucotte⁵⁵, F. Luehring⁶¹, W. Lukas⁶²,
 L. Luminari^{133a}, O. Lundberg^{147a,147b}, B. Lund-Jensen¹⁴⁸, M. Lungwitz⁸³, D. Lynn²⁵,
 R. Lysak¹²⁷, E. Lytken⁸¹, H. Ma²⁵, L.L. Ma^{33d}, G. Maccarrone⁴⁷, A. Macchiolo¹⁰¹,
 C.M. Macdonald¹⁴⁰, J. Machado Miguens^{122,126b}, D. Macina³⁰, D. Madaffari⁸⁵,
 R. Madar³⁴, H.J. Maddocks⁷², W.F. Mader⁴⁴, A. Madsen¹⁶⁷, S. Maeland¹⁴, T. Maeno²⁵,
 A. Maevskiy⁹⁹, E. Magradze⁵⁴, K. Mahboubi⁴⁸, J. Mahlstedt¹⁰⁷, S. Mahmoud⁷⁴,
 C. Maiani¹³⁷, C. Maidantchik^{24a}, A.A. Maier¹⁰¹, T. Maier¹⁰⁰, A. Maio^{126a,126b,126d},
 S. Majewski¹¹⁶, Y. Makida⁶⁶, N. Makovec¹¹⁷, B. Malaescu⁸⁰, Pa. Malecki³⁹,
 V.P. Maleev¹²³, F. Malek⁵⁵, U. Mallik⁶³, D. Malon⁶, C. Malone¹⁴⁴, S. Maltezos¹⁰,
 V.M. Malyshev¹⁰⁹, S. Malyukov³⁰, J. Mamuzic⁴², G. Mancini⁴⁷, B. Mandelli³⁰,
 L. Mandelli^{91a}, I. Mandić⁷⁵, R. Mandrysch⁶³, J. Maneira^{126a,126b}, A. Manfredini¹⁰¹,
 L. Manhaes de Andrade Filho^{24b}, J. Manjarres Ramos^{160b}, A. Mann¹⁰⁰, P.M. Manning¹³⁸,

A. Manousakis-Katsikakis⁹, B. Mansoulie¹³⁷, R. Mantifel⁸⁷, M. Mantoani⁵⁴, L. Mapelli³⁰,
 L. March^{146c}, G. Marchiori⁸⁰, M. Marcisovsky¹²⁷, C.P. Marino¹⁷⁰, M. Marjanovic¹³,
 F. Marroquim^{24a}, S.P. Marsden⁸⁴, Z. Marshall¹⁵, L.F. Marti¹⁷, S. Marti-Garcia¹⁶⁸,
 B. Martin⁹⁰, T.A. Martin¹⁷¹, V.J. Martin⁴⁶, B. Martin dit Latour¹⁴, H. Martinez¹³⁷,
 M. Martinez^{12,o}, S. Martin-Haugh¹³¹, V.S. Martoiu^{26a}, A.C. Martyniuk⁷⁸, M. Marx¹³⁹,
 F. Marzano^{133a}, A. Marzin³⁰, L. Masetti⁸³, T. Mashimo¹⁵⁶, R. Mashinistov⁹⁶, J. Masik⁸⁴,
 A.L. Maslennikov^{109,c}, I. Massa^{20a,20b}, L. Massa^{20a,20b}, N. Massol⁵, P. Mastrandrea¹⁴⁹,
 A. Mastroberardino^{37a,37b}, T. Masubuchi¹⁵⁶, P. Mättig¹⁷⁶, J. Mattmann⁸³, J. Maurer^{26a},
 S.J. Maxfield⁷⁴, D.A. Maximov^{109,c}, R. Mazini¹⁵², S.M. Mazza^{91a,91b},
 L. Mazzaferro^{134a,134b}, G. Mc Goldrick¹⁵⁹, S.P. Mc Kee⁸⁹, A. McCarn⁸⁹,
 R.L. McCarthy¹⁴⁹, T.G. McCarthy²⁹, N.A. McCubbin¹³¹, K.W. McFarlane^{56,*},
 J.A. Mcfayden⁷⁸, G. Mchedlidze⁵⁴, S.J. McMahon¹³¹, R.A. McPherson^{170,k},
 M. Medinnis⁴², S. Meehan^{146a}, S. Mehlhase¹⁰⁰, A. Mehta⁷⁴, K. Meier^{58a}, C. Meineck¹⁰⁰,
 B. Meirose⁴¹, C. Melachrinou³¹, B.R. Mellado Garcia^{146c}, F. Meloni¹⁷,
 A. Mengarelli^{20a,20b}, S. Menke¹⁰¹, E. Meoni¹⁶², K.M. Mercurio⁵⁷, S. Mergelmeyer²¹,
 N. Meric¹³⁷, P. Mermod⁴⁹, L. Merola^{104a,104b}, C. Meroni^{91a}, F.S. Merritt³¹, H. Merritt¹¹¹,
 A. Messina^{133a,133b}, J. Metcalfe²⁵, A.S. Mete¹⁶⁴, C. Meyer⁸³, C. Meyer¹²², J-P. Meyer¹³⁷,
 J. Meyer¹⁰⁷, R.P. Middleton¹³¹, S. Miglioranza^{165a,165c}, L. Mijović²¹, G. Mikenberg¹⁷³,
 M. Mikestikova¹²⁷, M. Mikuz⁷⁵, M. Milesi⁸⁸, A. Milic³⁰, D.W. Miller³¹, C. Mills⁴⁶,
 A. Milov¹⁷³, D.A. Milstead^{147a,147b}, A.A. Minaenko¹³⁰, Y. Minami¹⁵⁶, I.A. Minashvili⁶⁵,
 A.I. Mincer¹¹⁰, B. Mindur^{38a}, M. Mineev⁶⁵, Y. Ming¹⁷⁴, L.M. Mir¹², G. Mirabelli^{133a},
 T. Mitani¹⁷², J. Mitrevski¹⁰⁰, V.A. Mitsou¹⁶⁸, A. Miucci⁴⁹, P.S. Miyagawa¹⁴⁰,
 J.U. Mjörnmärk⁸¹, T. Moa^{147a,147b}, K. Mochizuki⁸⁵, S. Mohapatra³⁵, W. Mohr⁴⁸,
 S. Molander^{147a,147b}, R. Moles-Valls¹⁶⁸, K. Mönig⁴², C. Monini⁵⁵, J. Monk³⁶,
 E. Monnier⁸⁵, J. Montejó Berlingen¹², F. Monticelli⁷¹, S. Monzani^{133a,133b}, R.W. Moore³,
 N. Morange¹¹⁷, D. Moreno¹⁶³, M. Moreno Llácer⁵⁴, P. Morettini^{50a}, M. Morgenstern⁴⁴,
 M. Morii⁵⁷, V. Morisbak¹¹⁹, S. Moritz⁸³, A.K. Morley¹⁴⁸, G. Mornacchi³⁰, J.D. Morris⁷⁶,
 A. Morton⁵³, L. Morvaj¹⁰³, H.G. Moser¹⁰¹, M. Mosidze^{51b}, J. Moss¹¹¹, K. Motohashi¹⁵⁸,
 R. Mount¹⁴⁴, E. Mountricha²⁵, S.V. Mouraviev^{96,*}, E.J.W. Moyse⁸⁶, S. Muanza⁸⁵,
 R.D. Mudd¹⁸, F. Mueller¹⁰¹, J. Mueller¹²⁵, K. Mueller²¹, R.S.P. Mueller¹⁰⁰, T. Mueller²⁸,
 D. Muenstermann⁴⁹, P. Mullen⁵³, Y. Munwes¹⁵⁴, J.A. Murillo Quijada¹⁸,
 W.J. Murray^{171,131}, H. Musheghyan⁵⁴, E. Musto¹⁵³, A.G. Myagkov^{130,aa}, M. Myska¹²⁸,
 O. Nackenhorst⁵⁴, J. Nadal⁵⁴, K. Nagai¹²⁰, R. Nagai¹⁵⁸, Y. Nagai⁸⁵, K. Nagano⁶⁶,
 A. Nagarkar¹¹¹, Y. Nagasaka⁵⁹, K. Nagata¹⁶¹, M. Nagel¹⁰¹, E. Nagy⁸⁵, A.M. Nairz³⁰,
 Y. Nakahama³⁰, K. Nakamura⁶⁶, T. Nakamura¹⁵⁶, I. Nakano¹¹², H. Namasivayam⁴¹,
 G. Nanava²¹, R.F. Naranjo Garcia⁴², R. Narayan^{58b}, T. Nattermann²¹, T. Naumann⁴²,
 G. Navarro¹⁶³, R. Nayyar⁷, H.A. Neal⁸⁹, P.Yu. Nechaeva⁹⁶, T.J. Neep⁸⁴, P.D. Nef¹⁴⁴,
 A. Negri^{121a,121b}, M. Negrini^{20a}, S. Nektarijevic¹⁰⁶, C. Nellist¹¹⁷, A. Nelson¹⁶⁴,
 S. Nemecek¹²⁷, P. Nemethy¹¹⁰, A.A. Nepomuceno^{24a}, M. Nessi^{30,ab}, M.S. Neubauer¹⁶⁶,
 M. Neumann¹⁷⁶, R.M. Neves¹¹⁰, P. Nevski²⁵, P.R. Newman¹⁸, D.H. Nguyen⁶,
 R.B. Nickerson¹²⁰, R. Nicolaidou¹³⁷, B. Nicquevert³⁰, J. Nielsen¹³⁸, N. Nikiforou³⁵,
 A. Nikiforov¹⁶, V. Nikolaenko^{130,aa}, I. Nikolic-Audit⁸⁰, K. Nikolopoulos¹⁸, J.K. Nilsen¹¹⁹,
 P. Nilsson²⁵, Y. Ninomiya¹⁵⁶, A. Nisati^{133a}, R. Nisius¹⁰¹, T. Nobe¹⁵⁸, M. Nomachi¹¹⁸,

I. Nomidis²⁹, T. Nooney⁷⁶, S. Norberg¹¹³, M. Nordberg³⁰, O. Novgorodova⁴⁴,
 S. Nowak¹⁰¹, M. Nozaki⁶⁶, L. Nozka¹¹⁵, K. Ntekas¹⁰, G. Nunes Hanninger⁸⁸,
 T. Nunnemann¹⁰⁰, E. Nurse⁷⁸, F. Nuti⁸⁸, B.J. O'Brien⁴⁶, F. O'grady⁷, D.C. O'Neil¹⁴³,
 V. O'Shea⁵³, F.G. Oakham^{29,d}, H. Oberlack¹⁰¹, T. Obermann²¹, J. Ocariz⁸⁰, A. Ochi⁶⁷,
 I. Ochoa⁷⁸, S. Oda⁷⁰, S. Odaka⁶⁶, H. Ogren⁶¹, A. Oh⁸⁴, S.H. Oh⁴⁵, C.C. Ohm¹⁵,
 H. Ohman¹⁶⁷, H. Oide³⁰, W. Okamura¹¹⁸, H. Okawa¹⁶¹, Y. Okumura³¹, T. Okuyama¹⁵⁶,
 A. Olariu^{26a}, S.A. Olivares Pino⁴⁶, D. Oliveira Damazio²⁵, E. Oliver Garcia¹⁶⁸,
 A. Olszewski³⁹, J. Olszowska³⁹, A. Onofre^{126a,126e}, P.U.E. Onyisi^{31,q}, C.J. Oram^{160a},
 M.J. Oreglia³¹, Y. Oren¹⁵⁴, D. Orestano^{135a,135b}, N. Orlando¹⁵⁵, C. Oropeza Barrera⁵³,
 R.S. Orr¹⁵⁹, B. Osculati^{50a,50b}, R. Ospanov⁸⁴, G. Otero y Garzon²⁷, H. Otono⁷⁰,
 M. Ouchrif^{136d}, E.A. Ouellette¹⁷⁰, F. Ould-Saada¹¹⁹, A. Ouraou¹³⁷, K.P. Oussoren¹⁰⁷,
 Q. Ouyang^{33a}, A. Ovcharova¹⁵, M. Owen⁵³, R.E. Owen¹⁸, V.E. Ozcan^{19a}, N. Ozturk⁸,
 K. Pachal¹²⁰, A. Pacheco Pages¹², C. Padilla Aranda¹², M. Pagáčová⁴⁸, S. Pagan Griso¹⁵,
 E. Paganis¹⁴⁰, C. Pahl¹⁰¹, F. Paige²⁵, P. Pais⁸⁶, K. Pajchel¹¹⁹, G. Palacino^{160b},
 S. Palestini³⁰, M. Palka^{38b}, D. Pallin³⁴, A. Palma^{126a,126b}, Y.B. Pan¹⁷⁴,
 E. Panagiotopoulou¹⁰, C.E. Pandini⁸⁰, J.G. Panduro Vazquez⁷⁷, P. Pani^{147a,147b},
 S. Panitkin²⁵, L. Paolozzi^{134a,134b}, Th.D. Papadopoulou¹⁰, K. Papageorgiou¹⁵⁵,
 A. Paramonov⁶, D. Paredes Hernandez¹⁵⁵, M.A. Parker²⁸, K.A. Parker¹⁴⁰,
 F. Parodi^{50a,50b}, J.A. Parsons³⁵, U. Parzefall⁴⁸, E. Pasqualucci^{133a}, S. Passaggio^{50a},
 F. Pastore^{135a,135b,*}, Fr. Pastore⁷⁷, G. Pásztor²⁹, S. Patariaia¹⁷⁶, N.D. Patel¹⁵¹,
 J.R. Pater⁸⁴, T. Pauly³⁰, J. Pearce¹⁷⁰, B. Pearson¹¹³, L.E. Pedersen³⁶, M. Pedersen¹¹⁹,
 S. Pedraza Lopez¹⁶⁸, R. Pedro^{126a,126b}, S.V. Peleganchuk¹⁰⁹, D. Pelikan¹⁶⁷, H. Peng^{33b},
 B. Penning³¹, J. Penwell⁶¹, D.V. Perepelitsa²⁵, E. Perez Codina^{160a},
 M.T. Pérez García-Estañ¹⁶⁸, L. Perini^{91a,91b}, H. Pernegger³⁰, S. Perrella^{104a,104b},
 R. Peschke⁴², V.D. Peshekhonov⁶⁵, K. Peters³⁰, R.F.Y. Peters⁸⁴, B.A. Petersen³⁰,
 T.C. Petersen³⁶, E. Petit⁴², A. Petridis^{147a,147b}, C. Petridou¹⁵⁵, E. Petrolo^{133a},
 F. Petrucci^{135a,135b}, N.E. Pettersson¹⁵⁸, R. Pezoa^{32b}, P.W. Phillips¹³¹, G. Piacquadio¹⁴⁴,
 E. Pianori¹⁷¹, A. Picazio⁴⁹, E. Piccaro⁷⁶, M. Piccinini^{20a,20b}, M.A. Pickering¹²⁰,
 R. Piegaia²⁷, D.T. Pignotti¹¹¹, J.E. Pilcher³¹, A.D. Pilkington⁷⁸, J. Pina^{126a,126b,126d},
 M. Pinamonti^{165a,165c,ac}, J.L. Pinfold³, A. Pingel³⁶, B. Pinto^{126a}, S. Pires⁸⁰, M. Pitt¹⁷³,
 C. Pizio^{91a,91b}, L. Plazak^{145a}, M.-A. Pleier²⁵, V. Pleskot¹²⁹, E. Plotnikova⁶⁵,
 P. Plucinski^{147a,147b}, D. Pluth⁶⁴, R. Poettgen⁸³, L. Poggioli¹¹⁷, D. Pohl²¹,
 G. Polesello^{121a}, A. Policicchio^{37a,37b}, R. Polifka¹⁵⁹, A. Polini^{20a}, C.S. Pollard⁵³,
 V. Polychronakos²⁵, K. Pommès³⁰, L. Pontecorvo^{133a}, B.G. Pope⁹⁰, G.A. Popeneciu^{26b},
 D.S. Popovic¹³, A. Poppleton³⁰, S. Pospisil¹²⁸, K. Potamianos¹⁵, I.N. Potrap⁶⁵,
 C.J. Potter¹⁵⁰, C.T. Potter¹¹⁶, G. Poulard³⁰, J. Poveda³⁰, V. Pozdnyakov⁶⁵,
 P. Pralavorio⁸⁵, A. Pranko¹⁵, S. Prasad³⁰, S. Prell⁶⁴, D. Price⁸⁴, J. Price⁷⁴, L.E. Price⁶,
 M. Primavera^{73a}, S. Prince⁸⁷, M. Proissl⁴⁶, K. Prokofiev^{60c}, F. Prokoshin^{32b},
 E. Protopapadaki¹³⁷, S. Protopopescu²⁵, J. Proudfoot⁶, M. Przybycien^{38a}, E. Ptacek¹¹⁶,
 D. Puddu^{135a,135b}, E. Pueschel⁸⁶, D. Poldon¹⁴⁹, M. Purohit^{25,ad}, P. Puzo¹¹⁷, J. Qian⁸⁹,
 G. Qin⁵³, Y. Qin⁸⁴, A. Quadt⁵⁴, D.R. Quarrie¹⁵, W.B. Quayle^{165a,165b},
 M. Queitsch-Maitland⁸⁴, D. Quilty⁵³, A. Qureshi^{160b}, V. Radeka²⁵, V. Radescu⁴²,
 S.K. Radhakrishnan¹⁴⁹, P. Radloff¹¹⁶, P. Rados⁸⁸, F. Ragusa^{91a,91b}, G. Rahal¹⁷⁹,

S. Rajagopalan²⁵, M. Rammensee³⁰, C. Rangel-Smith¹⁶⁷, F. Rauscher¹⁰⁰, S. Rave⁸³,
 T.C. Rave⁴⁸, T. Ravenscroft⁵³, M. Raymond³⁰, A.L. Read¹¹⁹, N.P. Readioff⁷⁴,
 D.M. Rebuffi^{121a,121b}, A. Redelbach¹⁷⁵, G. Redlinger²⁵, R. Reece¹³⁸, K. Reeves⁴¹,
 L. Rehnisch¹⁶, H. Reisin²⁷, M. Relich¹⁶⁴, C. Rembser³⁰, H. Ren^{33a}, A. Renaud¹¹⁷,
 M. Rescigno^{133a}, S. Resconi^{91a}, O.L. Rezanova^{109,c}, P. Reznicek¹²⁹, R. Rezvani⁹⁵,
 R. Richter¹⁰¹, S. Richter⁷⁸, E. Richter-Was^{38b}, M. Ridel⁸⁰, P. Rieck¹⁶, C.J. Riegel¹⁷⁶,
 J. Rieger⁵⁴, M. Rijssenbeek¹⁴⁹, A. Rimoldi^{121a,121b}, L. Rinaldi^{20a}, E. Ritsch⁶², I. Riu¹²,
 F. Rizatdinova¹¹⁴, E. Rizvi⁷⁶, S.H. Robertson^{87,k}, A. Robichaud-Veronneau⁸⁷,
 D. Robinson²⁸, J.E.M. Robinson⁸⁴, A. Robson⁵³, C. Roda^{124a,124b}, L. Rodrigues³⁰,
 S. Roe³⁰, O. Røhne¹¹⁹, S. Rolli¹⁶², A. Romaniouk⁹⁸, M. Romano^{20a,20b},
 S.M. Romano Saez³⁴, E. Romero Adam¹⁶⁸, N. Rompotis¹³⁹, M. Ronzani⁴⁸, L. Roos⁸⁰,
 E. Ros¹⁶⁸, S. Rosati^{133a}, K. Rosbach⁴⁸, P. Rose¹³⁸, P.L. Rosendahl¹⁴, O. Rosenthal¹⁴²,
 V. Rossetti^{147a,147b}, E. Rossi^{104a,104b}, L.P. Rossi^{50a}, R. Rosten¹³⁹, M. Rotaru^{26a},
 I. Roth¹⁷³, J. Rothberg¹³⁹, D. Rousseau¹¹⁷, C.R. Royon¹³⁷, A. Rozanov⁸⁵, Y. Rozen¹⁵³,
 X. Ruan^{146c}, F. Rubbo¹⁴⁴, I. Rubinskiy⁴², V.I. Rud⁹⁹, C. Rudolph⁴⁴, M.S. Rudolph¹⁵⁹,
 F. Rühr⁴⁸, A. Ruiz-Martinez³⁰, Z. Rurikova⁴⁸, N.A. Rusakovich⁶⁵, A. Ruschke¹⁰⁰,
 H.L. Russell¹³⁹, J.P. Rutherford⁷, N. Ruthmann⁴⁸, Y.F. Ryabov¹²³, M. Rybar¹²⁹,
 G. Rybkin¹¹⁷, N.C. Ryder¹²⁰, A.F. Saavedra¹⁵¹, G. Sabato¹⁰⁷, S. Sacerdoti²⁷,
 A. Saddique³, H.F.W. Sadrozinski¹³⁸, R. Sadykov⁶⁵, F. Safai Tehrani^{133a},
 M. Saimpert¹³⁷, H. Sakamoto¹⁵⁶, Y. Sakurai¹⁷², G. Salamanna^{135a,135b}, A. Salamon^{134a},
 M. Saleem¹¹³, D. Salek¹⁰⁷, P.H. Sales De Bruin¹³⁹, D. Salihagic¹⁰¹, A. Salnikov¹⁴⁴,
 J. Salt¹⁶⁸, D. Salvatore^{37a,37b}, F. Salvatore¹⁵⁰, A. Salvucci¹⁰⁶, A. Salzburger³⁰,
 D. Sampsonidis¹⁵⁵, A. Sanchez^{104a,104b}, J. Sánchez¹⁶⁸, V. Sanchez Martinez¹⁶⁸,
 H. Sandaker¹⁴, R.L. Sandbach⁷⁶, H.G. Sander⁸³, M.P. Sanders¹⁰⁰, M. Sandhoff¹⁷⁶,
 C. Sandoval¹⁶³, R. Sandstroem¹⁰¹, D.P.C. Sankey¹³¹, A. Sansoni⁴⁷, C. Santoni³⁴,
 R. Santonico^{134a,134b}, H. Santos^{126a}, I. Santoyo Castillo¹⁵⁰, K. Sapp¹²⁵, A. Sapronov⁶⁵,
 J.G. Saraiva^{126a,126d}, B. Sarrazin²¹, O. Sasaki⁶⁶, Y. Sasaki¹⁵⁶, K. Sato¹⁶¹, G. Sauvage^{5,*},
 E. Sauvan⁵, G. Savage⁷⁷, P. Savard^{159,d}, C. Sawyer¹²⁰, L. Sawyer^{79,n}, J. Saxon³¹,
 C. Sbarra^{20a}, A. Sbrizzi^{20a,20b}, T. Scanlon⁷⁸, D.A. Scannicchio¹⁶⁴, M. Scarcella¹⁵¹,
 V. Scarfone^{37a,37b}, J. Schaarschmidt¹⁷³, P. Schacht¹⁰¹, D. Schaefer³⁰, R. Schaefer⁴²,
 J. Schaeffer⁸³, S. Schaepe²¹, S. Schaetzel^{58b}, U. Schäfer⁸³, A.C. Schaffer¹¹⁷, D. Schaile¹⁰⁰,
 R.D. Schamberger¹⁴⁹, V. Scharf^{58a}, V.A. Schegelsky¹²³, D. Scheirich¹²⁹, M. Schernau¹⁶⁴,
 C. Schiavi^{50a,50b}, C. Schillo⁴⁸, M. Schioppa^{37a,37b}, S. Schlenker³⁰, E. Schmidt⁴⁸,
 K. Schmieden³⁰, C. Schmitt⁸³, S. Schmitt^{58b}, S. Schmitt⁴², B. Schneider^{160a},
 Y.J. Schnellbach⁷⁴, U. Schnoor⁴⁴, L. Schoeffel¹³⁷, A. Schoening^{58b}, B.D. Schoenrock⁹⁰,
 E. Schopf²¹, A.L.S. Schorlemmer⁵⁴, M. Schott⁸³, D. Schouten^{160a}, J. Schovancova⁸,
 S. Schramm¹⁵⁹, M. Schreyer¹⁷⁵, C. Schroeder⁸³, N. Schuh⁸³, M.J. Schultens²¹,
 H.-C. Schultz-Coulon^{58a}, H. Schulz¹⁶, M. Schumacher⁴⁸, B.A. Schumm¹³⁸, Ph. Schune¹³⁷,
 C. Schwanenberger⁸⁴, A. Schwartzman¹⁴⁴, T.A. Schwarz⁸⁹, Ph. Schwegler¹⁰¹,
 Ph. Schwemling¹³⁷, R. Schwienhorst⁹⁰, J. Schwindling¹³⁷, T. Schwindt²¹, M. Schwoerer⁵,
 F.G. Sciacca¹⁷, E. Scifo¹¹⁷, G. Sciolla²³, F. Scuri^{124a,124b}, F. Scutti²¹, J. Searcy⁸⁹,
 G. Sedov⁴², E. Sedykh¹²³, P. Seema²¹, S.C. Seidel¹⁰⁵, A. Seiden¹³⁸, F. Seifert¹²⁸,
 J.M. Seixas^{24a}, G. Sekhniaidze^{104a}, S.J. Sekula⁴⁰, K.E. Selbach⁴⁶, D.M. Seliverstov^{123,*},

N. Semprini-Cesari^{20a,20b}, C. Serfon³⁰, L. Serin¹¹⁷, L. Serkin⁵⁴, T. Serre⁸⁵, R. Seuster^{160a},
 H. Severini¹¹³, T. Sfiligoj⁷⁵, F. Sforza¹⁰¹, A. Sfyrta³⁰, E. Shabalina⁵⁴, M. Shamim¹¹⁶,
 L.Y. Shan^{33a}, R. Shang¹⁶⁶, J.T. Shank²², M. Shapiro¹⁵, P.B. Shatalov⁹⁷, K. Shaw^{165a,165b},
 A. Shcherbakova^{147a,147b}, C.Y. Shehu¹⁵⁰, P. Sherwood⁷⁸, L. Shi^{152,ae}, S. Shimizu⁶⁷,
 C.O. Shimmin¹⁶⁴, M. Shimojima¹⁰², M. Shiyakova⁶⁵, A. Shmeleva⁹⁶, D. Shoaleh Saadi⁹⁵,
 M.J. Shochet³¹, S. Shojaii^{91a,91b}, S. Shrestha¹¹¹, E. Shulga⁹⁸, M.A. Shupe⁷,
 S. Shushkevich⁴², P. Sicho¹²⁷, O. Sidiropoulou¹⁷⁵, D. Sidorov¹¹⁴, A. Sidoti^{20a,20b},
 F. Siegert⁴⁴, Dj. Sijacki¹³, J. Silva^{126a,126d}, Y. Silver¹⁵⁴, D. Silverstein¹⁴⁴,
 S.B. Silverstein^{147a}, V. Simak¹²⁸, O. Simard⁵, Lj. Simic¹³, S. Simion¹¹⁷, E. Simioni⁸³,
 B. Simmons⁷⁸, D. Simon³⁴, R. Simoniello^{91a,91b}, P. Sinervo¹⁵⁹, N.B. Sinev¹¹⁶,
 G. Siragusa¹⁷⁵, A.N. Sisakyan^{65,*}, S.Yu. Sivoklokov⁹⁹, J. Sjölin^{147a,147b}, T.B. Sjursen¹⁴,
 M.B. Skinner⁷², H.P. Skottowe⁵⁷, P. Skubic¹¹³, M. Slater¹⁸, T. Slavicek¹²⁸,
 M. Slawinska¹⁰⁷, K. Sliwa¹⁶², V. Smakhtin¹⁷³, B.H. Smart⁴⁶, L. Smestad¹⁴,
 S.Yu. Smirnov⁹⁸, Y. Smirnov⁹⁸, L.N. Smirnova^{99,af}, O. Smirnova⁸¹, M.N.K. Smith³⁵,
 M. Smizanska⁷², K. Smolek¹²⁸, A.A. Snesarev⁹⁶, G. Snidero⁷⁶, S. Snyder²⁵, R. Sobie^{170,k},
 F. Socher⁴⁴, A. Soffer¹⁵⁴, D.A. Soh^{152,ae}, C.A. Solans³⁰, M. Solar¹²⁸, J. Solc¹²⁸,
 E.Yu. Soldatov⁹⁸, U. Soldevila¹⁶⁸, A.A. Solodkov¹³⁰, A. Soloshenko⁶⁵,
 O.V. Solovyanov¹³⁰, V. Solovyeu¹²³, P. Sommer⁴⁸, H.Y. Song^{33b}, N. Soni¹, A. Sood¹⁵,
 A. Sopczak¹²⁸, B. Sopko¹²⁸, V. Sopko¹²⁸, V. Sorin¹², D. Sosa^{58b}, M. Sosebee⁸,
 C.L. Sotiropoulou¹⁵⁵, R. Soualah^{165a,165c}, P. Soueid⁹⁵, A.M. Soukharev^{109,c}, D. South⁴²,
 S. Spagnolo^{73a,73b}, F. Spanò⁷⁷, W.R. Spearman⁵⁷, F. Spettel¹⁰¹, R. Spighi^{20a}, G. Spigo³⁰,
 L.A. Spiller⁸⁸, M. Spusta¹²⁹, T. Spreitzer¹⁵⁹, R.D. St. Denis^{53,*}, S. Staerz⁴⁴,
 J. Stahlman¹²², R. Stamen^{58a}, S. Stamm¹⁶, E. Stanecka³⁹, C. Stanescu^{135a},
 M. Stanescu-Bellu⁴², M.M. Stanitzki⁴², S. Stapnes¹¹⁹, E.A. Starchenko¹³⁰, J. Stark⁵⁵,
 P. Staroba¹²⁷, P. Starovoitov⁴², R. Staszewski³⁹, P. Stavina^{145a,*}, P. Steinberg²⁵,
 B. Stelzer¹⁴³, H.J. Stelzer³⁰, O. Stelzer-Chilton^{160a}, H. Stenzel⁵², S. Stern¹⁰¹,
 G.A. Stewart⁵³, J.A. Stillings²¹, M.C. Stockton⁸⁷, M. Stoebe⁸⁷, G. Stoicea^{26a}, P. Stolte⁵⁴,
 S. Stonjek¹⁰¹, A.R. Stradling⁸, A. Straessner⁴⁴, M.E. Stramaglia¹⁷, J. Strandberg¹⁴⁸,
 S. Strandberg^{147a,147b}, A. Strandlie¹¹⁹, E. Strauss¹⁴⁴, M. Strauss¹¹³, P. Strizenec^{145b},
 R. Ströhmer¹⁷⁵, D.M. Strom¹¹⁶, R. Stroynowski⁴⁰, A. Strubig¹⁰⁶, S.A. Stucci¹⁷,
 B. Stugu¹⁴, N.A. Styles⁴², D. Su¹⁴⁴, J. Su¹²⁵, R. Subramaniam⁷⁹, A. Succurro¹²,
 Y. Sugaya¹¹⁸, C. Suhr¹⁰⁸, M. Suk¹²⁸, V.V. Sulin⁹⁶, S. Sultansoy^{4d}, T. Sumida⁶⁸, S. Sun⁵⁷,
 X. Sun^{33a}, J.E. Sundermann⁴⁸, K. Suruliz¹⁵⁰, G. Susinno^{37a,37b}, M.R. Sutton¹⁵⁰,
 Y. Suzuki⁶⁶, M. Svatos¹²⁷, S. Swedish¹⁶⁹, M. Swiatlowski¹⁴⁴, I. Sykora^{145a}, T. Sykora¹²⁹,
 D. Ta⁹⁰, C. Taccini^{135a,135b}, K. Tackmann⁴², J. Taenzer¹⁵⁹, A. Taffard¹⁶⁴, R. Tafirout^{160a},
 N. Taiblum¹⁵⁴, H. Takai²⁵, R. Takashima⁶⁹, H. Takeda⁶⁷, T. Takeshita¹⁴¹, Y. Takubo⁶⁶,
 M. Talby⁸⁵, A.A. Talyshchev^{109,c}, J.Y.C. Tam¹⁷⁵, K.G. Tan⁸⁸, J. Tanaka¹⁵⁶, R. Tanaka¹¹⁷,
 S. Tanaka¹³², S. Tanaka⁶⁶, A.J. Tanasijczuk¹⁴³, B.B. Tannenwald¹¹¹, N. Tannoury²¹,
 S. Tapprogge⁸³, S. Tarem¹⁵³, F. Tarrade²⁹, G.F. Tartarelli^{91a}, P. Tas¹²⁹, M. Tasevsky¹²⁷,
 T. Tashiro⁶⁸, E. Tassi^{37a,37b}, A. Tavares Delgado^{126a,126b}, Y. Tayalati^{136d}, F.E. Taylor⁹⁴,
 G.N. Taylor⁸⁸, W. Taylor^{160b}, F.A. Teischinger³⁰, M. Teixeira Dias Castanheira⁷⁶,
 P. Teixeira-Dias⁷⁷, K.K. Temming⁴⁸, H. Ten Kate³⁰, P.K. Teng¹⁵², J.J. Teoh¹¹⁸,
 F. Tepel¹⁷⁶, S. Terada⁶⁶, K. Terashi¹⁵⁶, J. Terron⁸², S. Terzo¹⁰¹, M. Testa⁴⁷,

R.J. Teuscher^{159,k}, J. Therhaag²¹, T. Thevenaux-Pelzer³⁴, J.P. Thomas¹⁸,
 J. Thomas-Wilsker⁷⁷, E.N. Thompson³⁵, P.D. Thompson¹⁸, R.J. Thompson⁸⁴,
 A.S. Thompson⁵³, L.A. Thomsen³⁶, E. Thomson¹²², M. Thomson²⁸, R.P. Thun^{89,*},
 F. Tian³⁵, M.J. Tibbetts¹⁵, R.E. Ticse Torres⁸⁵, V.O. Tikhomirov^{96,ag},
 Yu.A. Tikhonov^{109,c}, S. Timoshenko⁹⁸, E. Tiouchichine⁸⁵, P. Tipton¹⁷⁷, S. Tisserant⁸⁵,
 T. Todorov^{5,*}, S. Todorova-Nova¹²⁹, J. Tojo⁷⁰, S. Tokár^{145a}, K. Tokushuku⁶⁶,
 K. Tollefson⁹⁰, E. Tolley⁵⁷, L. Tomlinson⁸⁴, M. Tomoto¹⁰³, L. Tompkins^{144,ah},
 K. Toms¹⁰⁵, E. Torrence¹¹⁶, H. Torres¹⁴³, E. Torró Pastor¹⁶⁸, J. Toth^{85,ai}, F. Touchard⁸⁵,
 D.R. Tovey¹⁴⁰, H.L. Tran¹¹⁷, T. Trefzger¹⁷⁵, L. Tremblet³⁰, A. Tricoli³⁰, I.M. Trigger^{160a},
 S. Trincaz-Duvoid⁸⁰, M.F. Tripania¹², W. Trischuk¹⁵⁹, B. Trocmé⁵⁵, C. Troncon^{91a},
 M. Trottier-McDonald¹⁵, M. Trovatelli^{135a,135b}, P. True⁹⁰, M. Trzebinski³⁹, A. Trzupek³⁹,
 C. Tsarouchas³⁰, J.C-L. Tseng¹²⁰, P.V. Tsiareshka⁹², D. Tsionou¹⁵⁵, G. Tsipolitis¹⁰,
 N. Tsirintanis⁹, S. Tsiskaridze¹², V. Tsiskaridze⁴⁸, E.G. Tskhadadze^{51a}, I.I. Tsukerman⁹⁷,
 V. Tsulaia¹⁵, S. Tsuno⁶⁶, D. Tsybychev¹⁴⁹, A. Tudorache^{26a}, V. Tudorache^{26a},
 A.N. Tuna¹²², S.A. Tupputi^{20a,20b}, S. Turchikhin^{99,af}, D. Turecek¹²⁸, R. Turra^{91a,91b},
 A.J. Turvey⁴⁰, P.M. Tuts³⁵, A. Tykhonov⁴⁹, M. Tylmad^{147a,147b}, M. Tyndel¹³¹,
 I. Ueda¹⁵⁶, R. Ueno²⁹, M. Ughetto^{147a,147b}, M. Ugland¹⁴, M. Uhlenbrock²¹,
 F. Ukegawa¹⁶¹, G. Unal³⁰, A. Undrus²⁵, G. Unel¹⁶⁴, F.C. Ungaro⁴⁸, Y. Unno⁶⁶,
 C. Unverdorben¹⁰⁰, J. Urban^{145b}, P. Urquijo⁸⁸, P. Urrejola⁸³, G. Usai⁸, A. Usanova⁶²,
 L. Vacavant⁸⁵, V. Vacek¹²⁸, B. Vachon⁸⁷, N. Valencic¹⁰⁷, S. Valentinetti^{20a,20b},
 A. Valero¹⁶⁸, L. Valery¹², S. Valkar¹²⁹, E. Valladolid Gallego¹⁶⁸, S. Vallecorsa⁴⁹,
 J.A. Valls Ferrer¹⁶⁸, W. Van Den Wollenberg¹⁰⁷, P.C. Van Der Deijl¹⁰⁷,
 R. van der Geer¹⁰⁷, H. van der Graaf¹⁰⁷, R. Van Der Leeuw¹⁰⁷, N. van Eldik¹⁵³,
 P. van Gemmeren⁶, J. Van Nieuwkoop¹⁴³, I. van Vulpen¹⁰⁷, M.C. van Woerden³⁰,
 M. Vanadia^{133a,133b}, W. Vandelli³⁰, R. Vanguri¹²², A. Vaniachine⁶, F. Vannucci⁸⁰,
 G. Vardanyan¹⁷⁸, R. Vari^{133a}, E.W. Varnes⁷, T. Varol⁴⁰, D. Varouchas⁸⁰, A. Vartapetian⁸,
 K.E. Varvell¹⁵¹, F. Vazeille³⁴, T. Vazquez Schroeder⁵⁴, J. Veatch⁷, F. Veloso^{126a,126c},
 T. Velz²¹, S. Veneziano^{133a}, A. Ventura^{73a,73b}, D. Ventura⁸⁶, M. Venturi¹⁷⁰, N. Venturi¹⁵⁹,
 A. Venturini²³, V. Vercesi^{121a}, M. Verducci^{133a,133b}, W. Verkerke¹⁰⁷, J.C. Vermeulen¹⁰⁷,
 A. Vest⁴⁴, M.C. Vetterli^{143,d}, O. Viazlo⁸¹, I. Vichou¹⁶⁶, T. Vickey^{146c,aj},
 O.E. Vickey Boeriu^{146c}, G.H.A. Viehhauser¹²⁰, S. Viel¹⁵, R. Vigne³⁰, M. Villa^{20a,20b},
 M. Villaplana Perez^{91a,91b}, E. Vilucchi⁴⁷, M.G. Vinciter²⁹, V.B. Vinogradov⁶⁵,
 I. Vivarelli¹⁵⁰, F. Vives Vaque³, S. Vlachos¹⁰, D. Vladoiu¹⁰⁰, M. Vlasak¹²⁸, M. Vogel^{32a},
 P. Vokac¹²⁸, G. Volpi^{124a,124b}, M. Volpi⁸⁸, H. von der Schmitt¹⁰¹, H. von Radziewski⁴⁸,
 E. von Toerne²¹, V. Vorobel¹²⁹, K. Vorobev⁹⁸, M. Vos¹⁶⁸, R. Voss³⁰, J.H. Vosseveld⁷⁴,
 N. Vranjes¹³, M. Vranjes Milosavljevic¹³, V. Vrba¹²⁷, M. Vreeswijk¹⁰⁷, R. Vuillermet³⁰,
 I. Vukotic³¹, Z. Vykydal¹²⁸, P. Wagner²¹, W. Wagner¹⁷⁶, H. Wahlberg⁷¹, S. Wahrmond⁴⁴,
 J. Wakabayashi¹⁰³, J. Walder⁷², R. Walker¹⁰⁰, W. Walkowiak¹⁴², C. Wang^{33c},
 F. Wang¹⁷⁴, H. Wang¹⁵, H. Wang⁴⁰, J. Wang⁴², J. Wang^{33a}, K. Wang⁸⁷, R. Wang⁶,
 S.M. Wang¹⁵², T. Wang²¹, X. Wang¹⁷⁷, C. Wanotayaroj¹¹⁶, A. Warburton⁸⁷,
 C.P. Ward²⁸, D.R. Wardrope⁷⁸, M. Warsinsky⁴⁸, A. Washbrook⁴⁶, C. Wasicki⁴²,
 P.M. Watkins¹⁸, A.T. Watson¹⁸, I.J. Watson¹⁵¹, M.F. Watson¹⁸, G. Watts¹³⁹, S. Watts⁸⁴,
 B.M. Waugh⁷⁸, S. Webb⁸⁴, M.S. Weber¹⁷, S.W. Weber¹⁷⁵, J.S. Webster³¹,

A.R. Weidberg¹²⁰, B. Weinert⁶¹, J. Weingarten⁵⁴, C. Weiser⁴⁸, H. Weits¹⁰⁷, P.S. Wells³⁰,
T. Wenaus²⁵, D. Wendland¹⁶, T. Wengler³⁰, S. Wenig³⁰, N. Wermes²¹, M. Werner⁴⁸,
P. Werner³⁰, M. Wessels^{58a}, J. Wetter¹⁶², K. Whalen²⁹, A.M. Wharton⁷², A. White⁸,
M.J. White¹, R. White^{32b}, S. White^{124a,124b}, D. Whiteson¹⁶⁴, D. Wicke¹⁷⁶,
F.J. Wickens¹³¹, W. Wiedenmann¹⁷⁴, M. Wielers¹³¹, P. Wienemann²¹, C. Wigglesworth³⁶,
L.A.M. Wiik-Fuchs²¹, A. Wildauer¹⁰¹, H.G. Wilkens³⁰, H.H. Williams¹²², S. Williams¹⁰⁷,
C. Willis⁹⁰, S. Willocq⁸⁶, A. Wilson⁸⁹, J.A. Wilson¹⁸, I. Wingerter-Seez⁵,
F. Winklmeier¹¹⁶, B.T. Winter²¹, M. Wittgen¹⁴⁴, J. Wittkowski¹⁰⁰, S.J. Wollstadt⁸³,
M.W. Wolter³⁹, H. Wolters^{126a,126c}, B.K. Wosiek³⁹, J. Wotschack³⁰, M.J. Woudstra⁸⁴,
K.W. Wozniak³⁹, M. Wu⁵⁵, M. Wu³¹, S.L. Wu¹⁷⁴, X. Wu⁴⁹, Y. Wu⁸⁹, T.R. Wyatt⁸⁴,
B.M. Wynne⁴⁶, S. Xella³⁶, D. Xu^{33a}, L. Xu^{33b,ak}, B. Yabsley¹⁵¹, S. Yacoub^{146b,al},
R. Yakabe⁶⁷, M. Yamada⁶⁶, Y. Yamaguchi¹¹⁸, A. Yamamoto⁶⁶, S. Yamamoto¹⁵⁶,
T. Yamanaka¹⁵⁶, K. Yamauchi¹⁰³, Y. Yamazaki⁶⁷, Z. Yan²², H. Yang^{33e}, H. Yang¹⁷⁴,
Y. Yang¹⁵², S. Yanush⁹³, L. Yao^{33a}, W-M. Yao¹⁵, Y. Yasu⁶⁶, E. Yatsenko⁴²,
K.H. Yau Wong²¹, J. Ye⁴⁰, S. Ye²⁵, I. Yeletsikh⁶⁵, A.L. Yen⁵⁷, E. Yildirim⁴²,
K. Yorita¹⁷², R. Yoshida⁶, K. Yoshihara¹²², C. Young¹⁴⁴, C.J.S. Young³⁰, S. Youssef²²,
D.R. Yu¹⁵, J. Yu⁸, J.M. Yu⁸⁹, J. Yu¹¹⁴, L. Yuan⁶⁷, A. Yurkewicz¹⁰⁸, I. Yusuff^{28,am},
B. Zabinski³⁹, R. Zaidan⁶³, A.M. Zaitsev^{130,aa}, A. Zaman¹⁴⁹, S. Zambito²³,
L. Zanello^{133a,133b}, D. Zanzi⁸⁸, C. Zeitnitz¹⁷⁶, M. Zeman¹²⁸, A. Zemla^{38a}, K. Zengel²³,
O. Zenin¹³⁰, T. Ženiš^{145a}, D. Zerwas¹¹⁷, D. Zhang⁸⁹, F. Zhang¹⁷⁴, J. Zhang⁶, L. Zhang¹⁵²,
R. Zhang^{33b}, X. Zhang^{33d}, Z. Zhang¹¹⁷, X. Zhao⁴⁰, Y. Zhao^{33d,117}, Z. Zhao^{33b},
A. Zhemchugov⁶⁵, J. Zhong¹²⁰, B. Zhou⁸⁹, C. Zhou⁴⁵, L. Zhou³⁵, L. Zhou⁴⁰, N. Zhou¹⁶⁴,
C.G. Zhu^{33d}, H. Zhu^{33a}, J. Zhu⁸⁹, Y. Zhu^{33b}, X. Zhuang^{33a}, K. Zhukov⁹⁶, A. Zibell¹⁷⁵,
D. Zieminska⁶¹, N.I. Zimine⁶⁵, C. Zimmermann⁸³, R. Zimmermann²¹, S. Zimmermann⁴⁸,
Z. Zinonos⁵⁴, M. Zinser⁸³, M. Ziolkowski¹⁴², L. Živković¹³, G. Zobernig¹⁷⁴,
A. Zoccoli^{20a,20b}, M. zur Nedden¹⁶, G. Zurzolo^{104a,104b}, L. Zwalinski³⁰.

¹ Department of Physics, University of Adelaide, Adelaide, Australia

² Physics Department, SUNY Albany, Albany NY, United States of America

³ Department of Physics, University of Alberta, Edmonton AB, Canada

⁴ ^(a) Department of Physics, Ankara University, Ankara; ^(c) Istanbul Aydin University, Istanbul; ^(d) Division of Physics, TOBB University of Economics and Technology, Ankara, Turkey

⁵ LAPP, CNRS/IN2P3 and Université de Savoie, Annecy-le-Vieux, France

⁶ High Energy Physics Division, Argonne National Laboratory, Argonne IL, United States of America

⁷ Department of Physics, University of Arizona, Tucson AZ, United States of America

⁸ Department of Physics, The University of Texas at Arlington, Arlington TX, United States of America

⁹ Physics Department, University of Athens, Athens, Greece

¹⁰ Physics Department, National Technical University of Athens, Zografou, Greece

¹¹ Institute of Physics, Azerbaijan Academy of Sciences, Baku, Azerbaijan

¹² Institut de Física d'Altes Energies and Departament de Física de la Universitat

Autònoma de Barcelona, Barcelona, Spain

¹³ Institute of Physics, University of Belgrade, Belgrade, Serbia

¹⁴ Department for Physics and Technology, University of Bergen, Bergen, Norway

¹⁵ Physics Division, Lawrence Berkeley National Laboratory and University of California, Berkeley CA, United States of America

¹⁶ Department of Physics, Humboldt University, Berlin, Germany

¹⁷ Albert Einstein Center for Fundamental Physics and Laboratory for High Energy Physics, University of Bern, Bern, Switzerland

¹⁸ School of Physics and Astronomy, University of Birmingham, Birmingham, United Kingdom

¹⁹ ^(a) Department of Physics, Bogazici University, Istanbul; ^(b) Department of Physics, Dogus University, Istanbul; ^(c) Department of Physics Engineering, Gaziantep University, Gaziantep, Turkey

²⁰ ^(a) INFN Sezione di Bologna; ^(b) Dipartimento di Fisica e Astronomia, Università di Bologna, Bologna, Italy

²¹ Physikalisches Institut, University of Bonn, Bonn, Germany

²² Department of Physics, Boston University, Boston MA, United States of America

²³ Department of Physics, Brandeis University, Waltham MA, United States of America

²⁴ ^(a) Universidade Federal do Rio De Janeiro COPPE/EE/IF, Rio de Janeiro; ^(b) Electrical Circuits Department, Federal University of Juiz de Fora (UFJF), Juiz de Fora; ^(c) Federal University of Sao Joao del Rei (UFSJ), Sao Joao del Rei; ^(d) Instituto de Fisica, Universidade de Sao Paulo, Sao Paulo, Brazil

²⁵ Physics Department, Brookhaven National Laboratory, Upton NY, United States of America

²⁶ ^(a) National Institute of Physics and Nuclear Engineering, Bucharest; ^(b) National Institute for Research and Development of Isotopic and Molecular Technologies, Physics Department, Cluj Napoca; ^(c) University Politehnica Bucharest, Bucharest; ^(d) West University in Timisoara, Timisoara, Romania

²⁷ Departamento de Física, Universidad de Buenos Aires, Buenos Aires, Argentina

²⁸ Cavendish Laboratory, University of Cambridge, Cambridge, United Kingdom

²⁹ Department of Physics, Carleton University, Ottawa ON, Canada

³⁰ CERN, Geneva, Switzerland

³¹ Enrico Fermi Institute, University of Chicago, Chicago IL, United States of America

³² ^(a) Departamento de Física, Pontificia Universidad Católica de Chile, Santiago; ^(b) Departamento de Física, Universidad Técnica Federico Santa María, Valparaíso, Chile

³³ ^(a) Institute of High Energy Physics, Chinese Academy of Sciences, Beijing; ^(b) Department of Modern Physics, University of Science and Technology of China, Anhui; ^(c) Department of Physics, Nanjing University, Jiangsu; ^(d) School of Physics, Shandong University, Shandong; ^(e) Department of Physics and Astronomy, Shanghai Key Laboratory for Particle Physics and Cosmology, Shanghai Jiao Tong University, Shanghai; ^(f) Physics Department, Tsinghua University, Beijing 100084, China

³⁴ Laboratoire de Physique Corpusculaire, Clermont Université and Université Blaise Pascal and CNRS/IN2P3, Clermont-Ferrand, France

- ³⁵ Nevis Laboratory, Columbia University, Irvington NY, United States of America
- ³⁶ Niels Bohr Institute, University of Copenhagen, Kobenhavn, Denmark
- ³⁷ ^(a) INFN Gruppo Collegato di Cosenza, Laboratori Nazionali di Frascati; ^(b) Dipartimento di Fisica, Università della Calabria, Rende, Italy
- ³⁸ ^(a) AGH University of Science and Technology, Faculty of Physics and Applied Computer Science, Krakow; ^(b) Marian Smoluchowski Institute of Physics, Jagiellonian University, Krakow, Poland
- ³⁹ Institute of Nuclear Physics Polish Academy of Sciences, Krakow, Poland
- ⁴⁰ Physics Department, Southern Methodist University, Dallas TX, United States of America
- ⁴¹ Physics Department, University of Texas at Dallas, Richardson TX, United States of America
- ⁴² DESY, Hamburg and Zeuthen, Germany
- ⁴³ Institut für Experimentelle Physik IV, Technische Universität Dortmund, Dortmund, Germany
- ⁴⁴ Institut für Kern- und Teilchenphysik, Technische Universität Dresden, Dresden, Germany
- ⁴⁵ Department of Physics, Duke University, Durham NC, United States of America
- ⁴⁶ SUPA - School of Physics and Astronomy, University of Edinburgh, Edinburgh, United Kingdom
- ⁴⁷ INFN Laboratori Nazionali di Frascati, Frascati, Italy
- ⁴⁸ Fakultät für Mathematik und Physik, Albert-Ludwigs-Universität, Freiburg, Germany
- ⁴⁹ Section de Physique, Université de Genève, Geneva, Switzerland
- ⁵⁰ ^(a) INFN Sezione di Genova; ^(b) Dipartimento di Fisica, Università di Genova, Genova, Italy
- ⁵¹ ^(a) E. Andronikashvili Institute of Physics, Iv. Javakhishvili Tbilisi State University, Tbilisi; ^(b) High Energy Physics Institute, Tbilisi State University, Tbilisi, Georgia
- ⁵² II Physikalisches Institut, Justus-Liebig-Universität Giessen, Giessen, Germany
- ⁵³ SUPA - School of Physics and Astronomy, University of Glasgow, Glasgow, United Kingdom
- ⁵⁴ II Physikalisches Institut, Georg-August-Universität, Göttingen, Germany
- ⁵⁵ Laboratoire de Physique Subatomique et de Cosmologie, Université Grenoble-Alpes, CNRS/IN2P3, Grenoble, France
- ⁵⁶ Department of Physics, Hampton University, Hampton VA, United States of America
- ⁵⁷ Laboratory for Particle Physics and Cosmology, Harvard University, Cambridge MA, United States of America
- ⁵⁸ ^(a) Kirchhoff-Institut für Physik, Ruprecht-Karls-Universität Heidelberg, Heidelberg; ^(b) Physikalisches Institut, Ruprecht-Karls-Universität Heidelberg, Heidelberg; ^(c) ZITI Institut für technische Informatik, Ruprecht-Karls-Universität Heidelberg, Mannheim, Germany
- ⁵⁹ Faculty of Applied Information Science, Hiroshima Institute of Technology, Hiroshima, Japan
- ⁶⁰ ^(a) Department of Physics, The Chinese University of Hong Kong, Shatin, N.T., Hong

- Kong; ^(b) Department of Physics, The University of Hong Kong, Hong Kong; ^(c) Department of Physics, The Hong Kong University of Science and Technology, Clear Water Bay, Kowloon, Hong Kong, China
- ⁶¹ Department of Physics, Indiana University, Bloomington IN, United States of America
- ⁶² Institut für Astro- und Teilchenphysik, Leopold-Franzens-Universität, Innsbruck, Austria
- ⁶³ University of Iowa, Iowa City IA, United States of America
- ⁶⁴ Department of Physics and Astronomy, Iowa State University, Ames IA, United States of America
- ⁶⁵ Joint Institute for Nuclear Research, JINR Dubna, Dubna, Russia
- ⁶⁶ KEK, High Energy Accelerator Research Organization, Tsukuba, Japan
- ⁶⁷ Graduate School of Science, Kobe University, Kobe, Japan
- ⁶⁸ Faculty of Science, Kyoto University, Kyoto, Japan
- ⁶⁹ Kyoto University of Education, Kyoto, Japan
- ⁷⁰ Department of Physics, Kyushu University, Fukuoka, Japan
- ⁷¹ Instituto de Física La Plata, Universidad Nacional de La Plata and CONICET, La Plata, Argentina
- ⁷² Physics Department, Lancaster University, Lancaster, United Kingdom
- ⁷³ ^(a) INFN Sezione di Lecce; ^(b) Dipartimento di Matematica e Fisica, Università del Salento, Lecce, Italy
- ⁷⁴ Oliver Lodge Laboratory, University of Liverpool, Liverpool, United Kingdom
- ⁷⁵ Department of Physics, Jožef Stefan Institute and University of Ljubljana, Ljubljana, Slovenia
- ⁷⁶ School of Physics and Astronomy, Queen Mary University of London, London, United Kingdom
- ⁷⁷ Department of Physics, Royal Holloway University of London, Surrey, United Kingdom
- ⁷⁸ Department of Physics and Astronomy, University College London, London, United Kingdom
- ⁷⁹ Louisiana Tech University, Ruston LA, United States of America
- ⁸⁰ Laboratoire de Physique Nucléaire et de Hautes Energies, UPMC and Université Paris-Diderot and CNRS/IN2P3, Paris, France
- ⁸¹ Fysiska institutionen, Lunds universitet, Lund, Sweden
- ⁸² Departamento de Física Teórica C-15, Universidad Autónoma de Madrid, Madrid, Spain
- ⁸³ Institut für Physik, Universität Mainz, Mainz, Germany
- ⁸⁴ School of Physics and Astronomy, University of Manchester, Manchester, United Kingdom
- ⁸⁵ CPPM, Aix-Marseille Université and CNRS/IN2P3, Marseille, France
- ⁸⁶ Department of Physics, University of Massachusetts, Amherst MA, United States of America
- ⁸⁷ Department of Physics, McGill University, Montreal QC, Canada
- ⁸⁸ School of Physics, University of Melbourne, Victoria, Australia
- ⁸⁹ Department of Physics, The University of Michigan, Ann Arbor MI, United States of

America

⁹⁰ Department of Physics and Astronomy, Michigan State University, East Lansing MI, United States of America

⁹¹ ^(a) INFN Sezione di Milano; ^(b) Dipartimento di Fisica, Università di Milano, Milano, Italy

⁹² B.I. Stepanov Institute of Physics, National Academy of Sciences of Belarus, Minsk, Republic of Belarus

⁹³ National Scientific and Educational Centre for Particle and High Energy Physics, Minsk, Republic of Belarus

⁹⁴ Department of Physics, Massachusetts Institute of Technology, Cambridge MA, United States of America

⁹⁵ Group of Particle Physics, University of Montreal, Montreal QC, Canada

⁹⁶ P.N. Lebedev Institute of Physics, Academy of Sciences, Moscow, Russia

⁹⁷ Institute for Theoretical and Experimental Physics (ITEP), Moscow, Russia

⁹⁸ National Research Nuclear University MEPhI, Moscow, Russia

⁹⁹ D.V. Skobeltsyn Institute of Nuclear Physics, M.V. Lomonosov Moscow State University, Moscow, Russia

¹⁰⁰ Fakultät für Physik, Ludwig-Maximilians-Universität München, München, Germany

¹⁰¹ Max-Planck-Institut für Physik (Werner-Heisenberg-Institut), München, Germany

¹⁰² Nagasaki Institute of Applied Science, Nagasaki, Japan

¹⁰³ Graduate School of Science and Kobayashi-Maskawa Institute, Nagoya University, Nagoya, Japan

¹⁰⁴ ^(a) INFN Sezione di Napoli; ^(b) Dipartimento di Fisica, Università di Napoli, Napoli, Italy

¹⁰⁵ Department of Physics and Astronomy, University of New Mexico, Albuquerque NM, United States of America

¹⁰⁶ Institute for Mathematics, Astrophysics and Particle Physics, Radboud University Nijmegen/Nikhef, Nijmegen, Netherlands

¹⁰⁷ Nikhef National Institute for Subatomic Physics and University of Amsterdam, Amsterdam, Netherlands

¹⁰⁸ Department of Physics, Northern Illinois University, DeKalb IL, United States of America

¹⁰⁹ Budker Institute of Nuclear Physics, SB RAS, Novosibirsk, Russia

¹¹⁰ Department of Physics, New York University, New York NY, United States of America

¹¹¹ Ohio State University, Columbus OH, United States of America

¹¹² Faculty of Science, Okayama University, Okayama, Japan

¹¹³ Homer L. Dodge Department of Physics and Astronomy, University of Oklahoma, Norman OK, United States of America

¹¹⁴ Department of Physics, Oklahoma State University, Stillwater OK, United States of America

¹¹⁵ Palacký University, RCPTM, Olomouc, Czech Republic

¹¹⁶ Center for High Energy Physics, University of Oregon, Eugene OR, United States of America

- ¹¹⁷ LAL, Université Paris-Sud and CNRS/IN2P3, Orsay, France
- ¹¹⁸ Graduate School of Science, Osaka University, Osaka, Japan
- ¹¹⁹ Department of Physics, University of Oslo, Oslo, Norway
- ¹²⁰ Department of Physics, Oxford University, Oxford, United Kingdom
- ¹²¹ ^(a) INFN Sezione di Pavia; ^(b) Dipartimento di Fisica, Università di Pavia, Pavia, Italy
- ¹²² Department of Physics, University of Pennsylvania, Philadelphia PA, United States of America
- ¹²³ Petersburg Nuclear Physics Institute, Gatchina, Russia
- ¹²⁴ ^(a) INFN Sezione di Pisa; ^(b) Dipartimento di Fisica E. Fermi, Università di Pisa, Pisa, Italy
- ¹²⁵ Department of Physics and Astronomy, University of Pittsburgh, Pittsburgh PA, United States of America
- ¹²⁶ ^(a) Laboratório de Instrumentação e Física Experimental de Partículas - LIP, Lisboa; ^(b) Faculdade de Ciências, Universidade de Lisboa, Lisboa; ^(c) Department of Physics, University of Coimbra, Coimbra; ^(d) Centro de Física Nuclear da Universidade de Lisboa, Lisboa; ^(e) Departamento de Física, Universidade do Minho, Braga; ^(f) Departamento de Física Teórica y del Cosmos and CAFPE, Universidad de Granada, Granada (Spain); ^(g) Dep Física and CEFITEC of Faculdade de Ciências e Tecnologia, Universidade Nova de Lisboa, Caparica, Portugal
- ¹²⁷ Institute of Physics, Academy of Sciences of the Czech Republic, Praha, Czech Republic
- ¹²⁸ Czech Technical University in Prague, Praha, Czech Republic
- ¹²⁹ Faculty of Mathematics and Physics, Charles University in Prague, Praha, Czech Republic
- ¹³⁰ State Research Center Institute for High Energy Physics, Protvino, Russia
- ¹³¹ Particle Physics Department, Rutherford Appleton Laboratory, Didcot, United Kingdom
- ¹³² Ritsumeikan University, Kusatsu, Shiga, Japan
- ¹³³ ^(a) INFN Sezione di Roma; ^(b) Dipartimento di Fisica, Sapienza Università di Roma, Roma, Italy
- ¹³⁴ ^(a) INFN Sezione di Roma Tor Vergata; ^(b) Dipartimento di Fisica, Università di Roma Tor Vergata, Roma, Italy
- ¹³⁵ ^(a) INFN Sezione di Roma Tre; ^(b) Dipartimento di Matematica e Fisica, Università Roma Tre, Roma, Italy
- ¹³⁶ ^(a) Faculté des Sciences Ain Chock, Réseau Universitaire de Physique des Hautes Energies - Université Hassan II, Casablanca; ^(b) Centre National de l'Energie des Sciences Techniques Nucleaires, Rabat; ^(c) Faculté des Sciences Semlalia, Université Cadi Ayyad, LPHEA-Marrakech; ^(d) Faculté des Sciences, Université Mohamed Premier and LPTPM, Oujda; ^(e) Faculté des sciences, Université Mohammed V-Agdal, Rabat, Morocco
- ¹³⁷ DSM/IRFU (Institut de Recherches sur les Lois Fondamentales de l'Univers), CEA Saclay (Commissariat à l'Energie Atomique et aux Energies Alternatives), Gif-sur-Yvette, France
- ¹³⁸ Santa Cruz Institute for Particle Physics, University of California Santa Cruz, Santa

Cruz CA, United States of America

¹³⁹ Department of Physics, University of Washington, Seattle WA, United States of America

¹⁴⁰ Department of Physics and Astronomy, University of Sheffield, Sheffield, United Kingdom

¹⁴¹ Department of Physics, Shinshu University, Nagano, Japan

¹⁴² Fachbereich Physik, Universität Siegen, Siegen, Germany

¹⁴³ Department of Physics, Simon Fraser University, Burnaby BC, Canada

¹⁴⁴ SLAC National Accelerator Laboratory, Stanford CA, United States of America

¹⁴⁵ ^(a) Faculty of Mathematics, Physics & Informatics, Comenius University, Bratislava;

^(b) Department of Subnuclear Physics, Institute of Experimental Physics of the Slovak Academy of Sciences, Kosice, Slovak Republic

¹⁴⁶ ^(a) Department of Physics, University of Cape Town, Cape Town; ^(b) Department of Physics, University of Johannesburg, Johannesburg; ^(c) School of Physics, University of the Witwatersrand, Johannesburg, South Africa

¹⁴⁷ ^(a) Department of Physics, Stockholm University; ^(b) The Oskar Klein Centre, Stockholm, Sweden

¹⁴⁸ Physics Department, Royal Institute of Technology, Stockholm, Sweden

¹⁴⁹ Departments of Physics & Astronomy and Chemistry, Stony Brook University, Stony Brook NY, United States of America

¹⁵⁰ Department of Physics and Astronomy, University of Sussex, Brighton, United Kingdom

¹⁵¹ School of Physics, University of Sydney, Sydney, Australia

¹⁵² Institute of Physics, Academia Sinica, Taipei, Taiwan

¹⁵³ Department of Physics, Technion: Israel Institute of Technology, Haifa, Israel

¹⁵⁴ Raymond and Beverly Sackler School of Physics and Astronomy, Tel Aviv University, Tel Aviv, Israel

¹⁵⁵ Department of Physics, Aristotle University of Thessaloniki, Thessaloniki, Greece

¹⁵⁶ International Center for Elementary Particle Physics and Department of Physics, The University of Tokyo, Tokyo, Japan

¹⁵⁷ Graduate School of Science and Technology, Tokyo Metropolitan University, Tokyo, Japan

¹⁵⁸ Department of Physics, Tokyo Institute of Technology, Tokyo, Japan

¹⁵⁹ Department of Physics, University of Toronto, Toronto ON, Canada

¹⁶⁰ ^(a) TRIUMF, Vancouver BC; ^(b) Department of Physics and Astronomy, York University, Toronto ON, Canada

¹⁶¹ Faculty of Pure and Applied Sciences, University of Tsukuba, Tsukuba, Japan

¹⁶² Department of Physics and Astronomy, Tufts University, Medford MA, United States of America

¹⁶³ Centro de Investigaciones, Universidad Antonio Narino, Bogota, Colombia

¹⁶⁴ Department of Physics and Astronomy, University of California Irvine, Irvine CA, United States of America

¹⁶⁵ ^(a) INFN Gruppo Collegato di Udine, Sezione di Trieste, Udine; ^(b) ICTP, Trieste; ^(c)

Dipartimento di Chimica, Fisica e Ambiente, Università di Udine, Udine, Italy

¹⁶⁶ Department of Physics, University of Illinois, Urbana IL, United States of America

¹⁶⁷ Department of Physics and Astronomy, University of Uppsala, Uppsala, Sweden

¹⁶⁸ Instituto de Física Corpuscular (IFIC) and Departamento de Física Atómica, Molecular y Nuclear and Departamento de Ingeniería Electrónica and Instituto de Microelectrónica de Barcelona (IMB-CNM), University of Valencia and CSIC, Valencia, Spain

¹⁶⁹ Department of Physics, University of British Columbia, Vancouver BC, Canada

¹⁷⁰ Department of Physics and Astronomy, University of Victoria, Victoria BC, Canada

¹⁷¹ Department of Physics, University of Warwick, Coventry, United Kingdom

¹⁷² Waseda University, Tokyo, Japan

¹⁷³ Department of Particle Physics, The Weizmann Institute of Science, Rehovot, Israel

¹⁷⁴ Department of Physics, University of Wisconsin, Madison WI, United States of America

¹⁷⁵ Fakultät für Physik und Astronomie, Julius-Maximilians-Universität, Würzburg, Germany

¹⁷⁶ Fachbereich C Physik, Bergische Universität Wuppertal, Wuppertal, Germany

¹⁷⁷ Department of Physics, Yale University, New Haven CT, United States of America

¹⁷⁸ Yerevan Physics Institute, Yerevan, Armenia

¹⁷⁹ Centre de Calcul de l'Institut National de Physique Nucléaire et de Physique des Particules (IN2P3), Villeurbanne, France

^a Also at Department of Physics, King's College London, London, United Kingdom

^b Also at Institute of Physics, Azerbaijan Academy of Sciences, Baku, Azerbaijan

^c Also at Novosibirsk State University, Novosibirsk, Russia

^d Also at TRIUMF, Vancouver BC, Canada

^e Also at Department of Physics, California State University, Fresno CA, United States of America

^f Also at Department of Physics, University of Fribourg, Fribourg, Switzerland

^g Also at Departamento de Física e Astronomia, Faculdade de Ciências, Universidade do Porto, Portugal

^h Also at Tomsk State University, Tomsk, Russia

ⁱ Also at CPPM, Aix-Marseille Université and CNRS/IN2P3, Marseille, France

^j Also at Università di Napoli Parthenope, Napoli, Italy

^k Also at Institute of Particle Physics (IPP), Canada

^l Also at Particle Physics Department, Rutherford Appleton Laboratory, Didcot, United Kingdom

^m Also at Department of Physics, St. Petersburg State Polytechnical University, St. Petersburg, Russia

ⁿ Also at Louisiana Tech University, Ruston LA, United States of America

^o Also at Institutio Catalana de Recerca i Estudis Avancats, ICREA, Barcelona, Spain

^p Also at Department of Physics, National Tsing Hua University, Taiwan

^q Also at Department of Physics, The University of Texas at Austin, Austin TX, United States of America

- ^r Also at Institute of Theoretical Physics, Ilia State University, Tbilisi, Georgia
- ^s Also at CERN, Geneva, Switzerland
- ^t Also at Georgian Technical University (GTU), Tbilisi, Georgia
- ^u Also at Ochanomizu Academic Production, Ochanomizu University, Tokyo, Japan
- ^v Also at Manhattan College, New York NY, United States of America
- ^w Also at Institute of Physics, Academia Sinica, Taipei, Taiwan
- ^x Also at LAL, Université Paris-Sud and CNRS/IN2P3, Orsay, France
- ^y Also at Academia Sinica Grid Computing, Institute of Physics, Academia Sinica, Taipei, Taiwan
- ^z Also at Laboratoire de Physique Nucléaire et de Hautes Energies, UPMC and Université Paris-Diderot and CNRS/IN2P3, Paris, France
- ^{aa} Also at Moscow Institute of Physics and Technology State University, Dolgoprudny, Russia
- ^{ab} Also at Section de Physique, Université de Genève, Geneva, Switzerland
- ^{ac} Also at International School for Advanced Studies (SISSA), Trieste, Italy
- ^{ad} Also at Department of Physics and Astronomy, University of South Carolina, Columbia SC, United States of America
- ^{ae} Also at School of Physics and Engineering, Sun Yat-sen University, Guangzhou, China
- ^{af} Also at Faculty of Physics, M.V.Lomonosov Moscow State University, Moscow, Russia
- ^{ag} Also at National Research Nuclear University MEPhI, Moscow, Russia
- ^{ah} Also at Department of Physics, Stanford University, Stanford CA, United States of America
- ^{ai} Also at Institute for Particle and Nuclear Physics, Wigner Research Centre for Physics, Budapest, Hungary
- ^{aj} Also at Department of Physics, Oxford University, Oxford, United Kingdom
- ^{ak} Also at Department of Physics, The University of Michigan, Ann Arbor MI, United States of America
- ^{al} Also at Discipline of Physics, University of KwaZulu-Natal, Durban, South Africa
- ^{am} Also at University of Malaya, Department of Physics, Kuala Lumpur, Malaysia
- * Deceased